INFORMATION TO USERS

This manuscript has been reproduced from the microfilm master. UMI films the text directly from the original or copy submitted. Thus, some thesis and dissertation copies are in typewriter face, while others may be from any type of computer printer.

The quality of this reproduction is dependent upon the quality of the copy submitted. Broken or indistinct print, colored or poor quality illustrations and photographs, print bleedthrough, substandard margins, and improper alignment can adversely affect reproduction.

In the unlikely event that the author did not send UMI a complete manuscript and there are missing pages, these will be noted. Also, if unauthorized copyright material had to be removed, a note will indicate the deletion.

Oversize materials (e.g., maps, drawings, charts) are reproduced by sectioning the original, beginning at the upper left-hand corner and continuing from left to right in equal sections with small overlaps.

ProQuest Information and Learning
300 North Zeeb Road, Ann Arbor, MI 48106-1346 USA
800-521-0600

University of Alberta

THE BRAGS ARE A NOVEL FAMILY OF ARF-GEFS

by

Troy K. Lasell

A thesis submitted to the Faculty of Graduate Studies and Research in partial fulfillment of the

requirements for the degree of *Master of Science*

Department of *Cell Biology*

Edmonton, Alberta
Spring, 2005

Abstract

ADP-ribosylation factors, or Arfs, function as regulators of vesicle budding and membrane remodeling, whose activation is catalyzed by Arf-GEFs. All Arf-GEFs known to date contain a characteristic 200-residue protein domain called Sec7 domain (Sec7d) that appears sufficient to promote Arf activation. Biostatistical analysis determined that three new human cDNAs encoding Sec7d, KIAA0522, KIAA0763 and KIAA1110, formed a new class of putative Arf-GEFs. Biochemical analysis of truncations containing the Sec7d of KIAA0522 and KIAA0763 confirmed that both cDNAs encode active Arf-GEFs. More detailed analysis with KIAA0522 established that this GEF acts on all three Arf classes and shows resistance to BFA. These proteins were renamed BFA-resistant Arf-GEFs, or BRAGs. 5'RACE demonstrated that the BRAG1/KIAA0522 gene yields several splice variants with alternate exons at the 5'end. Similar analysis for BRAG2/KIAA0763 identified an additional exon 100 kbp upstream from the first published exon. Multiple tissue Northern blots with splice-specific probes determined that some splice variants are expressed primarily in muscle, while others show a wider range of expression. These results suggest a model in which BRAGs are Arf-GEFs that contain an active Sec7d flanked by a variable N-terminus that confer tissue-specific function.

Acknowledgments

I would like to thank the various technicians that I have worked with, including Baoping Zhao, Heather Vandertol-vanier, and Anita Gilchrist.

I would also like to acknowledgment my lab-mates, both past and present, including Alex Claude, Xinhua Zhao, Mary Schneider, Florin Manolea

I would like to thank Paul Melancon for technical assistance both in the laboratory and with this thesis. Without Paul none of this would have happened.

I would like to give a huge thank-you to my mother Kathleen Lasell, whose support throughout the years has allowed me to achieve my potential. I love you mom.

Table of Contents

List of Tables

List of Figures

Figure 4.24 *FLAG-tagging BRAG1b and BRAG1c at the C-terminus interferes with localization*

List of Abbreviations

aa = amino acid
AP = Assembly Protein
AP = affinity purified
AP-OB4 = Affinity Purified 0b4 serum
Arf = ADP Ribosylation Factor
Arl = ARF like
ARNO = Arf Nucleotide binding site Opener
BIG = Brefeldin A Inhibited ARF-GEF
BFA = brefeldin A
BRAG = Brefeldin A Resistant ARF-GEF
COPI = Coat protein I
COPII = Coat protein II
DCB = Dimerization and Cyclophilin Binding Domain
EGF = Epidermal Growth Factor
ER = Endoplasmic Reticulum
tER = transitional ER
ERES = ER Exit Site
ERGIC = ER Golgi Intermediate Compartment
GA = Glutathione Agarose
GAP = GTPase Activating Protein
GBF = Golgi Brefeldin A resistance Factor
Gea = Guanine nucleotide Exchanger for ARF
GEF = Guanine nucleotide Exchange Factor
GEP = GTP Exchange Protein
GGA = Golgi localized Gamma ear containing ARF binding protein
GST = Glutathione-S-Transferase
HUS = Homology Upstream of Sec7d
IDT = Integrated DNA Technologies
MannII = mannosidase II
NEB = New England Biolabs
PCR = Polymerase Chain Reaction
PKC = Protein Kinase C
PLD = phospholipase D
PM = plasma membrane
PH domain = Pleckstrin Homology Domain
RACE = Rapid amplification of cDNA ends
Sec7d = Sec7 domain
SNARE = SNAP receptor
TAP = Tobacco Acid Phosphotase
UTR = Untranslated Region
VSV-G = Vesicular Stomatitis Virus glycoprotein
VTC = Vesicular-Tubular Clusters

Chapter 1

Introduction

1.0 Eukaryotic cells are compartmentalized

The cytoplasm of eukaryotic cells is filled with membrane-enclosed organelles that contain unique subsets of proteins and perform specialized functions. This organization, allows eukaryotic cells to tailor a number of micro-environments of specific pH or redox states to facilitate various aspects of metabolism. Furthermore, compartmentalization allows the separation of antagonistic processes, and the containment of potentially harmful components such as lysosomal proteases or mitochondrial cytochromes.

Some organelles such as peroxisomes, mitochondria, chloroplasts or the nucleus are able to import fully folded proteins directly from the cytoplasm. On the other hand, protein entry into nearly all the membrane-bound organelles comprising the central vacuolar system does not occur directly. The proteins of organelles such as the Golgi complex and the various compartments of the endo-lysosomal system are either imported by translocation into the endoplasmic reticulum (ER) or by endocytosis at the plasma membrane (PM). The final arrangement of membrane and lumenal content is then achieved through complex and selective transfer events between the many organelles.

1.1 Compartments of the exocytic pathway

Compartments of the exocytic pathway include the endoplasmic reticulum (ER), Golgi complex with its associated cis- and trans- tubular networks, and finally the plasma membrane (PM) (see Figure 1.1). Following translocation into the ER, proteins destined for other organelles such as the Golgi complex, endosomes or PM are first targeted to specialized regions of the ER called transitional ER (tER) or ER exit sites (ERES). Cargo proteins are then packaged into carriers and move sequentially from the ER, to an ER-Golgi intermediate compartment (ERGIC) and ultimately the cis-cisternae of the Golgi complex by a process that allows selective incorporation of cargo and transport machinery into forming carriers while retaining resident proteins in the ER. These pleiomorphic carriers are actively transported on microtubules towards the cell center where they accumulate, fuse into a tubulated network called the cis-Golgi network or CGN and eventually form new flattened Golgi cisternae near the microtubule organizing center.

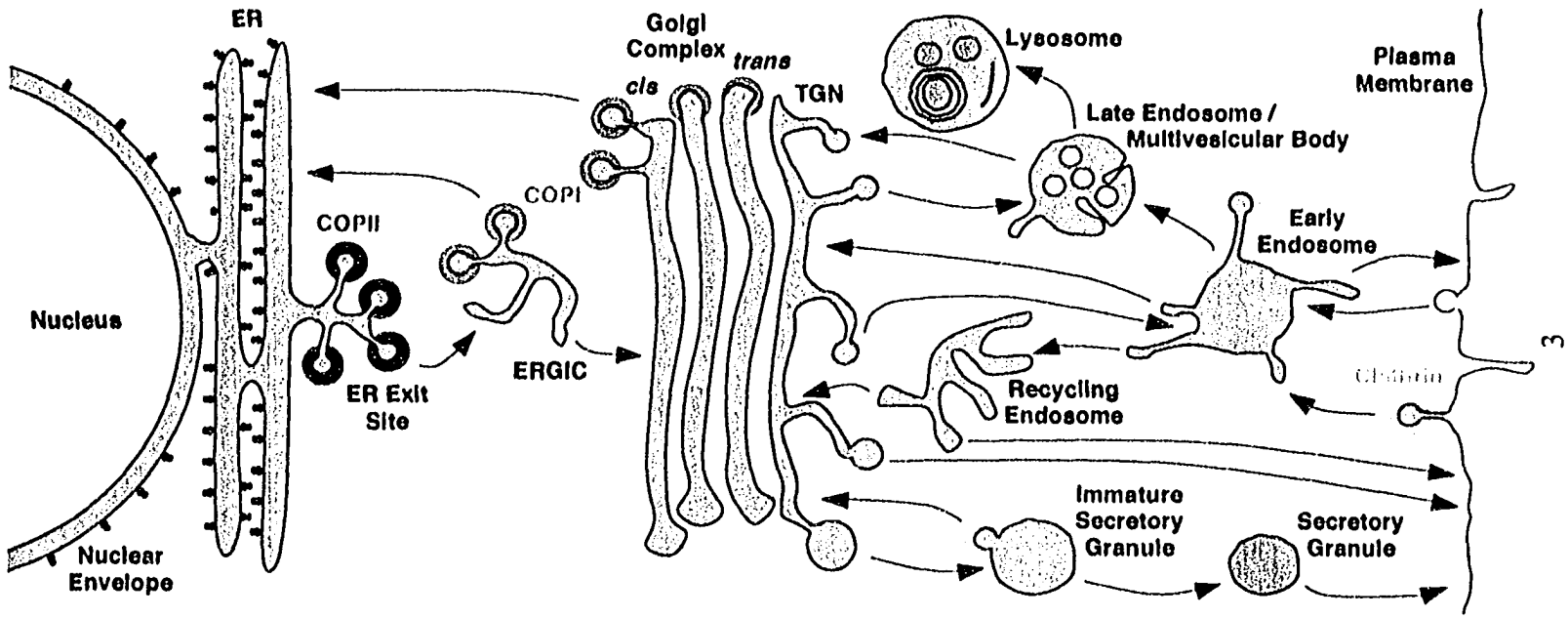

Figure 1.1 ***The Central Vacuolar system includes a number of organelles and the transport transport between them***

The central vacuolar system includes the ER, CGN, Golgi, TGN, endosomes, secretory granules and the PM. There is vectorial transport between the organelles, as is denoted with arrows This figure was adapted from Figure 1 of Bonifacino and Glick (2004) Cell 116:153-166.

Current evidence suggests that cargo molecules then progress through the Golgi stack by a process termed cisternal maturation whereby newly formed cis-cisternae with their anterograde cargo progressively move towards the trans side as they lose early-acting Golgi enzymes and acquire late-acting ones (Storrie and Nilsson, 2002). Golgi resident enzymes have been identified in small vesicles surrounding the Golgi stack and are thought to continuously move in a retrograde direction to facilitate the "maturation" process. Cargo molecules destined for the PM are shuttled to the PM from the penultimate cisterna, while those proteins destined to the endo-lysosomal system are selectively retrieved from the highly tubulated TGN (see Figure 1.1).

1.2 Compartments of the endocytic pathway

Proteins can also enter the central vacuolar system through one of several different types of endocytic reactions (see Figure 1.1). Receptor-mediated endocytosis at clathrin-coated pits is the best understood form of endocytosis. However, several clathrin-independent reactions can also facilitate internalization of components from the cell surface (Johannes and Lamaze, 2002),. Some of these alternate mechanisms include the constitutive uptake of liquid by pinocytosis, the triggered uptake of large pathogens by phagocytosis, and finally the internalization of plasma membrane patches enriched in cholesterol and glycopshingolipids. The latter mechanism appears regulated by a distinct type of coat protein called caveolin that binds and stabilizes these "lipid rafts" at the cell surface into characteristic flask-shaped structures called caveolae, (Nabi and Le, 2003);((Parton and Richards, 2003).

Following internalization and uncoating, the endocytic vesicles rapidly converge with several other intermediates at the "early endosome". This complex organelle displays both vesicular and tubular regions and contains the unique phospholipid phosphatidyl inositol 3-phosphate (PI3P). From the early endosome, internalized receptors can follow either of two routes. They can be uncoupled from their ligands in the acidic endosome lumen and targeted to the "recycling endosome" for their eventual recycling to the cell surface. Alternately, some receptors assemble with several other proteins in a complex mono-ubiquitylation-dependent process for their eventual incorporation into intra-lumenal vesicles of the "multivesicular endosome", also called

"multivesicular bodies" (Dupre et al., 2004). Once detached from early endosomes, the roughly spherical multivesicular endosome associate with microtubules and migrate in a motor-dependent manner towards the cell center where they eventually fuse with the more pleiomorphic "late endosome". From these structures, endocytosed material such as the EGF-receptor is subsequently transferred to lysosomes for degradation. Note that transport also occurs between the TGN and both early and late endosomal compartments for delivery of newly synthesized and cycling components of the endo-lysosomal pathway (see (Bonifacino and Jackson, 2003).

Recent analysis of entry mechanisms for bacterial toxins and viruses identified novel endocytic routes that allow these pathogens to evade degradation in lysosomes. For example, cholera toxin or simian-virus-40 associate with lipid rafts on the cell surface and internalize into small, tight fitting vesicles that are not immediately transported to acidic and PIP3-positive "early endosome", but rather to a new organelle with a neutral pH that has been called "caveosome". Like the early endosome, the caveosome appears capable of sorting as ligands such as cholera toxin are delivered to the Golgi complex, while others such as SV-40 are shuttled directly to the ER (Nabi and Le, 2003);(Parton and Richards, 2003).

1.3 FORMATION AND TARGETING OF CARGO CARRIERS:

1.3.1 Several types of coat proteins facilitate protein traffic

Formation of the various cargo carriers described in the previous sections depends on the spatially and temporally regulated recruitment of specific coat proteins from the cytoplasm onto membranes (Bonifacino and Lippincott-Schwartz, 2003). To date three major types of coat proteins have been identified, two of which, called COPI and COPII, function on exocytic compartments. COPI, the coat protein responsible for traffic between the ER and Golgi complex was first identified *in situ* as a dense fuzzy coat on the cisternal rims and vesicular profiles of Golgi cisternae (Orci et al., 1986). This material bound membranes weakly and its identification was only made possible following the demonstration that treatment of cell extracts with poorly hydrolysable analogs of GTP led the dramatic accumulation of coated structures near Golgi stacks (Melancon et al., 1987). Subsequent analysis with such Golgi-derived coated vesicles

identified a stable complex of seven distinct polypeptides that assembled on membranes of the cis-Golgi and was called coatomer protein, or COP (Waters et al., 1991). Interestingly, four of the COPI subunits are homologous to subunits of the clathrin adaptors AP-1 and AP-2 (Schledzewski et al., 1999), and appear to assemble in a similar structure (Bonifacino and Lippincott-Schwartz, 2003; Watson et al., 2004). This complex was renamed COPI following identification of a distinct coat system at the ER. As discussed below, subsequent work established that Arf-GAP1 also participates in COPI coat formation.

The coat complexes involved in the sorting and packaging of cargo from the ER for traffic to the Golgi complex were identified through genetic screens performed in the yeast Saccharomyces cerevisae (Lee et al., 2004). Subsequent functional characterization using cell-free assays established that four main gene products form two stable complexes, a Sec23p/Sec24p hetero-dimer and a Sec13p/Sec31p hetero-tetramer, that assemble sequentially at ER exit sites to form what is now called the COPII coat (Matsuoka et al., 1998); (Antonny and Schekman, 2001). Mammalian homologues of these proteins have been identified and shown to perform similar functions (Aridor et al., 1998). Interestingly, animals express several variants of hSec24 that may allow production of more than one type of COPII coated vesicles with potentially distinct functions (Bock et al., 2001).

The clathrin coat was the first type to be visualized by morphological methods, and the relative abundance of clathrin coated vesicles in brain extracts greatly facilitated its purification and subsequent characterization (Pearse and Robinson, 1990). The clathrin molecule is composed of three heavy chains and three light chains that readily form an easily recognized regular hexagonal lattice. Clathrin assembles at the plasma membranes to form coated patches and invaginations that ultimately lead to the budding of small 100 nm clathrin-coated vesicles. Clathrin was subsequently shown to also assemble on the trans-most cisternae of the Golgi stack and drive tubulation of the TGN. The recruitment and assembly of the clathrin coat requires assembly proteins (APs) with specific sites of action. The tetrameric AP-2 complex drives coated pit formation at the plasma membrane while the subsequently identified AP-1, AP-3 and AP-4 complexes direct assembly of clathrin on membranes of the TGN and endosomes. Further work

identified yet another family of 3 related adaptor proteins, the monomeric Golgi-localized, gamma ear containing, Arf-binding proteins, or GGAs, that also function on membranes of the TGN and endosome (for review see (Robinson, 2004); (Bonifacino and Lippincott-Schwartz, 2003).

1.3.2 Coat proteins can drive membrane deformation

Purified clathrin three-legged trimers, or triskelions, readily assemble *in vitro* into spherical or elongated cages that resemble the structures observed around the coated vesicles formed *in vivo*. This ability to self-assemble into spherical structures provided the initial basis for the hypothesis that coat proteins (COPs) facilitate deformation of flat membranes and ultimately drive budding of transport vesicles. Subsequent work established that addition of purified COPII proteins to synthetic uni-lamellar liposomes can drive formation of small vesicles (Matsuoka et al., 1998). Similar results were later obtained with purified COPI components (Bremser et al., 1999). More recently, the crystal structure of the Sec23p/24p hetero-dimer revealed that the membrane-binding face of the complex forms a natural curve that matches exactly that of a 60 nm COP II vesicle (Bi et al., 2002). Furthermore, this face displays a net positive charge that explains the observed preference of the COP II coat for binding synthetic liposomes containing acidic phospholipids (Matsuoka et al., 1998). Such observations strengthen the hypothesis that coat proteins drive membrane deformation.

Whereas purified coat proteins appear sufficient to drive release of individual vesicles *in vitro*, the process of vesicle scission likely involves additional factors *in vivo*. A newly described protein domain has drawn particular interest recently. The BAR (Bin/amphiphysin/Rvs) domain is the most phylogenetically conserved feature in amphiphysins, a class of proteins implicated in membrane tubulation. A crystal structure established that this module forms elongated crescent-shaped dimers that bind preferentially to highly curved negatively charged membranes (Carlton et al., 2004). Overexpression of BAR domains induces membrane tubules. Many proteins, including several Arf-GAPs, contain such BAR modules that depending on their membrane affinity may be important for either inducing or sensing membrane curvature (Lee and Schekman, 2004).

1.3.3 How does the coat sort cargo

A wide variety of cargo molecules are inserted into and across the ER membrane, and these must be sorted during their traffic through the central vacuolar system. Cargo molecules include both single spanning and multi-spanning membrane proteins that can expose either their N- or C-terminus for interaction with the cytosolic coat machinery. However, cargo also includes lumenal proteins that cannot interact directly with coat proteins and must rely instead on poorly characterized trans-membrane proteins that function as "cargo receptors". The sorting mechanism allowing the efficient recognition of such a variety of substrate is best understood for the export of proteins from the ER regulated by the COP II coat (Barlowe, 2003a).

Current evidence suggests that trans-membrane cargo is concentrated into nascent vesicles when sorting signals on the cytoplasmic domains of trans-membrane cargo interact with components of the coating system. To date, such interactions have been confirmed for both Sec24p and the small GTPase Sar1p. Using Sec23/24 binding assays and genetic approaches two groups recently identified multiple independent binding sites on the Sec24p membrane binding face that are critical for sorting of specific cargos into COPII vesicles (Miller et al., 2003); (Mossessova et al., 2003). Some molecules contain multiple ER export signals and these studies suggests that in some cases combination of export signals may be required for efficient packaging of cargo into COPII vesicles. Components of the COPI coat also recognize signals in the cytosolic domains of trans-membrane proteins and thus actively participate in selection of cargo into carriers (Letourneur et al., 1994); (Bremser et al., 1999). In this case, however, the signal targets proteins for retrieval from the ERGIC and Golgi complex back to the ER (Lee et al., 2004).

Some trans-membrane proteins such as Erv29p, the conserved p24 family and ERGIC53/p58 have been proposed to interact with lumenal proteins and act as "cargo receptors". Many of these receptors contain either a di-acidic motif or a di-hydrophobic motif in their cytoplasmic tail that explains their recruitment to COP II budding sites. On the other hand, the exit motif on the lumenal proteins have not yet been clearly identified. In the case of recognition by the lectin ERGIC53/p58, the interaction appears to depend on both calcium and carbohydrate modification on the soluble cargo (Barlowe, 2003b).

1.3.4 How are vesicles targeted?

Following scission and uncoating, proper delivery of the cargo carrier and its content involves a complex process with multiple discrete steps that include translocation, recognition, tethering/docking and fusion. Several factors with organelle specific distribution ensure the specificity of those reactions.

1.3.4.1 SNAREs Pioneering work by the Rothman group led to the identification of several "transport factors" implicated in membrane fusion. These included an "N-ethylmaleimide–Sensitive Factor", or NSF, and "Soluble NSF Attachment Proteins", or SNAPs, required for its association with Golgi membranes (Block et al., 1988);(Clary et al., 1990). A subsequent search in brain extracts for membrane "SNAP receptors", or SNAREs, led to the isolation of a complex of three integral membrane proteins previously implicated in docking and fusion of synaptic vesicles (Sollner et al., 1993).

Work from several laboratories has since identified a large number of proteins related to the original SNAREs that localize to distinct intracellular compartments (Santy et al., 2001). SNARES are C-terminally anchored integral membrane proteins that form heterotetramers, also called SNAREpins. Each SNAREpin contains one vesicle SNARE (v-SNARE) and 3 target membrane SNAREs (t-SNAREs) in a stable parallel coiled-coil bundle. Formation of a multimeric SNAREpin complex with subunits provided by two different membranes brings these membranes in close proximity and is responsible for reducing the free energy required for membrane fusion. Experiments with purified SNAREs and liposomes confirmed their ability to promote membrane fusion (Weber et al., 1998); (Jahn et al., 2003).

Individual SNAREs show restricted intracellular distribution and can provide a level of specificity in membrane fusion. Purified t-SNAREs and v-SNAREs can pair promiscuously *in vitro*, but only those pairs representing physiologically relevant v- and t-SNARE combinations actually promote membrane fusion when tested with liposomes (McNew et al., 2000). However, SNARE pairing cannot be the sole determinant of specificity because some SNAREs are used at multiple steps in vesicular transport. Tethering factors that act prior to SNAREpin formation provide the additional specificity.

1.3.4.2 Tethering factors. Tethering factors have been implicated in facilitating the initial contact between a transport vesicle and its intended target membrane. These

tethers serve to increase the local concentration of vesicles near the acceptor membrane and provide some specificity to the pre-fusion events. Two broad families of proteins have been implicated in tether formation. The first family consists of multi-component complexes that, as in the case of TRAPP, can contain upward of 10 distinct subunits (Oka and Krieger, 2005). Three different types of complexes called TRAPP, COG and GARP regulate various steps between the ER and Golgi, within the Golgi and between the endosome and Golgi; a different complex called the exocyst operates at the PM (Whyte and Munro, 2002).

The second family consists of proteins that form elongated, rod-like, coiled-coil structures (Gillingham and Munro, 2003). Most of these proteins are found associated with the Golgi complex and are often called golgins. Golgins have been proposed to form long elongated complexes that can form bridges between the vesicle and target membranes. Freeze fracture EM studies have confirmed the presence of long fibrous elements tethering vesicles to nearby acceptor membranes (Orci et al., 1998).

1.3.4.3 *rabs* Several of the tethering factors interact with specific members of the rab family GTPases. These interactions may contribute to the assembly of the tethers and or regulate conformational changes that collapse the tether and brings the vesicle in closer proximity to the target membrane (Barr and Short, 2003).

1.4 Small GTPases and regulation of protein traffic

1.4.1 Regulation of coat assembly by cycles of GTP binding and hydrolysis

Two main sub-families of related GTPases called Sar1p and Arfs have been implicated in the regulation of the recruitment and assembly of the coat proteins described in section 1.3.1. Unlike most other small GTPases, Sar1p and Arfs localize primarily to the cytosol when in the GDP-bound "inactive" form. However, upon activation to the GTP-bound form, these proteins associate tightly with the membrane where they promote coat assembly and vesicle budding. Arfs are myristoylated at their N-terminus and this lipid modification plays a critical role in this membrane association (Franco et al., 1996). Sar1p lacks the myristate modification but use a similar mechanism that takes advantage of a very hydrophobic N-terminal extension (Huang et al., 2001).

The spatial and temporal regulation of small GTPase activation therefore allows the cell to determine where and when to initiate coat recruitment.

Under physiological concentrations of Mg and nucleotides, Sar1p and Arfs do not spontaneously release GDP to bind GTP. Furthermore, these proteins lack a critical residue required for GTP hydrolysis and are particularly poor GTPases (Pasqualato et al., 2001). Ancillary factors are therefore required to catalyze guanine nucleotide exchange and facilitate GTP hydrolysis. A large family of Guanine nucleotide Exchange Factors (or GEFs), which share a common Sec7 domain, catalyze the exchange on Arfs (Jackson and Casanova, 2000). Several members of this family, those that function at the Golgi complex, are direct targets of the drug Brefeldin A. As a consequence, treatment with Brefeldin A blocks Arf activation and loading on Golgi membranes and causes rapid release of both the COP1 coat and various clathrin accessory proteins from the Golgi complex (Lippincott-Schwartz et al., 1991). The mechanism of GDP exchange and the properties of the Arf-GEFs will be discussed in more detail in section 1.10 below.

Whereas a separate class of enzymes regulates Arf and Sar1p activation, it is the coat itself that regulates subsequent deactivation. Indeed, detailed biochemical characterization of the COP II components established that the Sec23p/24p complex acts a weak GTPase activating protein, or GAP, on the Sar1p protein. As is the case for most small GTPase GAPs, Sec23p provides a critical arginine residue (the so-called "arginine finger") that inserts into the guanine nucleotide binding site and promotes GTP hydrolysis. This weak Sar1p-GAP activity increases more than 10 fold upon recruitment of the Sec13/31 complex onto sar1p•GTP-bound Sec23/24p (Antonny et al., 2001; Antonny and Schekman, 2001; Yoshida et al., 1991). This complex dependence on COP II components for Sar1p inactivation is thought to lead to formation COP II patches lacking Sar1p in the center but maintained in a transient meta-stable state by a ring of Sar1p-GTP on their edges (Antonny and Schekman, 2001).

Several classes of Arf-GAPs have been characterized that all share a conserved GAP domain consisting of a zinc-finger motif. However, Arf-GAPs vary widely in size and domain organization and many of these enzymes perform a variety of additional functions independent of GAP activity (Nie et al., 2003a). For example, Arf-GAP1 was initially isolated as a negative regulator of Arf recruitment on Golgi membranes but

subsequently shown to be a structural component of the COPI coat directly involved in cargo sorting (Reinhard et al., 2003). Furthermore, as was the case for the Sec23/24 complex, the ability of Arf-GAP1 to deactivate and release Arf1 is regulated by interaction with other coat components such as COPI (Goldberg, 1999). A particularly intriguing property of Arf-GAPI is its sensitivity to membrane curvature (Bigay et al., 2003). Current evidence suggests the following model: activated Arf recruits both Arf-GAP and COPI to Golgi membranes through direct interactions; the low activity of Arf-GAPI on flat bilayers allows the formation of COPI patches that recruit and concentrate cargo molecules; as the COPI patch grows and leads to formation of a bud, GAP activity is stimulated allowing release of COPI vesicles lacking Arfs but still coated with COP1 and Arf-GAP; the metastable coat lacking Arf dissociates following vesicle scission (Holthuis and Burger, 2003).

1.4.2 Other GTPases implicated in membrane traffic

Coat recruitment and membrane remodeling are not the only steps of protein traffic regulated by small GTPases. Several other classes of small GTPases regulate a variety of subsequent steps. These include rab proteins, Arf-like proteins (Arl) and several members of the rho family. Like Arfs, most of these GTPases are lipidated for membrane association.

1.4.2.1 ***Rabs.*** The large family of small GTPases of the rab family encompasses more than 63 different members in mammals, many of which are restricted to specialized cell types (Bock et al., 2001). Importantly, each rab localizes to a particular sub-cellular compartment. Current evidence suggests that rabs are recruited directly to their intracellular target membranes and that the presence of two geranyl-geranyl groups is critical for delivery. However, the fundamental question of how localization specificity is imparted to Rabs remains unanswered (Seabra and Wasmeier, 2004).

Upon activation to the GTP-bound form, rabs regulate a large and diverse group of effectors, and have been implicated in organizing functionally distinct sub-domains within a particular membrane, thereby defining organelle identity (Pfeffer, 2003). As mentioned in section 1.3.4.2, several rabs regulate the selective assembly of tethering

factors on cargo carriers and target membranes. Rabs also play important regulatory roles in motility by recruiting molecular motors to organelles and transport vesicles (Hammer and Wu, 2002).

1.4.2.2 ***Arls.*** Some members of the Arf-like, or Arl, protein family have also been implicated in protein traffic. Arls show 60-80% protein sequence similarity to Arfs but lack the defining ability to stimulate ADP-ribosylation of Gs by cholera toxin. Subsequently, Arls were shown to also lack the ability to stimulate the activities of phospholipase D (PLD) and PI4P5 kinase.

Bio-statistical analysis reveals that the human genome contains more than ten genes encoding Arls. As a whole, Arls are poorly characterized and the localization of most Arls remains unknown (Burd et al., 2004). Arl 4 and Arl5 localize to the nucleus and are not likely to be involved in protein traffic. However, 2 Arls, Arl1 and Arl3, associate with microtubules, localize to the Golgi complex and have been implicated in protein traffic. Current evidence demonstrates that recruitment of Arl3 to the TGN promotes activation and recruitment of Arl1. At the TGN, Arl1 functions in part to regulate the subsequent tethering of endosome-derived transport vesicles mediated by GRIP domain proteins (Burd et al., 2004; Graham, 2004). Interestingly, Arl1 binds some Arf effectors such as Arfaptin2/POR1 and MKLP1 (Van Valkenburgh et al., 2001) and may yet have other functions.

1.4.2.3 ***rho-family proteins.*** Rho family proteins play a critical role at various steps of both exocytosis and endocytosis through their regulation of actin dynamics (Engqvist-Goldstein and Drubin, 2003). Morphological studies established early that actin filaments form a dense network below the plasma membrane. This actin cortex acts as a barrier to the docking of secretory vesicles and internalization of endocytic vesicles. As a consequence, transient depolymerization of this network must occur to allow vesicles to reach their appropriate docking and fusion sites. The actin cytoskeleton can also have a facilitatory role in protein traffic. The movement of cargo carriers to specific cellular sites depends in many instances on the presence of the actin cables and actin-based motors. Polarized secretion to bud site in yeast is a prime example of this phenomenon.

Analysis of the human genome has identified 20 genes encoding proteins with a small GTPase domain of the rho consensus type (Wherlock and Mellor, 2002). These twenty proteins can be further divided into 5 groups on the basis of sequence and functional similarities: rho-like, rac-like, cdc42-like, Rnd and RhoBTB (Burridge and Wennerberg, 2004). The rho-like GTPases (RhoA,B,C) are very similar and their activation promotes myosin contractility, stress fibers formation, integrin clustering and assembly of focal adhesions. In contrast, members of the rac-like subfamily (rac1-3, rhoG) stimulate formation of lamellipodia and membrane ruffles, whereas the Cdc42-like proteins (Cdc42, TC10, TCL, Wrch1,2) all bind WASP and stimulate formation of filipodia.

The involvement of rho proteins in protein traffic is not limited to their effects on the cytoskeleton. Recent studies revealed that rho proteins perform essential functions in membrane fusion, independent of the cytoskeleton (Eitzen, 2003). For example, Rho1p and cdc42p are enriched on yeast vacuole membranes and both GTPases are required for homotypic vacuole fusion reconstituted in a cell-free assay lacking cytoskeleton (Eitzen et al., 2001); (Muller et al., 2001). Current evidence suggests that such effects on membrane fusion could be related to activation of PI, 5-kinase or PKC and subsequent stimulation of F-actin assembly on the membrane surface (Eitzen, 2003).

1.5 Molecular details for exocytosis

1.5.1 Regulation of ER export by Sar1p and COP II

In most eukaryotes, the endoplasmic reticulum is not a homogeneous environment. The COPII coat forms on ER sub-domains called transitional ER (tER) sites, or alternatively ERES for ER exit sites that function as transport active zones. ERES are long-lived structures defined by the presence of components of the COPII coat assembly machinery (Bevis and Glick, 2002). At the ultrastructural level, ERES appear as ribosome-free ER sub-domains approximately 0.5 μm in diameter, with tubular protrusions of various lengths but constant diameter (Palade, 1975); (Bannykh and Balch, 1997). Several such ER budding sites on distinct but adjacent ER cisternae often cluster around a central cavity filled with vesiculo-tubular elements (Bannykh et al., 1996). ER buds are coated by small particles with distinctive spacing corresponding to the COPII

coat.

The small GTPase Sar1p plays a critical role in assembly of ERES and can initiate cargo selection (Aridor et al., 2001). *In vitro* studies established that activation of Sar1p alone, in the absence of other cytosolic components, leads to the formation of ER-derived tubular domains that resemble ER transitional elements. These transient Sar1-generated tubular domains perform cargo selection and behave as functional intermediates in ER to Golgi transport *in vitro*. Live cell imaging has confirmed that ER export *in vivo* is also characterized by the formation of dynamic tubular structures.

As mentioned in section 1.4.1 above, accumulation of activated Sar1p at ERES ultimately leads to sequential recruitment of the Sec23/24 tetramer and Sec13/31 dimer (Antonny and Schekman, 2001). Activation of Sar1p is catalyzed by the trans-membrane guanine exchange factor (GEF) Sec12p. Interestingly, in mammalian cells (Weissman et al., 2001) and the yeast S cerevisiae (Rossanese et al., 1999), Sec12p does not accumulate at ERES but rather localizes throughout the ER. The site of COP II coat assembly is therefore not determined by the location of the Sar1p-specific GEF. Recent experiments in the yeast *P. pastoris* suggest instead the presence of a regulatory and saturable scaffold at ERES that collects and organizes components of the COP II coat (Soderholm et al., 2004). The nature of the scaffold remains unknown, but several lines of evidence suggest the involvement of Sec16p (Bonifacino and Glick, 2004).

Some abundant cargo molecules are picked up in COPII vesicles at their prevalent concentration in the ER, without any detectable concentration, by a process termed bulk flow (Martinez-Menarguez et al., 1999). However, the majority of cargo molecules appear enriched in COPII vesicles through interaction between sorting signals and either the COPII coat or a variety of cargo receptors mentioned in section 1.3.3. Some of the cargo molecules sorted in this manner include SNAREs involved in targeting of the nascent vesicle.

ERES appear to generate at least two distinct classes of COPII vesicles. Analysis of the transport of the GPI-anchored protein Gas1p revealed that it utilizes the trans-membrane protein Emp24 as cargo receptor. Loss of Emp24 prevents packaging of Gas1p into vesicles with minimal impact on other cargos. Furthermore, when present, Gas1p and other GPI-anchored proteins enter transport vesicles that are distinct from

those that carry other cargo proteins such as α-factor and amino acid permeases (Muniz et al., 2001; Watanabe and Riezman, 2004).

The presence of multiple isoforms of COPII components may explain the production of distinct types of vesicles. For example, the yeast Sec24 homolog, Lst1, is required for ER export of an abundant plasma membrane protein and vesicles generated with Lst1 in place of Sec24 package a distinct subset of cargo (Miller et al., 2002). Humans express two homologues of Sar1p and several Sec24 isoforms have been described (Bock et al., 2001). The unique function of each isoform remains unknown but their relative abundance may facilitate differential regulation of packaging and transport.

1.5.2 Sorting in VTCs and Golgi stack by COPI

In S. cerevisiae, COPII vesicles are thought to fuse and target directly cis-Golgi cisternae dispersed throughout the cytoplasm. In animal cells, COPII vesicles first form intermediate vesiculo-tubular clusters, or VTCs, that rapidly associate with microtubules and move towards the juxta-nuclear Golgi complex in a dynein-dependent manner (Corthesy-Theulaz et al., 1992). This collection of intermediates has also been described as an ER-Golgi intermediate compartment, or ERGIC. The ERGIC serves as the first sorting compartment in the exocytic pathway, where proteins that have escaped are recycled back to the ER (Pelham, 1988). Quantitative immuno-electron microscopy in rat exocrine pancreas revealed significant concentration for several secretory proteins during transit from the ER to the Golgi complex (Martinez-Menarguez et al., 1999); (Oprins et al., 2001). These studies led to a model wherein secretory proteins are concentrated as a consequence of their exclusion from membrane recycling from VTCs back to the ER (Martinez et al., 1997; Martinez-Menarguez et al., 1999; Oprins et al., 2001; Warren and Mellman, 1999).

Current evidence suggests that the COPI coat facilitates the maturation of VTCs using mechanisms similar to those described above for the COPII coat. Live-imaging studies with GFP-chimeras revealed that COPI associates with transport intermediates shortly after their formation and release from ERES (Presley et al., 1997);(Scales et al., 1997). Subsequent experiments with the drug BFA confirmed that COPII and COPI both

perform essential but distinct functions in production of transport intermediates (Pelham, 2001). As expected, treatment with Brefeldin A had no impact on COPII assembly and maintenance of ERES, but effectively blocked recruitment of Arf and COP1 on these structures and interfered with concentration of secretory cargo such as VSV-G and Golgi resident enzymes (Ward et al., 2001).

Assembly of the COPI coat is thought to promote the sorting of retrograde cargo into tubules and budding vesicles. Purified COPI both facilitates membrane deformation and can interact with retrograde cargo. Proteins retrieved to the ER display a characteristic and essential KKXX motif at their C-terminus that binds directly with several subunits of the COP1 complex (Cosson and Letourner, 1994). Arf-GAP1, the other structural component of COP1, also interacts with KKXX-containing proteins. Interestingly, Arf-GAP1 and COPI display slightly different affinities for KKXX-containing peptides with varying N-terminal sequences (Reinhard et al., 2003). The COPI coat performs similar functions at the Golgi complex where it is found associated with cisternal rims and small 60-90 nm vesicular structures near the Golgi stack (Orci et al., 1986); (Oprins et al., 1993).

In contrast to the COPII system, the functions of Arf/COPI may not be limited to membrane deformation and cargo sorting but also include extensive local remodeling of the membrane bilayer. Upon activation and membrane recruitment, Arfs interacts with and activate several effectors that include PI4P-5 kinase and PLD (Nie et al., 2003b). In combination with the ongoing sorting and budding of retrograde cargo, the action of these lipid modifying enzymes leads to progressive changes in both the protein and the lipid content of the cargo carriers.

1.6 Sorting to the endosomal system from the TGN

Recent work suggests that sorting and exit from the Golgi complex occurs from the last 2-3 of cisternae of the stack and may involve two distinct mechanisms (Mogelsvang et al., 2004). In contrast to the flattened appearance of cisternae in the middle of the Golgi stack, the trans cisternae show a highly tubulated structure (Ladinsky et al., 1999); (Marsh et al., 2001). The extreme fenestration often observed on those trans cisternae gives the impression of a network that results from the actual consumption of

the cisterna. The trans-most cisterna of the Golgi complex clearly displays buds with the characteristic pentagonal/hexagonal pattern of the clathrin triskelion. Clathrin coats only this trans-most cisterna and it is here that cargo destined to the endosomal-lysosomal pathway is recruited. It is currently assumed that material targeted to the plasma membrane must exit from the two previous trans-cisternae. Those cisternae show a distinct type of coat called lace-like or non-clathrin (Ladinsky et al., 1999; Ladinsky et al., 2002), whose identify remains unknown.

As observed for COPI on early compartments of the exocytic pathway, recruitment of the clathrin coat on the trans-most cisterna of the Golgi complex depends on Arf activation. Members of the BFA-sensitive BIG/Sec7p family of Arf-GEFs catalyze this activation. In contrast to the COPI system, activated Arfs do not recruit the clathrin triskelion directly, but instead promote the recruitment of several adaptor proteins of the AP (AP-1, AP-3 and AP-4) and GGA (GGA1, GGA-2 and GGA-3) families. Arfs can also regulate recruitment of adaptors indirectly by affecting the levels of phospho-inositides either directly by activation of phosphatidyl-inositol 4-phosphate 5 kinase, or either indirectly through activation of PLD and production of the phosphatidic acid (Donaldson, 2003). For example, the recruitment of AP-1 on the TGN depends critically on the presence of phosphatidyl-inositol 4-phosphate (PI4P), a phospho-inositide produced preferentially on the Golgi complex (Wang et al., 2003).

On the TGN and endosome membranes, these adaptors have been shown to interact with Arfs and the intracellular tails of several types of transport receptors (Bonifacino, 2004). Note that AP-3 and GGA-3 function primarily on the endosome while AP-4 localizes predominantly to the TGN. Interestingly, none of these three "adaptors" are recovered in clathrin-coated vesicles and they appear instead to function independently of clathrin (Robinson, 2004). Whether these adaptors recruit an alternate lattice distinct from clathrin has yet to be determined.

Current evidence does not permit one to clearly determine whether APs and GGAs function sequentially, on parallel trafficking pathways or on opposite trafficking pathways. However, the recent demonstration that transfer of a single ubiquitin can act as a targeting signal in the endo-lysosomal pathway may shed new light on this question (Reggiori and Pelham, 2002). Indeed, recent work showed that the GAT domain of

GGAs not only recognizes Arf-GTP but also acts as binding site for mono-ubiquitinated proteins. Binding of Arf to GGAs actually facilitates binding of the ubiquitinated protein to the adaptor (Shiba et al., 2004). The GGAs themselves are ubiquitinated and could thus participate in the complex network of ubiquitin-binding proteins responsible for formation of multivesicular bodies (Pelham, 2004). Thus, unlike APs, GGAs likely play a role not only in delivery of cargo to the endosome but also in its transfer to multivesicular bodies.

1.7 Molecular mechanisms for Arf6 regulated endocytosis

1.7.1 Arf6 displays unique properties

Arf6 is unique among Arfs in showing restricted distribution to endosomes and the PM. Most eukaryotes express a homologue of Arf6, and all have a predicted pI in the range of 8.5-9.5, significantly higher than the range of 6-7 predicted for other Arf isoforms. As a consequence, Arf6 has a net positive charge that is thought to play a role in its preferential association with the PM (Donaldson, 2003). A conserved signature di-peptide sequence (Glu-Ser) adjacent to the effector's binding site has been implicated in Arf6 recognition and likely plays a critical role in Arf6-specific function (Al-Awar et al., 2000).

1.7.2 Arf6 plays multiple roles at the PM

The first indication that Arf6 functions at the PM came from the observation that over-expression of an activated form of Arf6 generates protrusive structures at the cell surface (Radhakrishna et al., 1996). Subsequent work with either activated or GTP-binding defective mutants implicated Arf6 in a variety of PM-associated processes such as cell spreading, cell migration, wound healing and some forms of phagocytosis (for review, see (Donaldson, 2003)). Arf6 also localizes to endosomal membranes in many cell types and is required for a clathrin-independent form of endocytosis (Radhakrishna and Donaldson, 1997).

In contrast to the well-characterized regulation of Golgi coats by Arfs described in section 1.4.1 above, Arf6 does not exert it effects at the PM and endosome by regulating AP-2 and clathrin. Instead, Arf6 is involved in regulating membrane lipid composition

and cortical actin rearrangement. Specifically, Arf6-GTP activates PI4,P 5-kinase, the enzyme responsible for generating PI(4,5)P2. Arf6-GTP also activates PLD, which produces phosphatidic acid (PA), a known activator of PI4P 5-kinase. Phosphoinositides, PIP2 in particular, can then recruit and influence the activity of a variety of other factors. As discussed in 1.7.2 below, Arf6 also affects the actin regulators rho and rac through several classes of Arf6-specific GAPs.

1.7.3 Arf6 and remodeling of the actin cytoskeleton

By far the most striking and complex effects of Arf6 are on actin dynamics. Many of those effects arise indirectly through the activation of the rho GTPase rac (Franco et al., 1999). Further work identified several potential mechanisms for this cross-talk between Arfs and the cdc42/rac/rho subfamily. For example, Arfaptin-2/POR1 binds rac in either nucleotide-bound form but only associates with Arfs in the GTP-form. Upon activation, Arf6-GTP displaces rac, which is then freed for regulation of membrane ruffling (Tarricone et al., 2001). The effects of Arf6 on lipid composition can also modulate the dynamics of cortical actin, possibly synergistically with this rac activation. Increased PIP2 levels at the PM recruit a number of actin-binding proteins that regulate the actin network.

A second important mechanism for cross-talk comes from the observation that Arf6-GAPs serve both as Arf6 regulators and Arf6 effectors. As discussed in more detail in section 1.9 below, many of these proteins are multi-domain enzymes that include binding sites for rho GEF or display GAP activity for Rac and/or Rho. Arf6 activation in this case leads to the recruitment of Arf-GAPs to Arf6-GTP, which then act as scaffold organizing rho and rac activities.

1.7.4 Arf6 and membrane traffic

Cortical actin acts as a barrier to endocytosis and as mentioned above, Arf6 plays a key but indirect role in endocytosis by increasing actin dynamics to facilitate formation and movement of endocytic carriers. Similarly, Arf6-dependent activation of PI4P-5 kinase at the PM (Aikawa and Martin, 2003) or of PLD activity on dense core granules has also been shown to facilitate fusion (Bader et al., 2004). However, Arf6 has been

observed on specialized endocytic structures that contain PM proteins internalized independently of AP-2 and clathrin, and may therefore have more direct functions in endocytosis (for review, see (Donaldson, 2003)) Interestingly, whereas Arf6 activation is not required for entry of these proteins into Arf6-positive endosomes, its inactivation must occur for the subsequent sorting and recycling (Brown et al., 2001).

Several studies suggested that Arf6 also plays a direct role in desensitization and endocytosis of G-protein coupled receptors, or GPCRs (Hunzicker-Dunn et al., 2002). Most GPCRs do not internalize constitutively: upon ligand-binding and activation, these receptors are targeted by specific kinases, and subsequent phosphorylation of the receptor in turn recruits proteins of the arrestin family (Perry and Lefkowitz, 2002). Arrestins also interact with a large number of endocytic factors such as AP-2 and clathrin, and were shown to coordinate the subsequent internalization of GPCRs in a manner dependent on their ubiquitination and de-ubiquitination (Lefkowitz and Whalen, 2004). Early studies showed that the Arf-GEF ARNO forms a complex with arrestin that would also recruit Arf6 upon receptor activation (Claing, 2001). The presence of arrestin in the complex stimulated ARNO activity and provided a mechanism to couple receptor activation and Arf6-GTP production. An Arf6-targeted siRNA knockdown study recently confirmed that Arf6 was indeed required for endocytosis of several different GPCRs (Houndolo et al., 2005). However, the exact role of activated Arf6 in GPCR endocytosis remains unclear and may ultimately be limited to lipid remodeling.

1.8 The properties of Arfs

Mammals express six Arfs grouped in three classes based on sequence similarity (Boman and Kahn, 1995). The class I Arfs which include Arfs 1, 2 and 3 have been implicated in Golgi to ER recycling, intra-Golgi traffic and traffic from the TGN. These Arfs show greater than 95% sequence identity but likely have distinct function (Taylor et al., 1992). The class II Arfs which include Arfs 4 and 5 have remained largely uncharacterized; like class I Arfs, they localize primarily to the Golgi complex. Arf6 is the only class III Arf and is the most divergent. It localizes primarily to the endosomal compartment and has been implicated in endocytosis (D'Souza-Schorey et al., 1995), sub-cortical actin cytoskeleton rearrangement (Radhakrishna et al., 1996), and cell spreading

(Song et al., 1998). Interestingly, all six Arfs acquire co-translationally a myristate on an N-terminal glycine (Berger et al., 1995; Boman and Kahn, 1995). Mutations that prevent this modification abolish cellular Arf activity (Kahn et al., 1995).

Arfs differ from other small GTPases in that their GTP cycle correlates with membrane association (Bonifacino and Lippincott-Schwartz, 2003), independent of GDP-dissociation inhibitors. Crystal structures have been obtained initially for nucleotide-free Arf-Sec7 complex and recently for two GDP-bound intermediates that, remarkably, can be ordered to provide snapshots of a "3D movie" of the exchange reaction (Renault et al., 2003). While in the inactive GDP conformation Arfs localize primarily to the cytoplasm but can associate weakly with membranes through a myristoylated N-terminal amphipathic helix (Antonny et al., 1997). In absence of membranes, this amphipathic helix fits in a hydrophobic groove on the Arf core and acts as locking device that physically blocks a conformational change required to allow interaction with the GEF and release of the GDP (Pasqualato et al., 2002). Insertion of the helix in the membrane removes the lock and now permits the GEF–induced conformational change and GDP release. GTP binding locks in the conformational change, prevents re-docking of the helix on the Arf core and traps the activated Arf on the membrane.

The switch I and switch II regions of Arfs are responsible for interaction with regulators (GEFs and GAPs) as well as several of the Arf effectors (Liang et al., 1997). Crystal structures of GDP and GTPγS bound Arfs demonstrate that residues of the switch I and II responsible for effector and GAP interaction are almost completely conserved among Arfs (Goldberg, 1999). Interestingly, whereas these two regions adopt nearly identical conformations in the GTP-bound form of Arf1 and Arf6 they differ significantly in conformation when bound to GDP (Pasqualato et al., 2001). This may explain the differential activation of Arfs by specific exchange factors, but does not address the issue of specific interaction with effectors.

Arf activation is a highly regulated process involving not only GEFs and GAPs, but also cargo and effectors. It has been demonstrated that a variety of Arf effectors are capable of potentiating Arfs for activation, such that the extent of GTP binding in *in vitro* studies is significantly increased in the presence of effectors without affecting the rates of GTP binding or hydrolysis (Boman et al., 2000). Some effectors such as GGAs interact

with activated Arfs through the switch I and switch II regions and as a consequence compete with Arf-GAPs, prevent their action and maintain Arfs in an active state (Puertollano et al., 2001). Other Arf effectors such as coatomer interact with a different surface of activated Arf and actually increase GAP mediated GTP hydrolysis (Goldberg, 1999; Szafer et al., 2001). Cargo can further modulate Arf activation by interacting with and decreasing the rate of GAP mediated GTP hydrolysis (Lanoix et al., 2001).

1.9 The properties of the Arf-GAPs

Analysis of the human genome identified 16 genes encoding a characteristic GAP domain, which consists of a zinc-finger motif (Cukierman et al., 1995; Randazzo and Hirsch, 2004). Four of these encode proteins similar to Arf-GAP1, and can be distinguished by the location of the GAP domain at the immediate N-terminus and by the absence of a PH domain. Arf-GAP1 and Arf-GAP3, the smallest and best characterized GAPs, localize to the Golgi complex through distinct targeting signals in their C-terminal region (Aoe et al., 1999). Their function in cargo sorting as components of the COPI coat was discussed above in section 1.4.1. The other 2 Arf-GAPs in this group, called Git1 and Git2, are much larger, contain a paxillin binding site and multiple ankyrin repeats. They were first identified as interactors of G-protein coupled receptor kinases and current evidence indicates that their GAP activity critically regulates Arf6-GTP levels at the PM. Increased Arf6-GDP levels decrease endocytosis of G-protein coupled receptors by both limiting the amount of free arrestin and reducing production of PI4,5P2 that contributes to AP-2 recruitment (Bader et al., 2004).

The remaining twelve Arf-GAPs have internal GAP domains immediately preceded by a PH domain; they also contain various combinations of ankyrin repeats, and in some cases additional PH domains. These Arf-GAPs with Ankyrin repeats and PH domains, or A(X)AP, are sub-divided into four groups, depending on the presence of SH3 domains (ASAP), coiled-coiled domains (ACAP), GTP-binding protein-like domains (AGAP), or a Rho GAP domain (ARAP). Like Git1/2, these large multi-domain Arf-GAPs can be considered as scaffolds serving to assemble large protein complexes that contain regulators of both membrane traffic and the actin cytoskeleton.

The 16 Arf-GAPS clearly outnumber the 6 Arfs and for this reason are thought to have site- and Arf-specific functions. The PH domains of the various GAPs show slightly different specificities towards phospho-inositides, and several GAP domains also show specificity towards their Arf substrate. For example, Arf-GAP1 acts preferentially on class I Arfs *in vitro*. AGAP-1 shows even greater preference for Arf1 and its overexpression, like that of Arf-GAP1 causes dissolution of the Golgi complex, in agreement for the key role of Arf1 in Golgi traffic. On the other hand, several GAPs localize to the PM and their overexpression reduces intracellular levels of Arf6-GTP. This is clearly the case for Gits and ACAP1/2. The substrate specificities of ARAPs and ASAPs have not been resolved (for review see (Randazzo and Hirsch, 2004).

The presence of PH domains in most Arf-GAPs suggests lipids as regulators of GAP activity. This has been best described for ASAP1. The PH domain is essential for activity since its deletion yields a protein with less than 0.001% the activity of the wt protein. The presence of acidic lipids such as phosphatidic acid and PI(4,5)P2 stimulated 10,000 fold the activity of an ASAP-1 truncation containing the PH, GAP and ANK domains. Limited proteolysis experiments indicated that the lipid-induced increase in activity coincided with a conformational change. On this basis, Randazzo and colleagues propose that the PH domain acts as negative regulator that folds over the catalytic GAP domain and prevents access to the substrate. Binding of PIP2 to the PH domain leads to its dissociation from the GAP domain and consequent activation of the GAP (Kam et al., 2000). Lipids have more moderate effects on other Arf-GAPs.

Arf6 and its GAPs have been implicated in regulation of cytoskeletal structures such as focal adhesions and actin-rich membrane ruffles. Some of these effects clearly result from Arf6-dependent regulation of lipid composition and subsequent changes in membrane traffic (Randazzo and Hirsch, 2004). However, several of the Arf6 GAPs are large multi-domain proteins that act as scaffolds that coordinate the presence of activated Arf6 and a multitude of signaling molecules that more directly impact the actin cytoskeleton. For example, Gits have binding sites for both paxillin, a focal adhesion adaptor, and for PIX, an exchange factor for both rac and cdc42 (Turner et al., 2001). Similarly, ARAPs contain a second GAP domain with activity towards the actin regulators cdc42 and rhoA (Miura et al., 2002). ASAPs, on the other hand, interact

through their proline-rich domain with several tyrosine kinases involved in regulating turnover of focal adhesions (Randazzo and Hirsch, 2004).

1.10 THE PROPERTIES OF ARF-GEFS

1.10.1 Phylogenetic analysis identifies seven groups of sec7d proteins

Arf-GEFs are characterized by a central 200 amino acids (aa) Sec7 domain (Sec7d) that has been demonstrated both necessary and sufficient for promoting nucleotide exchange on Arfs (Chardin, 1996; Mansour et al., 1999). Subsequent structural and biochemical analysis identified a critical "glutamate finger" that inserts in the Arf nucleotide binding site and promotes dissociation of the tightly bound GDP nucleotide, thereby favoring the binding of the more abundant cellular GTP (Goldberg, 1998). Mutation of this glutamate to aspartate significantly reduces activity, while charge reversal mutation to a lysine completely abrogates GEF activity (Beraud-Dufour et al., 1998).

Extensive bio-informatics analysis of the fully sequenced genome of seven model organisms identified a total of 7 different families of Arf-GEFs (Cox et al., 2004). Only two of these families, the GBF1 (Gea1p/Gea2p) and BIGs (Sec7p), are present in all organisms. Plants and fungi express two unique families, while animal genomes encode 3 unique types that are called: Exchange factor for Arf6 (EFA6), Arf nucleotide opener (ARNO) and BFA resistant Arf-GEFs (BRAGs). The human genome encodes 13 distinct Sec7d containing proteins that can be separated into these five groups on the basis of domain organization and sequence similarity, as shown in Figure 1.2 and 1.3.

1.10.2 Properties of ARNOs

ARNOs (also called cytohesins) are a family of four 40kDa GEFs unique to metazoans. In addition to the canonical Sec7d, all ARNOs contain a coiled-coil domain at their N-terminus and a PH domain downstream of the Sec7d (see Fig 1.3). ARNOs are active on both class I and class II Arfs *in vitro* but activate preferentially Arf6 *in vivo* (Frank et al., 1998); (Macia et al., 2001). ARNOs are primarily cytosolic but can redistribute to the PM where they function in cytoskeletal dynamics (Frank et al., 1998) and cell spreading (Santy et al., 2001). Some studies involving very high levels of overexpression have

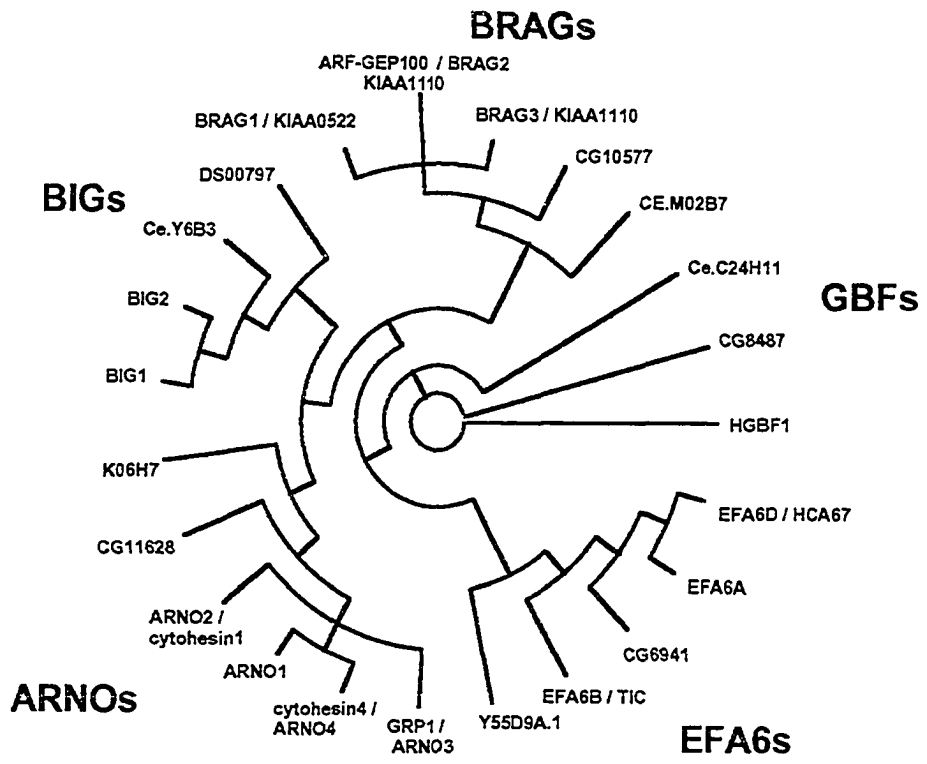

Figure 1.2 ***The BRAGs are a novel family of ARF GEFs***

Sec7 domain proteins present in the H. *sapiens*, C. *elegans* and D. *melanogaster* genomes were identified by BLASTp searches of genome specific databases as of January 2001. Maximal parsimony using PAUP of consensus alignments generated with SOAP (1.5) yielded 6 phylogenetic trees with similar distribution and of equal length. This demonstrated that there are 5 families of ARF-GEFs: The BIGs,GBFs, EFA6s, ARNOs and now the BRAGs.

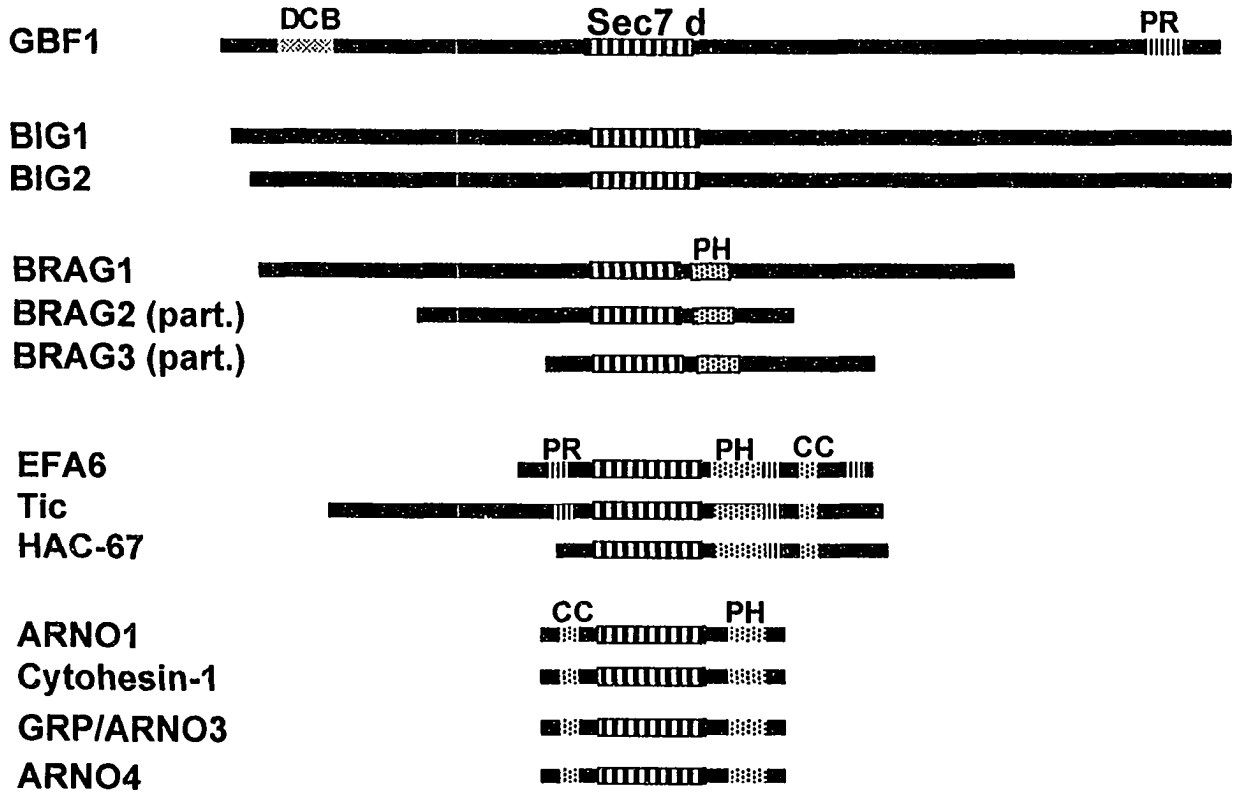

Figure 1.3 ***ARF-GEF families possess similar domain organization***

Each mammalian ARF-GEF possesses the cannonical sec7 domain. Other domains include the dimerization and cyclophillin binding domain (DCB), proline rich domains (PR), pleckstrin homology domains (PH) and the coiled coil domain. The ARF-GEFs have been grouped by family, yielding the GBFs, the BIGs, the BRAGs, the EFA6s and the ARNOs families, respectively.

implicated ARNO at the Golgi complex (Franco et al., 1998). The coiled-coil domain promotes dimerization (Chardin, 1996) and has also been implicated in cellular localization (Lee and Pohajdak, 2000).

Initial studies on ARNO1 (cytohesin 2) revealed that its PH domain regulates membrane association. Further work established that the PH domain contributes to PM association by binding selectively the PIP3 (PI3,4,5P) produced in response to receptor stimulation and subsequent PI3kinase activation (Klarlund et al., 1998). Two alternate splice variants of ARNO1, 3 and 4 mRNAs have since been described that differ by the presence of a 3 nt exon encoding a glycine within the PH domain (Ogasawara et al., 2000). Interestingly, the presence of this additional gly residue in one of the PIP interacting loop of the PH domain eliminates the specificity towards PI(3,4,5)P2 relative to PIP2 (Cullen and Chardin, 2000; Klarlund et al., 2000).

1.10.3 Properties of EFA6s

EFA6s consist of a family of three small metazoan-specific GEFs of approximately 60kDa. Whereas the expression of the related EFA6A and EFA6C is restricted to brain tissues, that of EFA6B appears ubiquitous (Derrien et al., 2002). In contrast to the primarily cytosolic ARNOs, EFA6s associate with membranes and localize at the plasma membrane / endosomal system (Franco et al., 1999). Furthermore, EFA6s are the only known GEFs to date that display no GTP exchange activity towards Arf1 *in vitro*, and shows instead strong activity on Arf6 (Franco et al., 1999). Like ARNOs, EFA6s contain a PH domain downstream of the sec7d, that appears sufficient to target to Arf6 and actin-rich membrane ruffles and microvilli structures at the PM (Derrien et al., 2002). The specificity of the PH domain of this class has not been reported. EFA6s contain a C-terminal coiled-coil domains that appear essential but whose function in dimerization has not been investigated in detail (Derrien et al., 2002).

1.10.4 Properties of BIGs

BIG1 was first identified from brain extracts through it ability to promote GTP-loading on purified Arfs (Morinaga et al., 1996). This activity co-purified with a 200 kDa protein, showed sensitivity to BFA and was therefore called BFA inhibited GEF, or

BIG (Morinaga et al., 1997). Subsequent cloning of BIG1 facilitated the identification of a second isoform, called BIG2, which co-purified with BIG1 in a large macro-molecular complex (Yamaji et al., 2000). BIGs are active on all 3 classes of Arfs (Morinaga et al., 1997); (Sata et al., 1998), and are the only mammalian family whose GEF activity shows clear inhibition *in vitro* by the uncompetitive inhibitor Brefeldin A (Mansour et al., 1999).

BIG1 and BIG2 are ubiquitously expressed proteins (Mansour et al., 1999) that localize to trans-most cisternae of the Golgi complex where they are thought to regulate recruitment of adaptors for the clathrin coat (Yamaji et al., 2000); (Zhao et al., 2002). Overexpression of Arf-GEFs can partially compensate for their inhibition by BFA. However, protection resulting from GEF overexpression appears selective. Not surprisingly, overexpression of BIG2 protects the clathrin coat from dissociation caused by BFA at the TGN but does not prevent BFA-induced release of COP1 from earlier Golgi compartments (Shinotsuka et al., 2002). Co-immunoprecipitation analysis using tagged forms of BIG1 and BIG2 established that greater than 75% of these two GEFs exist as heterodimers (Yamaji et al., 2000). However, pools of homodimers with unique function appear to exist, since under some conditions BIG1 and BIG2 localize to overlapping but distinct regions within the TGN (Melancon et al., 2004); (Shin et al., 2004).

1.10.5 Properties of GBF1

GBF1 was first identified by expression cloning for its ability to permit growth of transfected cells in the presence of BFA (Claude et al., 1999). The effect of over-expression appeared Golgi-specific and the new cDNA was thus called Golgi-specific BFA resistance factor. Mammals express a single GBF1 member but two isoforms are present in fungi (Gea1p and Gea2p) and plants express three related proteins called GNOM and GNOM-like 1 2 (GNL-1) and GNL-2. GBF1 is expressed ubiquitously (Mansour et al., 1998) and functions in early compartments of the Golgi complex where it regulates recruitment of the COP1 coat (Zhao et al., 2002); (Kawamoto et al., 2002). GBF1 is most active on Arf5 *in vitro* (Claude et al., 1999) but its over-expression was

shown to protect both class I and class II Arfs from BFA-induced dispersal in vivo (Kawamoto et al., 2002).

GBF1, like all other Arf-GEFs, likely functions as a dimer. The possibility that GNOM is a homodimer was first suggested by unusual allelic complementation between three classes of GNOM alleles (Busch et al., 1996). Subsequent characterization using a yeast two-hybrid assay confirmed that GNOM is a homodimer and established that the region responsible for dimerization is present at the N-terminus (residues 1 to 246), in the region encoded by the first exon (Grebe et al., 2000). This region is also able to bind cyclophilin-5, a protein with folding activity that may be important for regulation of GNOM dimerization and function. This dimerization and cyclophilin-binding, or DCB domain, is also found in Geas and GBF1 but its function in these proteins has not been confirmed. However, GBF1 and Geas likely function as dimers because other well-characterized Arf GEFs such as BIGs (Yamaji et al., 2000) and ARNOs (Chardin, 1996) clearly form dimers.

1.10.6 Properties of BRAGs

The BRAGs are the focus of my research and the current thesis. There are 3 human homologues, the most similar of which are BRAG1 and BRAG2 (also called ArfGEP100). While BRAG2 localizes to the endosomal compartment and is most active towards Arf6 (Someya et al., 2001), my research indicates that BRAG1 may localize to the cis-Golgi complex and is more active on class I than class II Arfs. The D. melanogaster genome encodes a single BRAG gene, called LONER, whose product has been implicated in muscle development and activation of Arf6 in the endosomal system (Chen et al., 2003). Furthermore, LONER appears to be a cytosolic protein whose proper localization requires the presence of the trans-membrane receptor Duf. Interestingly, the LONER gene yields three distinct splice variants with potentially tissue-specific function (Chen and Olson, 2004; Chen et al., 2003). Variable localization and Arf specificity is not observed in other families and may be considered a novel feature of this family.

Chapter 2

Materials and Methods

2.1 General DNA manipulation techniques

The following methodology was used in the generation of all DNA constructs, except where otherwise noted.

2.1.1 Primer design

Primers were generally designed to meet the following criteria: (1) a melting temperature (Tm) of 60°C ±5 °C (2) a GC content of approximately 50%, and if not possible, of similar value between the primer pairs; (3) inability to form stable homo or hetero-dimers as determined by Oligo-calculator on the integrated DNA technologies (IDT) website (http://scitools.idtdna.com/Analyzer/). I further rejected any primer pairs for which approximately 3 of the 5 terminal residues are complementary, with special emphasis on the 3' most nucleotide; (4) absence of low complexity sequences such as poly-n tracts, especially near the 3' ends of primers, as this is the location of polymerization. (5) a length of 20-30 nucleotides. Restriction sites were often engineered into the 5' ends of primers to facilitate directional cloning of the fragment, often in a specific translational frame (N-and C-tagging). Additional nucleotides were usually included at the 5' end to increase the efficiency of subsequent cleavage with restriction enzymes. The number of additional nucleotides used was based on information provided in the reference appendix of the New England Biolabs (NEB) catalogue which lists the efficiency of cleavage close to the end of DNA fragments as a function of the length of overhangs. These additional nucleotides were chosen to be homologous to the gene sequence.

2.1.2 PCR reactions

The number of cycles was initially set at 25-30, but was further optimized after the yield of the first set of reactions was determined. The annealing temperature was usually chosen to be between 5-10°C below the Tm for the primers. Because we have a Robo-cycler, which allows the simultaneous use of multiple annealing temperatures, I often chose the Tm as the highest annealing temperature, with several lower temperature conditions as well. This allowed me to determine the most specific and productive

conditions. Primers were used at a final concentration of 0.2pmol/μl, and 0.75μl of enzyme was used per 50μl reaction.

After the last reaction cycle, one tenth of each sample was analyzed on an analytical agarose gel. Following analysis, the remainder of productive reactions was purified on Qiaex PCR purification columns. In cases when amplification reactions performed at multiple temperatures gave moderate but clean products, I would often load all reactions on the same column. This would concentrate the otherwise dilute PCR products.

2.1.3 Subcloning

The DNA of interest usually consisted of Qiagen mini-/maxi-prep DNA, or Polymerase Chain Reaction (PCR products). In most cases, DNA fragments were cloned directionally into the vector of interest using a pair of non-complementary restriction sites at the two ends. Whenever possible, the restriction enzyme pair was chosen so that both enzymes were active under similar incubation conditions. This allowed simultaneous digestion with both restriction enzymes, and eliminated the need to purify DNA fragments between digests. When intermediate purification of digested fragments was required, the restriction reaction was subjected to standard phenol:chloroform purification followed by ethanol precipitation.

Generally, 1μg of vector and insert were digested and half the products were separated on a low melting agarose gel and recovered using Sigma GenElute MINUS EtBr SPIN COLUMNS (cat# 5-6501) or Qiagen Qiaex II Gel Extraction Kit (cat no. 20021). One tenth of each DNA preparation was run a standard analytical agarose gel, and the relative concentrations of vector and insert were estimated based on ethidium fluorescence following staining and illumination on a UV light box. Ligation reactions were then assembled so that the vector to insert ratio (mol : mol) were either 1:1 or 1:3 (where "1 part" is usually 1μL)

To recover plasmids, the ligation reactions were electroporated into TOP10 or DH5α *E. coli* and one tenth of the bacteria was plated. DNA was extracted from overnight cultures using Qiagen miniprep kit, and was subjected to a diagnostic digest (most often using the

enzymes which were used in the original insertion). Where noted, the resulting clones were sequenced.

2.2 Kazusa Institute clones

The KIAA0522, KIAA0763 and KIAA1110 clones were obtained from the Kazusa Institute. cDNA synthesis from human brain polyA RNA was initiated with a Not1 oligo dT primer and the resulting cDNAs were repaired and ligated with a SalI adapter at the 5' end prior to insertion into the SalI – NotI site of pBluescript2 SK+. Initial analysis at the Kazusa Institute revealed interruption of the ORF that suggested a potential problem with the original KIAA1110 cDNA, clone hh04831b. Further analysis by RT-PCR confirmed the presence of several mistakes in clone hh04831b (http://www.kazusa.or.jp/huge/full/goal/hh/hh04831bmrp1/w3open/compare.html). Although the correct sequence is now available, an intact cDNA has not yet been reconstructed.

2.3 Construction of prokaryotic expression vectors for BRAG truncations

The overall strategy for recombinant expression of truncations containing the Sec7 domain of BRAG1 and BRAG2 is described in Chapter 3. The first set of truncation was amplified using the KIAA0522For – KIAA0522Rev and KIAA0763For-KIAA0763Rev primer pairs (see Table 2.1). Coded within the primers were an EcoRI site at the N-terminus and an XhoI site at the C-terminus. KIAA0522 and KIAA0763 were each amplified with the appropriate primers, digested with EcoRI and XhoI. The KIAA0522For primer was abandoned once I realized that the BRAG1 ORF contains 2 EcoRI sites. I therefore re-ordered the KIAA0522For primer, this time with a BamH1 site in place of the EcoR1 site. This new primer was named 0522R0.

The KIAA0522R0-KIAA0522 fragment was amplified by PCR and the fragment was inserted into pCEP4 at the BamH1-Xho1 sites. This "R0" construct was then induced in *E. coli*-BL21DE3 as described in chapter 2, and purified on GST-agarose beads. This fragment was then tested for GEF activity on Arf5.

The KIAA0763 fragment was ligated into pGEX4-t-1 exhaustively digested with

Table 2.1

Primer name	Enzyme	Primer sequence	Tm
KIAA0522for:	EcoRI	5'- tgg **aat tca** acc tgt gca agc aga ctt acc agc ggg aga c–3'	67
KIAA0522 rev:	XhoI	5'- tgt tgc **tcg agg** act ttt cgc tcc cca ggt act gc –3'	69
KIAA0763 for:	EcoRI	5'– tgg **aat tca** agc tca gca agc aga cct aac aca agg agg c –3'	66
KIAA0763 rev:	XhoI	5'- tgt tgc **tcg agg** gtg aat ttc ttc cgg tct tga ggg ttg gg – 3'	64
0522F2:	BamHI	5'- gag **gga tcc** gag agc tcc agc aat tcc aat gag ac –3'	59
0522R2:	XhoI	5'- acc tgc **tcg aga** tgg tca tcg ttg gtc cgc agt tc –3'	62
0522R3:	XhoI	5'- asc **gac tcg agg** ctg tta cgc cgc ccc cgc ttg –3'	70
0763F2:	EcoRI	5'- acg **aat tca** aca gca cgt cca act cca acg ata cc –3'	62
0763R2:	XhoI	5'- acc tgc **tcg aga** tgg tcc tca ttg gtc ttt agc tc –3'	57
0763R3:	XhoI	5'- ctg **tac tcg agc** gag ttc ttc ttc ttc tgg aag at –3'	54
FATG (for pCEP4-N1):	KpnI	5'- cgc **cgg tac** cga ggc ggg gtc ggg g –3'	62
FUTR (for pCEP4-N1):	KpnI	5'- tcc **ggg tac** ccg gca gcc tca gct cct gct –3'	65
Rstop:	XhoI	5'- ctg ttc **ctc gag** tca ctc tct cca ttc atc aga cca cg –3'	60
R2St:	XhoI	5'- agg tcc **ctc gag** tgt ggc tcc cca gac ttt cct –3'	61
B1RaceF1:		5'- cgt gga gta cct gct gga gct gaa –3'	76
B1RaceR1:		5'- cgc cga ata gcc cgc ttc ctt ct –3'	74
B1RaceR2:		5'- gcc ggg act gga gct cct gga t –3'	74
B3RaceR1:		5'- cgt gac gtc ccg gaa agc cat ca –3'	74
B3RaceR2:		5'- gta gcg cgg cag gct cag gat ca –3'	76
B1Race R3:		5'- tgg tac tgg ctc tcg cgg ccc ggg cta t –3'	71
B1RaceR4:		5'- ccg ggc cgc ctg gtg gaa ctg gct ct –3'	73
B1RaceF2:		5'- cgggatccgagagcccaaatcgggccgt –3'	70
B1RaceR5:		5'- gc tga ccc tgg ctc ctc aga cat –3'	74
B1RaceR6:		5'- atc cag gta gag ggg aag atc act g –3'	76
B1RaceR7:		5'- tga tgg cac tgg tgg agg aac tg –3'	72
B2RaceR1:		5'- cag tgt gca ggc tgc ggc agt tga –3'	78
B2RaceR2:		5'- gac atc act gta cga ggc cgt cat –3'	74
B2RaceR3:		5'- agg ggg cga cag ctc ctc ctc atc –3'	80
RP12-5UTR:	KpnI	5'- agg agg **gta** ccc ttc tag gga agg gct ggg ga –3'	61
RP18-5UTR:	KpnI	5'- agg agg **gta** cca ggg aag ggc tgg gga gga –3'	63
RclaI:		5'- gac atg ggc cct gac ggg tgg ca –3'	68
Gtag-5ATG:		5'- cca gag gta ccg agc ccc ccg gga gga gca gc –3'	70
B1R3RT:		5'- ctc tcc aca gac ctg cag gac aag –3'	61
PH-NorFor:		5'- ccc ctc gtg gaa atg cac atg –3'	60
PH-NorRev:		5'- gga tgt aaa gcg cag ccg gtc –3'	62
RP18-NorFor:		5'- agg gaa ggg ctg ggg agg agg –3'	66
RP18-NorRev:		5'- ctg ctg ctc ctc ccg ggg ggc t –3'	71

5cDNAFor:		5'- gga ggg tgg cgc cgt gag aga –3'	67
5cDNARev:		5'- tca gct cca gca ggt act cca cg -3	64
BRAG1-FLAGfor:	KpnI	5'- aaa **ggt acc** cag gcc ctg cat gcc cag tat tgc –3'	66
BRAG1-FLAGrev-5t0-r:	XhoI	5'- aaa aaa **ctc gag** tda cgg ccg ctt gtc gtc gtc atc ctt gta gtc ctc tct cca ttc atc aga cca cgg tgc -3'	64
BRAG1-unFLAG-rev:	XhoI	5'- aaa aaa **ctc gag** tca ctc tct cca ttc atc aga cca cgg tgc –3'	64
StopNorFor:		5'- gaa ttc cca tcc cca ctg ctg t –3'	60
StopNorRev:		5'- agg ttc caa gct cca agc tcc a –3'	61

the same enzymes. This construct encodes a protein of expected size 63 kDa (GST + 37,204 Da). Several colonies were obtained, none of the clones showed reproducible induction of the recombinant protein, and therefore were not analyzed further.

Following the failure of the first set of BRAG1 and BRAG2 truncations, new forward and reverse primers were developed. In particular, the EcoRI site in the 0522For was replaced with a BamHI site at the 5'end of a new forward primer (0522F2) for the KIAA0522 truncation. The new forward primer (0763F2) for the KIAA0763 truncation retained the EcoR1 site. Two new reverse primers were also designed for each truncations (see Fig 3.1 for relative position). The resulting clones from the 0522F2 – KIAA0522Rev, 0522R2 and 0522R3 amplifications of KIAA0522 have been named 5r1, 5r2 and 5r3, respectively. The chimeric proteins encoded by these constructs were expected to have masses of 63 kDa (GST + 41,408 Da), 55 kDa (GST + 28, 588 Da) and 78 kDa (GST +52,475 Da), respectively. The clones obtained from the KIAA0763F2 – KIAAO763rev, 0763R2 and 0763R3 were named 7r1, 7r2 and 7r3, respectively.. The chimeric proteins encoded by these constructs were expected to have masses of 70 kDa (GST + 44,136 Da), 54 kDa (GST + 28,579 Da) and 63 kDa (GST +37,578 Da), respectively.

2.4 General methods for protein analysis

To rapidly analyze recombinant protein expression, I inoculated and grew small cultures overnight. The next morning, cultures were diluted one in three into fresh LB broth, and incubated for one hour prior to induction with 0.4mM IPTG for one hour. Cells were recovered by centrifugation in a microfuge, and then resuspended and boiled in sample buffer for analysis on a 10% poly-acrylamide gel (Laemmli and Eiserling, 1968). The relative mobility of recombinant proteins was estimated by comparison with commercial molecular weight standards (Broad range standards, BD Biosciences) analyzed in parallel.

For protein isolation, I first inoculated 2 ml of LB broth that were used following overnight growth, for inoculation of larger cultures by dilution in the range of 1/500 to 1/1000. Cells were then grown to a density of $O.D._{600}$ of 0.4-0.6, and induced by further culture for 2-4 hours in the presence of 0.4mM IPTG. Cells were recovered by

centrifugation at 5,000g for 5 minutes at 4°C, washed in PBS, resuspended in 1/10 volume of wet cell mass and disrupted in French Press. The resulting lysates were adjusted to 0.1% Tween-20 to increase solubility and then cleared by centrifugation at 20,000g for 20 minutes at 4°C. For isolation of glutathione S-transferase (GST)– tagged proteins, the cleared lysates were incubated by mixing end over end for 12-16 hours at 4°C with glutathione-agarose beads (BioRad) equilibrated in PBS containing 10 mM beta-mercapto-ethanol. Beads were recovered and washed by repeated centrifugation at 500g for 5 min.

I tested two methods for releasing GST-tagged proteins from the glutathione-agarose beads. The standard method involves competing the interaction of GST with the beads though addition of excess free glutathione. The other method, in theory more selective, involves cleavage of the linker between the GST and KIAA0522 by virtue of an engineered thrombin cleavage site. Several attempts at recovering protein 5r1 by this method showed very poor yields (<10% release from beads) and no improvement in purity over the simpler glutathione elution method. Two separate attempts to improve thrombin cleavage yields by addition of hirudin, a known thrombin enhancer, were unsuccessful.

In the end, I chose to elute proteins by sequential incubation with PBS containing increasing concentrations of glutathione in the range of 5-100 mM. Eluates were flash-frozen and stored at –80°C. Where indicated, proteins retained on GA-beads were released by boiling in a volume of SDS sample buffer equivalent to that used for elution.

2.5 Purification of 5r0 construct

5r0 and mock-transfected E.coli were analyzed for expression as described above. The mock transfected *E. coli* showed no specific increase in protein levels with IPTG induction, but the 5r0 transfected *E. coli* reproducibly expressed a new protein of the expected size, 63 kDa.

When the 5r0 bacterial lysates were cleared of insoluble material by centrifugation there was a considerable loss of recombinant protein, suggesting that the majority this protein may be insoluble (Fig 2.1). When these cleared lysates were incubated with glutathione beads, there was binding and elution of several proteins from

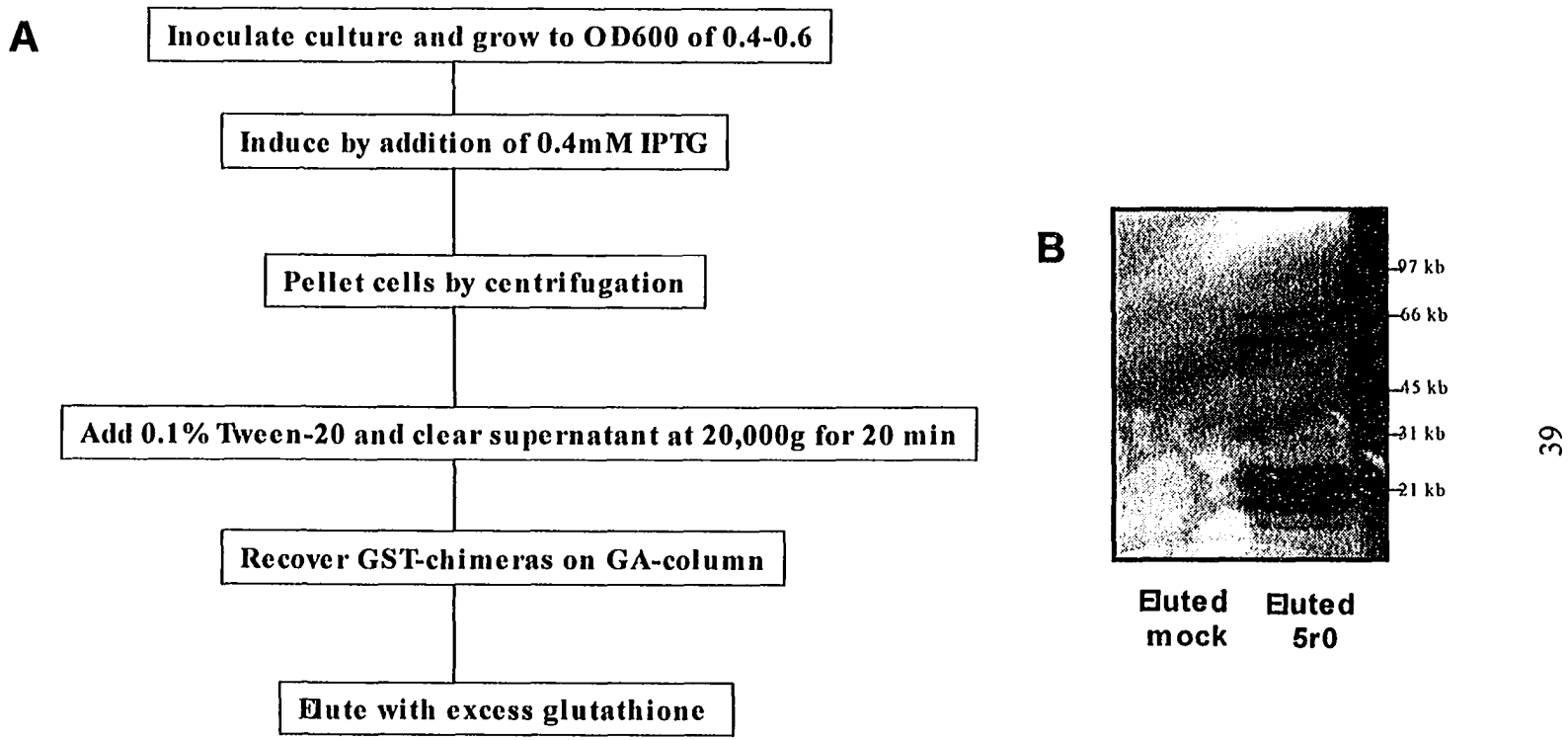

Figure 2.1 ***Purified 5r0 is suited for biochemical analysis***

Panel A. Flowchart of procedure for expression and isolation of GST-BRAG chimeras. For details see the text.

Panel B. The 5r0 fusion protein was purified from low speed supernatants of E.coli lysates using glutathione-agarose beads. Eluted product was visualized by SDS-PAGE and compared to elution from mock-transformed lysates.

the 5r0 expressing lysates. In contrast, no proteins were bound from lysates of mock-transfected cells (Fig 2.1). This suggests that multiple proteins are made from the transcript, there has been proteolysis or several E.coli proteins bind to the recombinant protein of interest.

Preliminary studies established that most contaminants on the beads could be released by extensive washing with 5-7 volumes of PBS. Serial elutions with wash buffer containing 5mM, 10mM and 15mM glutathione released the majority of bound proteins because very little is left on the beads after elution. This method yielded a 5r0 preparation with several bands migrating around the size expected of 63 kDa (GST + 38,500 kDa) and a 70kDa protein as a contaminant (Fig 2.1). According to GST purification manual the 70kDa band is likely a chaperone which can be selectively eluted / removed from a sample by washing with an ATP containing buffer. This preparation was then tested in a standard GTP exchange reaction for GDP release on Arf5.

2.6 Purification of R1, R2 and R3 constructs of KIAA0522

E. coli transformed with the three new KIAA0522 constructs, 5r1, 5r2 and 5r3, all expressed new recombinant proteins of the expected size:67 kDa, 54 kDa and 78 kDa, respectively (Fig. 2.2A). Sec7 domain truncation 5r2 accumulated in *E. coli* BL21DE3 to the highest level, while the 5r1 and 5r3 constructs were only moderately overexpressed (Fig 2.2A).

When incubated with glutathione beads, the three KIAA0522-sec7 domain constructs bound GA-beads with varying efficiency. The 5r1 truncation bound the GA-beads weakly and for this reason was not further purified and assayed for GTP exchange activity. Both the 5r2 and 5r3 constructs bound efficiently to GA-beads and could be recovered by elution with glutathione.

A number of low molecular weight products in the 30 kDa range co-purified with the 5r2 and 5r3 fractions (Fig 2.2A). Although these contaminants did not interfere with preliminary analysis in the GEF assay, we chose to obtain a more highly purified preparation for the detailed biochemical analysis described in Chapter 3. Batch binding experiments first established the BRAG1 sec7 domain truncation bound cationic resins such as FastFlow-S under salt concentrations as high as 100 mM KCl. In contrast, most

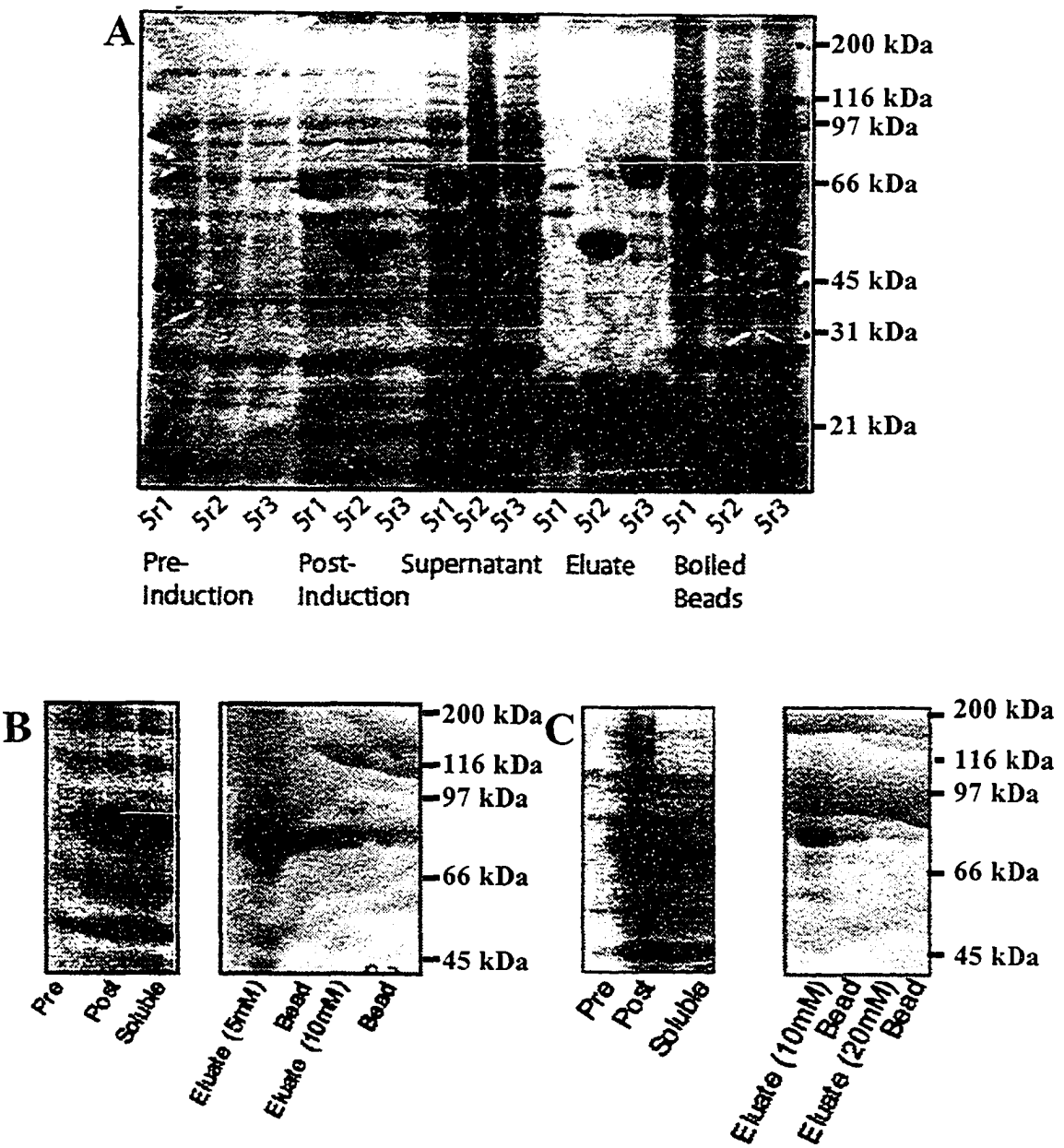

Figure 2.2 ***Expression and purification of the KIAA-522 and KIAA0763 chimeras***

Panel A. SDS-PAGE analysis of intermediate fractions obtained during the isolation of GST-chimeras containing three different truncations of KIAA0522. (see diagram in Figure 2.1)

Panel B and C. SDS-PAGE analysis of intermediate fractions of the 7R2 and 7R3 chimeras containing truncations of KIAA0763. Shown are equivalent amounts of pre-induction, post-induction, and soluble post induction samples. Elution profiles for 7r2 and 7r3 suggest that 5mM glutathione is acceptable for elution of 7r2 and 10mM elution is sufficient for elution of 7r3.

contaminant were recovered in the flow through fraction. For large scale purification, eluates from the GA beads were loaded on a 1 ml Mono-S column equilibrated in phosphate buffer (pH 7) containing 100 mM KCl. After extensive washing with loading buffer, the BRAG1 Sec7d was eluted a with step gradient containing 350 mM KCl. Fractions containing BRAG1 were identified by SDS-PAGE electrophoresis, pooled and stored as aliquots at –80°C.

2.7 Purification of R1, R2 and R3 constructs of KIAA0763

E. coli transformed with the two new KIAA0763 constructs 7r2 and 7r3 expressed new recombinant proteins of the expected size:73 kDa and 81 kDa, respectively. Several preliminary experiments with *E. coli* BL21DE3 transformed with the 7r2 and 7r3 constructs established that induction with 0.4mM IPTG at 37°C yielded the best expression. Both of these constructs are highly expressed, with a considerable fraction of recombinant protein remaining soluble after a 10, 000xg spin (Fig 2.2B,C). The 7r2 truncation bound GA-beads well under all conditions, while the 7r3 construct bound more poorly under similar conditions. Elution with glutathione yielded final protein preparations that were >90% pure (see Fig 2.2).

These preparations were tested in a standard GTP exchange reaction for GTP exchange on Arf5.

2.8 GTP exchange assays

GTP exchange assays were performed as previously described by Mansour, Claude and colleagues (Mansour et al., 1999); (Claude et al., 1999). Briefly, a pre-mix was assembled that contained sufficient amounts of salts and buffers to yield final concentrations of 50 mM HEPES (pH 7.5) / 100 mM KCl / 1 mM $MgCl_2$ / 1 mM DTT. Also added was the GEF of interest, sonicated azolectin vesicles (1.5 mg/ml), GTPγS (40 μM containing radioactive [^{35}S]GTPγS) and the volume is adjusted with water. The assay begins when the appropriate amount of Arf is added to give a final volume 50-100 μl.

Reactions were initiated by adding the appropriate ARF. This is because the ARF will begin to load GTPγS as soon as it is available. Reactions were performed at 30 °C

rather than 37 °C since unpublished experiments established that GTP loading occurs more slowly but to greater extent at this reduced temperature.

Time points were taken by removing (typically) 15-20 µl of a 100µl reaction, and diluting into 2ml of ice cold stop buffer (50mM HEPES (pH 7.5) / 100mM KCl / 10mM $MgCl_2$). At the end of the reaction, the 2mL samples are filtered through pre-wetted 0.45µm MF membrane filters (Millipore, cat# HAWP02500) to trap protein and bound nucleotides. Filters are then washed twice with 2ml of ice cold stop buffer and dried under a heat lamp. The extent of radioactivity trapped on each filter was determined using a Beckman-Coulter (model LS 6500) multi-purpose liquid scintillation counter.

2.9 Calculating adjusted GEF values

The raw data obtained from each reaction must be corrected to obtain the number of moles of GTP exchange on Arfs in GEF-dependent manner. Background values that must be determined and used for correction include the amount of filter trapped GTP when reactions contain (1) buffer without proteins; (2) GEF alone = (GEF - buffer) and (3) Arf alone = (Arf – buffer). To calculate the extent of GEF-dependent exchange on Arf in a typical incubation I used the following equation to correct the raw value:

GTP exchange = Value - buffer – (GEF-buffer) – (Arf-buffer)

or, following rearrangement

GTP exchange = Value – GEF - Arf + buffer

To calculate the number of moles of GTP exchanged above background, this value is then divided by the specific activity of GTPγS in the reaction.

2.10 Construction of eukaryotic expression vectors for BRAG1

To allow for expression of the cDNA in mammalian cells, BRAG1 was first subcloned into the Invitrogen vector pCEP4. This vector was chosen because a strong cytomegalovirus promoter drives transcription of the cloned cDNA. Furthermore, this plasmid can be used to generate stable lines at high frequency since it contains the Epstein-Barr virus origin of replication and can be readily maintained as an episome in cells expressing the EBNA-1 protein.

Because the pCEP4 vector does not provide an initiating ATG, the first one within the cloned cDNA is used. Therefore there was no concern as to the reading frame of the inserted fragment. As illustrated in Fig 2.3, the KIAA0522 cDNA was directionally sub-cloned into the KpnI-NotI sites of pCEP4. These sites were chosen because they are present in the multiple cloning site of both pBluescript2 and pCEP4, and are absent from KIAA0522. The resulting plasmid was termed BRAG1-pCEP4. The sequence of the cDNA was not confirmed by sequencing but subsequent experiments demonstrated that it encoded a protein of 63kDa.

2.11 Tagging of BRAG1 at N-terminus with VSV-G epitope

Our first attempt at constructing an epitope-tagged form of BRAG1 took advantage of a derivative of pCEP4 generated by Dr. Sam Mansour by insertion of an oligo in the KpnI-XbaI MCS (p-CEP4-N1). The additional sequence encodes a short peptide segment derived from the C-terminus of the VSV-G protein (G-tag) in-frame with an initiating methionine. Several restriction sites located downstream allowed insertion of a coding sequence to produce of N-terminally tagged form of the protein of interest. Because there were no convenient, unique restriction sites at the 5'end of KIAA0522, I chose to amplify the entire coding region of BRAG1 by PCR using primers containing restriction sites suitable for insertion into pCEP4-N1 (see Table 2.1). The amplified region encodes an ORF that starts at the first residue after the initiation AUG and ends immediately after the first in-frame stop codon of the cDNA. This initiating methionine was omitted from the G-tagged vector to avoid alternate initiation of translation.

As indicated in Fig 2.3, the forward primer FATG introduced a KpnI site at the 5'end and the reverse primer RSTOP an XhoI at the 3'end (see Table 2.1). The PCR reaction yielded a product of the expected size (1487 bp) that was purified and ligated into pCEP4-N1 using standard methods. A single clone, called G-BRAG1-pCEP4, was sequenced from the 5'end. The insertion was in frame, without errors over the region sequenced. This plasmid drives production of a protein of the expected size (163kDa kDa) in transfected cells (see Fig 4.3C).

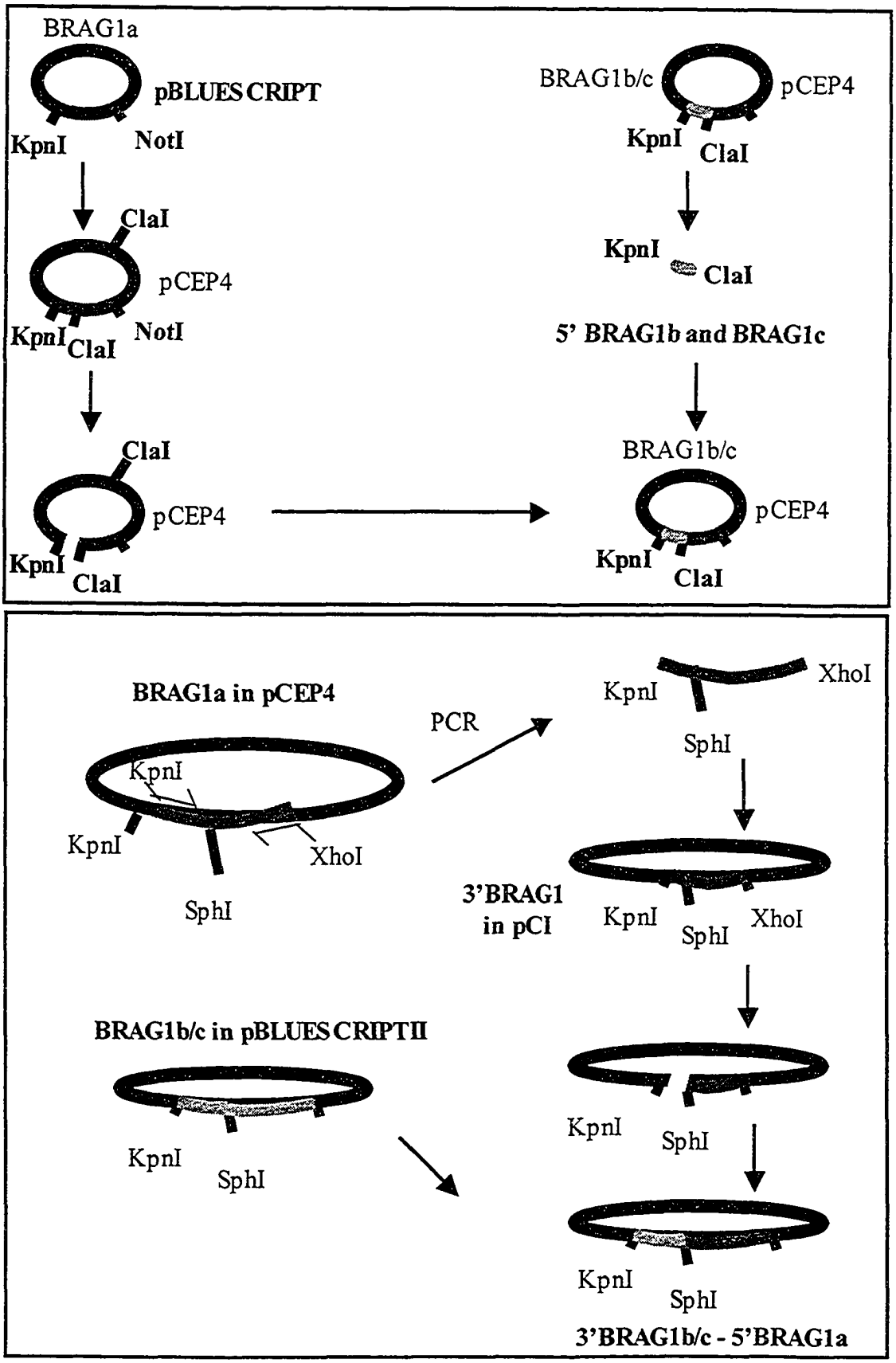

Figure 2.3 ***Construction of expression vectors for BRAG1 encoding cDNAs***

2.12 Synthesis and cloning of 5' RACE products

To estimate the amount of cells required for mRNA isolation and cDNA synthesis, I took advantage of manufacturer's recommendations. The Oligotex manual suggested that extraction from cultured cells yield 3-6μg of mRNA per $1x10^7$ cells (I used the lower value for calculations), and the Qiashredder manual suggested that a 10cm plate will yield 2.1-4.2μg of mRNA at 90% confluency. I concluded that a single 10cm plate of HEK 293 would yield enough RNA for several reactions with the Generacer kit, which requires 50-250ng of mRNA per reaction.

RNA was isolated from sub-confluent cultured HEK293. The cells were trypsinized, spun down and resuspended in Qiagen buffer OL1 (lysis buffer). The cells were then lysed according to the Qiashredder (cat #79654) protocol and poly mRNA was isolated using Qiagen Oligotex Direct mRNA Mini Kit. I used 2 μl of the isolated mRNA (estimate 200ng based on typical yield) of this product for each of the Generacer "libraries" generated. First strand synthesis was performed using either random hexamers (RP library), or a combination of the 3 reverse primers KIAA0522 rev, 0522R2, 0522R3 used in the construction of plasmids encoding the 5r1, 5r2 and 5r3 Sec7 domain truncations of BRAG1 (Gene Specific Primed, or GSP library). HeLa total RNA provided with the kit was reverse transcribed with random hexamers and amplified with β-actin primers as a positive control. 5'-RACE was performed using the Invitrogen Generacer™ kit as per manufacturer's instructions. Products from reactions yielding high molecular weight species were cloned using the Zero Blunt® TOPO® PCR Cloning Kit provided with the 5'RACE kit.
The following regime was used for 5'RACE of BRAGs 1, 2 and 3.

Temperature	Time	Cycles
94	2 min	1
94	30 sec	5
72	2.5 min	
94	30 sec	5
70	2.5 min	
94	30 sec	30
65	30 sec	
72	2.5 min	
72	10 min	1

The DNA was amplified using the Expand High Fidelity PCR kit (cat# 03300242001). Reactions were typically 50µl of which 1µl was template. The primers were all used at 10 pM (final) except the Generacer 5' primer, which was used at 3x the standard concentration (as suggested).

2.13 Assembly of full-length cDNAs containing the alternate 5' ends of RP12 and RP18

To determine if the RP12 and RP18 splice variants of BRAG1 have distinct localization or function, I chose to assemble full-length cDNAs by substituting the alternate 5' ends present in the RP12 and RP18 RACE products for those present in the KIAA-0522 cDNA. Construction of cDNAs encoding tagged and untagged forms of BRAG1b and BRAG1c involved sub-cloning the RP12 and RP18 sequences into either the BRAG1-pCEP4 or G-BRAG1-pCEP4 plasmids described above (Fig 2.3).

The RP12 and RP18 clones share a 993 bp sequence with KIAA0522 at their 3' ends which contain a ClaI site that could be used for this construction. KIAA0522 contains an additional Cla1 site that is not cleaved when plasmid DNA is prepared from a bacterial, strain capable of methylation (TOP10, dam+, dcm+). The RP12 and RP18 regions were amplified by PCR from the TOPO-RP12 and TOPO-RP18 clones using a forward primer that introduced a KpnI site at the 5' end. The untagged RP12 and RP18

sequences include the 5' UTR of each sequence, in case this region was important for mRNA stability or localization. The purified RP12/RP18 PCR products and the G-BRAG1-pCEP4 vector were digested to completion with KpnI. After phenol:chloroform purification the inserts were digested to completion with ClaI.

Preparation of the vector turned out to be more problematic. pCEP4 is a very large vector (14kb) which includes a single ClaI site, thereby necessitating partial digests for RP12 and RP18 insertion. The purified G-BRAG1-pCEP4 vector was digested to completion with KpnI. After phenol : chloroform purification the vector was subjected to a partial ClaI digest for several time points. The products were then run on a Low Melting Point (LMP) gel and well-resolved species of appropriate size were extracted. These vector and inserts were ligated, yielding G-BRAG1b-pCEP4 and G-BRAG1c-pCEP4.

This cloning of partial digests proved to be much more difficult than originally imagined. Therefore I added an intermediate cloning step, in which the BRAG1b and BRAG1c termini were substituted into the KIAA0522 clone. This vector harbors an appropriate KpnI site, and lacks the extraneous ClaI site. These chimeric cDNAs were then sub-cloned into pCEP4 using the unique KpnI and NotI sites yielding BRAG1b-pCEP4 and BRAG1c-pCEP4.

These procedures yielded two pCEP4 constructs, with or without a G-tag, for each of BRAG1a, BRAG1b and BRAG1c. Of these 6 clones I have only sequenced the 5' end of untagged BRAG1c. The first 620nt of this clone are without mistake.

2.14 Construction of vectors for regulated expression of FLAG-tagged forms of BRAG1a, BRAG1b and BRAG1c

To overcome the low transfection efficiency, potential cytotoxicity and mis-localization problems encountered with the G-BRAG1-pCEP4 plasmids, I chose to construct new vectors based on pcDNA 5/TO (Invitrogen). These expression vectors are significantly smaller than pCEP4 (5.6 kb vs 10.4 kb) and harbor a promoter containing multiple copies of the Tet operator that allows regulation of transcription by addition of either tetracycline or its stable analog, doxycycline. The smaller vector size should yield

higher transfection rates while the ability to regulate expression should allow us to select expression levels and overcome cytotoxicity.

To overcome problems related to tagging the N-terminus with the G epitope, we switched to the FLAG epitope and chose to append the tag at the C-terminus. The FLAG epitope is relatively small, and can be recognized by several well-characterized and commercially available antibodies; interestingly, some of these are sensitive to Ca^{+2} levels and could be used at a later stage in co-immunoprecipitation experiments to identify BRAG interactants. Tagging at the C-terminus may avoid disrupting targeting signals, which in the case of BIG1 and cytohesin1 appear to be present at the N-terminus (Lee and Pohajdak, 2000; Mansour et al., 1999)

The construction was performed in three stages. In the first stage, I used PCR to amplify a short 670 nt segment with a forward primer located slightly upstream of a unique Sph1 site in the coding region near the 3'end and a reverse primer located at the stop codon. This PCR product was then cloned in vector pCI using Kpn1 and Xho1 sites engineered during amplification at the 5' and 3' ends, respectively. pCI was chosen for this purpose because unlike pCEP4 and p5/TO it lacks a Sph1 site. In the second stage, the 5' end of the BRAG1 cDNAs was inserted in front of the PCR product within pCI using the unique Sph1 site. In the final stage, the 3'end-modified BRAG1 cDNAs were moved into pcDNA 5/TO using flanking Kpn1 and Xho1 sites. This approach produced modified BRAG1 cDNAs with only a short stretch at the 3'end derived from PCR amplification. As such there would be little BRAG1 to be sequenced for PCR mistakes.

PCR was performed on BRAG1a-pCEP4 under standard conditions using forward primer BRAG1-FLAGfor and either BRAG1-FLAGrev-5t0-r or BRAG1-unFLAG-rev as reverse primers. The forward and reverse primers contained Kpn1 and Xho1 sites, respectively, to facilitate subsequent manipulations of the DNA fragment (see Table 2.1). The reverse primer BRAG1-FLAGrev-5t0-r contained in addition the sequence coding for the FLAG epitope (sequence: DYKDDDDK, as is used in the pCAL-n-FLAG vector) in frame with the last codon of BRAG1. Note that this procedure removes the extensive 3' UTR from both the tagged and non-tagged fragments. The PCR products were isolated, exhaustively digested with KpnI and XhoI and ligated into vector pCI within its unique KpnI and XhoI sites. Plasmids 3'-BRAG1-FLAG-pCI and 3'-BRAG1-pCI

containing PCR products with or without the FLAG epitope were recovered. This construct cannot be used for mammalian expression because the cDNA is in the wrong orientation.

To assemble a complete cDNA, the 936 nt fragment encoding the 5'end of BRAG1a was isolated from an exhaustive digest of KIAA0522 with Kpn1 and Sph1. Corresponding fragments for BRAG1b and BRAG1c were obtained from similar digests of BRAG1b and BRAG1c – pCEP4. Those fragments were inserted into (3'-BRAG1-pCI) DNA and (3'-BRAG1-FLAG)-pCI DNA cleaved with KpnI and SphI. From these ligations, I recovered full length tagged and untagged versions BRAG1b and BRAG1c, which were subsequently transferred to p5/TO. An undergraduate student in our lab, Chris Smith has since confirmed the sequence at the 5' and 3' ends of the BRAG1b and BRAG1c inserts of both tagged and untagged forms in p5/TO. I have not yet recovered p5/TO vectors containing the tagged and untagged form of BRAG1a. Therefore, the BRAG1a FLAG-tagged constructs will have to be isolated to determine the function of the multiple 5' variants of BRAG1.

2.15 Northern blot analysis

Three probes were designed for the northern blot analysis of BRAG1 expression. The design and target of these probes within the BRAG1 mRNA is discussed in more detail in Chapter 4. The probes were generated by PCR using the following primer – DNA combinations and PCR conditions:

PH-probe: PH-NorFor and PH-NorRev on KIAA0522

BRAG1a-probe: 5cDNAFor and 5cDNARev on KIAA0522

BRAG1b/c probe: RP18-NorFor and RP18-NorRev on BRAG1c in pCEP4

These 3 reactions were initially optimized for annealing temperature using the RoboCycler's gradient feature. All 3 probes could be specifically amplified under the conditions outlined in the table below using cold dNTPs. As expected, the products of the amplifications of probes selective for the PH-domain, BRAG1a and BRAG1b/c were 147nt, 112 and 150 nucleotides, respectively.

Temperature	Time	Cycles
94°C	2 mins	1
94°C	30 secs	25
60°C	45 secs	
72°C	1 min	
72°C	10 mins	1

Radioactive probes were generated by replacing the 0.2 mM dCTP with 0.2 mM (3000Ci/mmol [α^{32}P] dCTP). The probes were purified using a Qiaquick PCR purification kit, as instructed by the manufacturer (cat# 28104). To ensure that unincorporated nucleotides were removed, I washed the columns with wash buffer twice instead of the recommended single wash. The amounts of purified radiolabeled PCR products were measured by analyzing a small aliquot in a liquid scintillation counter. The radioactive probes had the following activities: PH-probe: 157, 000 CPM/μL; BRAG1a-probe: 206, 000 CPM/μL; BRAG1b/c probe: 188, 000 CPM/μL; Actin: 402, 000 CPM/μL. The actin probe was generated using random hexamers, at 4 times the concentration of the other primers.

The MTN manual suggests using $2x10^6$ CPM / mL of blotting buffer. Because I was blotting in 5mL of Express Hyb, a total of $1x10^7$ CPM worth of probe were used for each blotting experiment. The blot was probed at 68°C for 1.5 hours, as suggested by the manufacturer.

Each of the wash was performed with 10x the blotting volume, or 50mL of appropriate buffer, as listed in the MTN manual. The wash with solution 1 was performed at room temperature as suggested by the manufacturer. Over the course of this 40 minute wash the buffer was changed 4 times. The wash with solution 2 was incubated at 50°C as suggested by the manufacturer, with 2 changes of buffer. At the end of the washes, the blot was wrapped twice in Saran Wrap™, exposed to PhosphorImager plate (Storm; Molecular Dynamics) and resolved on a Storm-840 PhosphorImager from Molecular Dynamics. The exposure times for the pictures are as follows: PH-probe: 50 hrs; BRAG1a-probe: 53 hrs; BRAG1b/c probe: 48 hrs; Actin: 48 hrs.

The blot was stripped by incubation in 0.5% SDS at 90-100°C for 10 minutes. The blot was then exposed for 24 hours, to ensure that the probe has been successfully removed.

2.16 INDIRECT IMMUNO-FLUORESCENCE

Most experiments were performed with cells grown on coverslips within in a 6 well plate. Media was aspirated and the cells were washed twice with 2ml of PBS pre-warmed of 37°C. To prevent redistribution of proteins prior to fixation, the wash procedure was performed as quickly as possible.

2.16.1 Acetone-methanol fixation

Washed cells were covered with 5 ml of 1:1 methanol : acetone from a bottle kept in a freezer at –20°C. The solvent was removed after 5 min. incubation at room temperature and the cells were washed twice with 2 ml/well of PBS. Cells were blocked in preparation for immuno-staining by incubation with PBS containing 0.2% gelatin *(PBS-g) three times for 5 minutes each.

2.16.2 Parafomaldehyde fixation

Washed cells were fixed by adding to each well 1.5 ml of 3% paraformaldehyde solution. After a 15 min. incubation at room temperature, each coverslip was washed three times with 2 ml of PBS and finally incubated for ten min. with 2 mL of a 50mM NH4Cl solution prepared in PBS buffer to quench any remaining cross-liker. The cells were then washed quickly wash 3 times with PBS + 0.2% gelatin (PBS-g) prior to permeabilization with 2 ml of 0.1% TX-100 in PBS. As before, the cells were blocked in preparation for immuno-staining by incubation three times with PBS containing 0.2% gelatin for 5 minutes each.

2.16.3 *bis* (sulfosuccinamidyl) suberate (BS^3) fixation

Each coverslip was dropped into individual 50 ml falcon tubes containing pre-cooled 1:1 acetone-methanol and put back in a -20°C freezer. After a minimum of thirty min., each coverslip was removed from the solvent, drained of excess solvent by blotting

a corner on a paper towel, and then held vertically in a stream of air until dry. To re-hydrate, the coverslip was laid face-up and covered with 500 µl of PBSO (PBS + 0.1% n-octyl-β-D-glucopyranoside) containing 17.4 mg / ml of the cross-linker *bis* (sulfosuccinamidyl) suberate (BS^3). After three rapid washes with 500µl of PBSO, excess cross-linker was quenched for 15 min. with 500 µl of 1M Tris pH 7.0. The cells were blocked in preparation for immuno-staining by incubation for 1 hour with PBS containing 1% gelatin and 1% nonfat milk.

2.16.4 Immuno-staining

To minimize the amount of antibodies required for staining, incubations were performed by inverting coverslips onto a 75µl drop deposited onto a sheet of parafilm. Antibodies were diluted in PBS-0.2% gelatin and first incubation usually lasted 1 hour. Coverslips were removed from the parafilm after "floating" them on top of 400µl of PBS-g gently transferred under the coverslips. Coverslips were returned to the 6 well plate, and washed a total of three times for 5 minutes each at room temperature. To stain with the secondary antibody, coverslips were again transferred face-down onto 75µl of PBS-g with an appropriate dilution of secondary antibody (usually alexa495 or 594 for green and red channels respectively). Following a 45 minutes to 1 hour incubation, coverslips were removed as before and washed three times with PBS-g, at room temperature, for 5 minutes each time. This was followed by a final wash in PBS lacking gelatin. Coverslips were mounted face down on a drop of 1x PBS containing 80% vol : vol glycerol and 1 mg/ml antifading agent.

Chapter 3:

Biochemical characterization:
KIAA0522 and KIAA0763 define a new family of BFA-resistant Arf-GEFs

3.1 Introduction

Bio-statistical analysis of fully sequenced genomes identified several new genes encoding Sec7 d proteins. To identify closest relatives, BLASTp searches were performed with each of the cDNAs listed in column 1 of Table 3.1. The absolute values of the exponents of E-values obtained for each pairwise comparison are tabulated. This analysis yielded 5 groupings (Table 3.1), a result that was confirmed by phylogenetic analysis (Fig. 1.2) and comparison of domain organization (Fig. 1.3). Three human cDNAs KIAA0522, KIAA0763 and KIAA1110 form a novel family of ARF-GEFs. In characterizing these cDNAs, several questions must be asked. Do these ARF-GEFs possess measurable GEF activity *in vitro*? If so, to which ARFs are they specific? Is this activity sensitive or resistant to the fungal toxin Brefeldin A?

3.2 Design of GST-chimeras with Sec7d of BRAG1 and BRAG2

To demonstrate that the translated products of these genes encode *bona fide* Arf-GEFs it is essential to obtain sufficiently large quantities of protein for biochemical analysis. We chose *E. coli* as a host for the overexpression of recombinant protein. Because E.coli expression systems are not able to efficiently translate larger proteins it is unlikely that we would be able to produce full length KIAA0522 or KIAA0763, which are predicted to be 169.6 kDa and 108.5 kDa, respectively.

I chose to generate Sec7d truncations from each of these two longest cDNAs, KIAA0522 and KIAA0763 (Fig 3.1). This approach has been used successfully by P. Chardin and S. Mansour to demonstrate that the Sec7d of ARNO and BIG1/p200 are sufficient to catalyze GDP release on Arf1 (Franco et al., 1996; Mansour et al., 1999). Further work demonstrated that truncations containing the Sec7d of EFA6 and ARNO retained not only GEF activity but also their respective substrate specificities (Chardin, 1996); (Macia et al., 2001)).

Table 3.1 ***Pairwise comparison of E - values suggest the BRAGs define a novel family of GEFs*** [A]

	0522	0763	1110	Dros	C.E.	Monkey	Arab	Aco 2	BIG 1	BIG 2	sec7	cyto 1	cyto2	cyto3	cyto4	rat cyto	Gnom	GBF1	GEA 1	GEA 2	C24h11	EFA 6
0522	∞	∞	133	113	61	60	38	37	33	30	30	29	31	29	27	29	26	25	18	17	16	12
0763	∞	∞	143	122	62	66	40	38	33	31	30	33	35	33	29	34	27	26	19	18	16	14
1110	133	144	∞	102	56	119	38	37	31	30	29	32	33	32	26	32	27	25	18	16	16	15
Monkey	66	73	121	45	15	∞	24	23	22	20	18	23	25	25	20	23	18	17	11	11	10	5
Drosoph	124	131	108	∞	76	45	38	36	35	32	31	38	37	35	32	38	27	27	20	22	24	15
Elegans	66	66	61	76	∞	15	29	29	21	20	22	23	23	23	20	24	19	16	21	17	13	13
Arabidops	42	45	42	38	28	23	[illegible]	[illegible]	[illegible]	[illegible]	[illegible]	49	51	50	46	51	84	55	30	32	44	24
Aco2 (elegans)	42	43	41	36	28	23	[illegible]	[illegible]	[illegible]	[illegible]	[illegible]	50	52	51	45	51	91	60	30	31	44	24
BIG 1	37	38	35	35	21	21	[illegible]	[illegible]	[illegible]	[illegible]	[illegible]	49	46	47	44	49	53	55	25	29	41	17
BIG2	29	31	29	29	18	19	[illegible]	[illegible]	[illegible]	[illegible]	[illegible]	43	38	40	37	43	57	60	19	23	40	10
sec7	34	35	32	31	22	17	[illegible]	[illegible]	[illegible]	[illegible]	[illegible]	42	43	40	37	42	49	40	29	30	27	21
cyto1	35	39	37	40	24	23	50	51	50	49	42	∞	∞	∞	162	∞	38	35	25	25	29	25
cyto2	36	41	38	39	23	25	52	53	47	44	43	∞	∞	∞	166	∞	37	34	23	23	25	23
cyto3	34	39	37	36	23	25	51	52	48	46	41	∞	∞	∞	168	∞	38	36	24	23	26	25
cyto4	32	34	31	33	20	20	46	45	45	42	38	162	166	173	∞	164	33	32	25	24	22	19
rat cyto	35	39	38	40	24	23	52	51	50	49	43	∞	∞	∞	164	∞	38	35	26	27	29	26
Gnom	29	31	30	27	19	17	85	89	65	64	47	37	36	38	33	37	∞	95	51	63	112	22
GBF1	29	31	29	26	15	16	52	58	53	60	39	34	33	35	30	34	92	∞	44	41	∞	18
GEA1	23	24	23	20	20	10	31	31	25	24	29	25	22	24	25	26	50	41	∞	∞	53	11
GEA2	23	23	21	22	17	10	31	31	27	26	30	25	22	22	23	26	63	43	∞	∞	63	12
C24h11 (elegans)	20	20	21	24	12	10	41	42	42	45	25	28	24	25	21	29	108	∞	44	35	∞	14
EFA6	15	16	19	15	13	5	23	24	17	15	21	25	23	25	19	25	22	21	12	13	14	∞

[A] BLASTp searches were performed with each of the cDNAs listed in column 1. Tabulated are the absolute values of the exponents of E-values for each obtained for each pairwise comparison. Greater values represent a greater degree of similarity. ∞ represents an E - value of 0 . Recognized families of genes are represented as similarily coloured number boxes. Red = family X, Blue = BIG family, Purple = cytohesin family Orange = GEA family.

3.2.1 Choice of N-and C- termini for Sec7d truncations

To determine the activity, specificity and BFA sensitivity of KIAA0522 and KIAA0763, truncated cDNAs encoding the Sec7d fused to glutathione-S-transferase (GST) were generated for each putative Arf-GEF (Fig 3.1). Selection of the C-terminus was intended to maximize proper folding and solubility of each product. Terminal stretches of hydrophobic residues are particularly unfavorable because they have been observed to promote aggregation. Because the N-terminal portion of the protein is GST, I expected no solubility problems related to the choice of the N-terminus of the Sec7d.

The N-terminus was chosen to contain a region corresponding to what is known as the Homology Upstream of Sec7d (HUS) box, as defined by Mansour (Mansour et al., 1999). This short amino acid stretch first identified in BIG1 is highly conserved amongst Arf-GEFs and therefore may play an important role for GDP release (Mouratou et al., 2005). Unfortunately I was unable to identify sequences encoding a HUS box in either KIAA0522 or KIAA0763. I therefore chose the N-termini of the chimeras based on similar distance upstream of the motif 1 region of the sec7d of BIG1. The BIG1 HUS box is 120 amino acids upstream of the switch 1, which itself is a stretch of 29 amino acid residues Mansour (Mansour et al., 1999).

3.2.2 GST-fusion protein purification

Two methods are generally used to elute GST fusion proteins from glutathione agarose (GA) beads: competition with free glutathione or thrombin proteolysis. The first method uses a thrombin cleavage site, which had been engineered between the MCS and the GST domain. When thrombin is added to GA-beads with bound protein it is expected that thrombin will release the recombinant protein while GST remains bound to the beads. This method provides an extra level of specificity as only proteins bound to the GA-beads with a thrombin cleavage site should be released. As such, most bound contaminants should remain on the GA-beads. This method is not suitable for proteins with exposed thrombin cleavage sites as these will be cleaved as well.

The second method for removing GST-fusion proteins from the GA-beads involves competing the interaction between immobile glutathione to GST with soluble

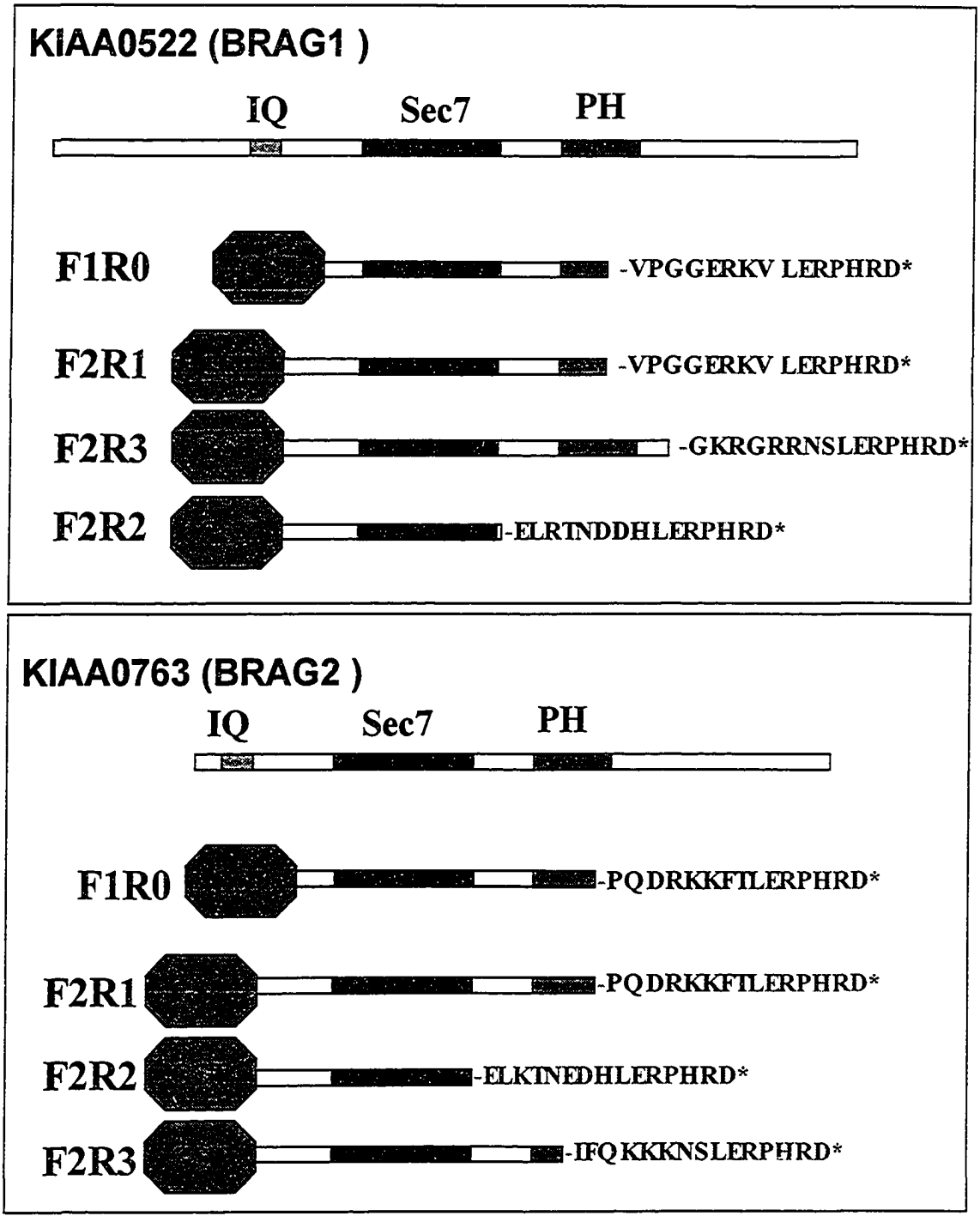

Figure 3.1 ***The KIAA0522 and KIAA0763 Sec7 domain GST-chimeras have hydrophilic termini***

Multiple truncations of BRAG1 (top panel) and BRAG2 (lower panel) were generated by PCR using various combinations of forward and reverse primers (see Table 2.1). PCR products were inserted in pGEX4 to produce GST fusion proteins for biochemical analysis. Black lettering represents terminal BRAG1 sequence, grey lettering represents sequence derived from the vector and * is a stop codon.

glutathione. This is the easiest method for eluting proteins. As described in section 2.4, this was the approach used to purify all GST-chimeras.

3.2.3 Purification of KIAA0522-r0 and KIAA0763-r0

Expression in *E. coli*, and the subsequent purification were optimized for the KIAA0522-r0 construct, abbreviated as 5r0 (see Materials and Methods in Chapter 2). The purified product is very clean with a major band at about 66kDa and a minor band at 70kDa (Fig 2.1b). According to the GST purification manual this 70kDa band is a chaperone which can be selectively eluted / removed from a sample by washing with an ATP containing buffer. Because the overall yield and purity of this preparation were sufficient, it was tested in a standard GTP exchange reaction for GDP release on Arf5.

The KIAA0763-r0 product, or 7r0, was mostly insoluble with roughly <10% of induced protein remaining soluble after a 10, 000g spin for 5min. Several separate isolates harboring this construct were tested for expression and I was never able to reproduce the induction of this clone or any 7r0 clones.

3.2.4 GTP exchange reactions

In a standard GTP-exchange reaction, we incubate myristoylated GDP-Arf, GEF, azolectin vesicles and excess GTPγ[^{35}S] in a physiological buffer (see section 2.8). An active GEF will promote the release of GDP from the Arf, then allowing the apo-Arf to bind GTPγS. At the end of the incubation, the samples are filtered through a nitrocellulose filter that binds proteins, and the amount of bound radioactivity is then quantitated by scintillation counting. To determine the level of loading of GTP on Arfs that is GEF-dependent, the raw data obtained must be further processed to account for self-loading of GTPγS onto Arf and for nonspecific binding of nucleotides to the GEF and/or the filter. Further details of the correction procedure are described in section 2.9. For all experiments described below, I will present the raw and processed data on the left and right side, respectively. This is exemplified in the GTP exchange reaction of KIAA0522-5r0.

3.2.5 KIAA0522-5r0 is inactive on Arf5.

Graphing the raw data from this GTP-exchange assay gives the impression that there has been loading of Arf5 by both the ARNO control and 5r0 (Fig. 3.2A). Once the total values of Arf5 loaded are corrected for GEF-independent GTP binding (see section 2.9 for details), we see a different picture (3.2B). Where it seemed that ARNO and 5r0 had similar levels of GTP loading in figure 3.2A, we also see that the background binding of radio-labeled GTPγS to the 5r0 preparation is much higher than the ARNO preparation. When the values are corrected for background it is evident that the purified 5r0 has no exchange activity for Arf5 (3.2B). The ARNO control had weak Arf-GEF activity, with 0.75pmol of enzyme loading 2pmol of Arf5 after a 20 minute incubation. This represents a 2.7 fold excess of substrate loaded over enzyme (3.2B). Because of the poor results with each of the two initial GST-fusion proteins, a new set of truncations was constructed (Fig. 3.1).

3.2.6 Design of alternate sec7d truncations

The 5' ends of the Sec7d-encoding truncations of KIAA0522 and 0763 were expanded using a new forward primer (F2) to include more upstream sequences such that the HUS box is not missed (Fig. 3.1). Analysis of the original C-terminus for 5r0 demonstrated that this end is situated in the middle of the PH domain. As this region may be vital for phospho-inositide binding, having a partial domain may not have been the best choice. I therefore designed the new truncations of KIAA0522 to include either all, or none of the PH domain.

To ensure that I was not pursuing a poor rational for choice of C-termini, I designed the new KIAA0763 C-termini such that one truncation would be longer than the original, and one would be shorter.

3.2.7 Protein expression / purification

The three new KIAA0522 truncations, 5r1, 5r2 and 5r3 were all expressed in E.coli (Fig. 2.2A). The 5r2 construct was expressed in *E. coli* while the 5r1 and 5r3 constructs were moderately overexpressed (Fig 2.2A).

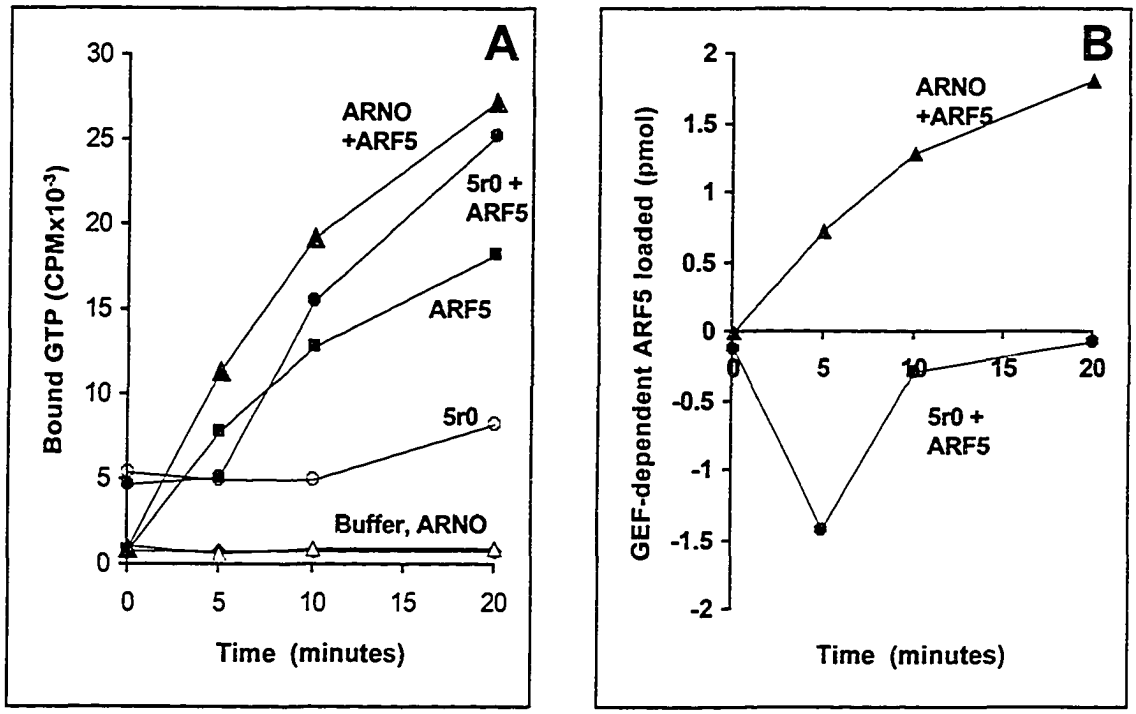

Figure 3.2 ***The KIAA0522-R0 construct is an inactive ARF-GEF***

Panel A. Recombinant 5R0 and ARNO were assayed at the same final concentration in the standard Arf-GTP exchange assay described in section 2.8 . 5R0 and ARNO promote retention of similar levels of GTP on nitrocellulose filters.
Panel B. Raw data from panel A was corrected to determine the extent of GTP binding on Arf5. The graph reveals that ARNO is active on ARF5 while 5R0 is not.

When incubated with glutathione beads, the three KIAA0522-sec7 domain constructs bound GA-beads with varying efficiency. The 5r1 preparation had a very weak affinity for the GA-beads and for this reason was not purified and assayed for GTP exchange activity. Both the 5r2 and 5r3 constructs bound efficiently to the GA-beads. A number of low molecular weight products co-purified with the 5r2 and 5r3 fractions (Fig 2.2A).

The 7r2 and 7r3 constructs were expressed in *E. coli* BL21DE3 and purified on GA-beads (Fig 2.2 B & C). Both of these constructs are highly expressed, with a considerable fraction of recombinant protein remaining soluble after a 10, 000xg spin. The final 7r2 eluate (10mM glutathione) was >90% pure while the 7r3 preparation (10mM glutathione) was about 70% pure.

3.3 Screening the KIAA0522 and KIAA0763 constructs for GTP exchange activity

Concentrations for each of the protein preparations were estimated based on Coomassie stained gels. While I was unable to determine the absolute concentrations of each preparation, I was able to ensure that roughly equal amounts of enzyme were added to each reaction. Recombinantly expressed BIG1-sec7d was used as a positive control for GTP exchange. This construct was previously characterized by Mansour *et al* (Mansour et al., 1999).

The protein preparations were tested in a standard GTP exchange reaction using Arf5 as a substrate (Fig 3.3). The most active preparation tested was the 5r3 truncation of KIAA0522, loading a total of 5 pmol of myr-Arf5 after a 10-minute incubation. The 7r3 construct loaded 1 pmol of myr-Arf5. The Sec7d of BIG 1 loaded 2.1 pmol of myr-Arf5. It is interesting to note that BRAG1-5r3 is the most active construct and the only one with a complete PH domain (Fig. 3.1). Because the 5r3 construct of KIAA0522 has proven the most active of my constructs, I decided to focus my direction on this, the longest cDNA of the family. In collaboration with Heather Vandertol-Vanier, I scaled up production of the 5r3 truncation of KIAA0522 and optimized the purification procedure to remove contaminants (see section 2.6 in Chapter 2 for details).

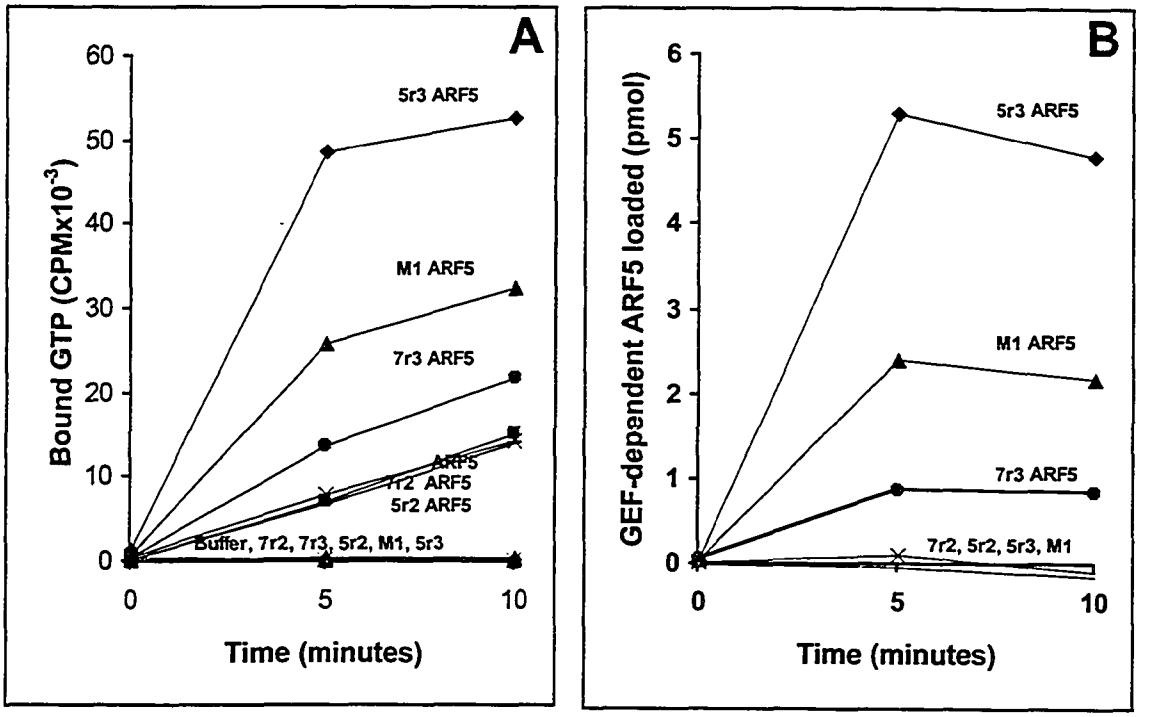

Figure 3.3 ***The 5r3 and 7r3 constructs are active ARF-GEFs***

Panel A. Raw data obtained from Arf-GEF assays of the four GST-chimeras containing the Sec7domain and PH domains of either KIAA0522 (5R2 and 5R3) or KIAA0763 (7R2 and 7R3). A previously characterized chimera containing the Sec7 domain of BIG1 (M1) was used as a positive control.
Panel B. The raw data shown in panel A was processed to reveal GEF-dependent GTP exchange on Arf5. Only the BRAG1 5r3 and BRAG2 7r3 chimeras display clear ARF-GEF activity.

3.4 CATALYTIC PROPERTIES 5R3

Quantitative studies demonstrate that the FPLC purified 5r3 (Fig. 2.3 panels A & B) was able to load 1.9pmol of myr-Arf5 in a standard GTP exchange reaction, using 1μM Arf5 and 50nM 5r3 (Fig. 3.4). This represents a 20-fold excess of substrate loaded over enzyme, demonstrating that the enzyme acts catalytically. Furthermore, Fig 3.5 (panels C & D) shows that an increase in enzyme levels leads to a proportional increase in the amount of GTP exchange on Arfs since 50nM enzyme loaded 5.7pmol of Arf5, which is roughly 2.5x as much Arf5 as was loaded in reactions containing 20nM 5r3.

In addition to demonstrating that KIAA0522 is an active Arf-GEF, it is also essential that we determine its substrate specificity. Because the three classes of Arfs act at different stages in the exocytic pathway, substrate specificity might provide clues to the *in vivo* role of KIAA0522. When tested comparatively against class I, class II and class III Arfs, there is greater activity on myr-Arf3/1 than myr-Arf5 (Fig. 3.5). 5r3is also active on myr-ARF6 (Fig. 3.6), but because of poor overall loading by both 5r3 and the positive ARNO control it is difficult to draw any conclusions. If these data were reliable it would suggest that 5r3 is more active than ARNO on Arf6.

3.5 BFA RESISTANCE OF BRAG1 GEF ACTIVITY

Brefeldin A is a toxic metabolite produced by *Penicillium brefeldinium*. It is an uncompetitive inhibitor of the brefeldin A Inhibited Arf GEFs (or BIGs). This means that the toxin does not compete with substrate / enzyme for an active site or binding site. Instead the toxin locks the substrate and enzyme into a non-productive complex. In this scenario the ternary complex consists of Arf-GDP, GEF and BFA.

Arf-GEFs are divided into 2 groups, based on sensitivity to this drug. Several groups have performed mutagenesis studies to determine which residues are vital to BFA sensitivity or resistance (Fig. 3.7). A number of residues have been identified in the Sec7d of ySec7p (Sata et al., 1999) and Gea1p (Peyroche et al., 1999), which are able to convert a BFA sensitive Arf-GEF to a BFA resistant Arf-GEF.

The mechanism for this sensitivity or resistance has recently been elucidated further through the crystal structure of Arf-GDP bound to GEF and BFA (Renault et al., 2003). As a whole those studies strongly suggest that the BRAGs should be BFA

resistant (Fig. 3.7). As predicted by analysis of the primary sequence of KIAA0522 and the crystal structure (Fig. 3.7) the GEF activity of 5r3 on Arf5 is resistant to BFA under conditions where BIG1 is completely inhibited (Fig. 3.8). As such I have named this family the Brefeldin A Resistant Arf-GEFs (BRAGs). cDNAs KIAA0522, KIAA0763 and KIAA1110 from the Kazusa Institute have been named BRAG1, BRAG2 and BRAG3, respectively.

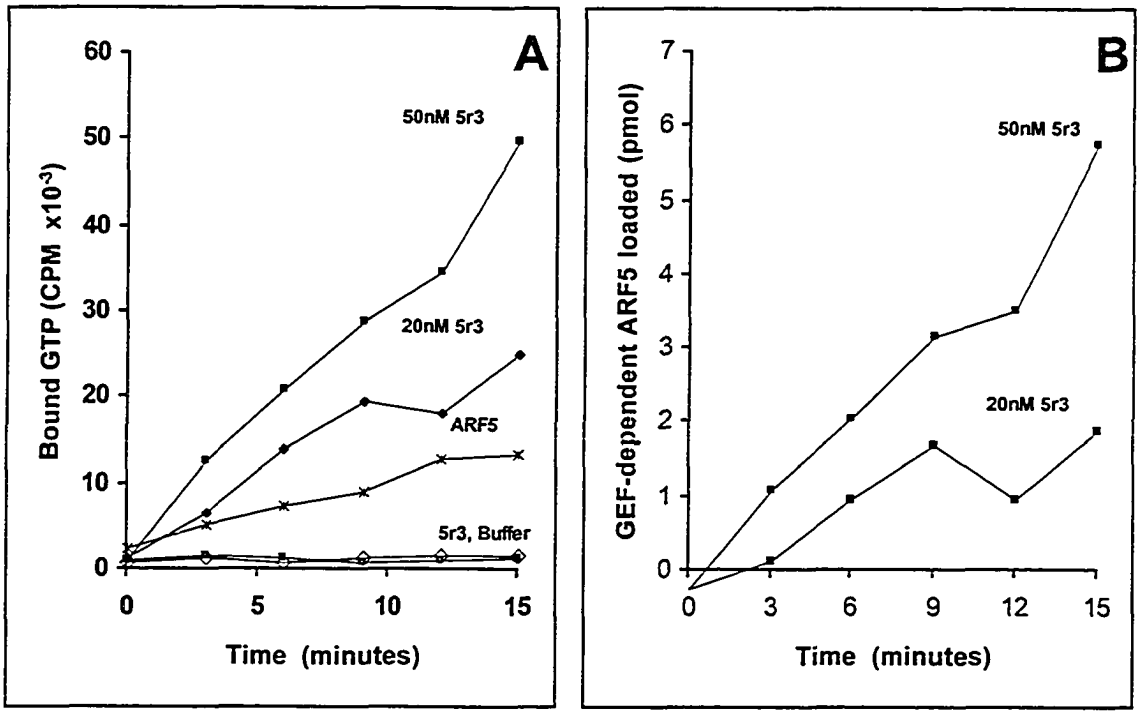

Figure 3.4 *The BRAG1-5r3 construct acts catalytically*

Panel A. Raw data obtained from Arf-GEF assays of BRAG1 5r3 performed at 20nM and 50nM enzyme concentrations. About 2.5 times as much GTP remains filter-bound when using 50nM rather than 20 nM enzyme.
Panel B. Corrected data from panel A also shows increased GEF activity when increasing enzyme concentration.

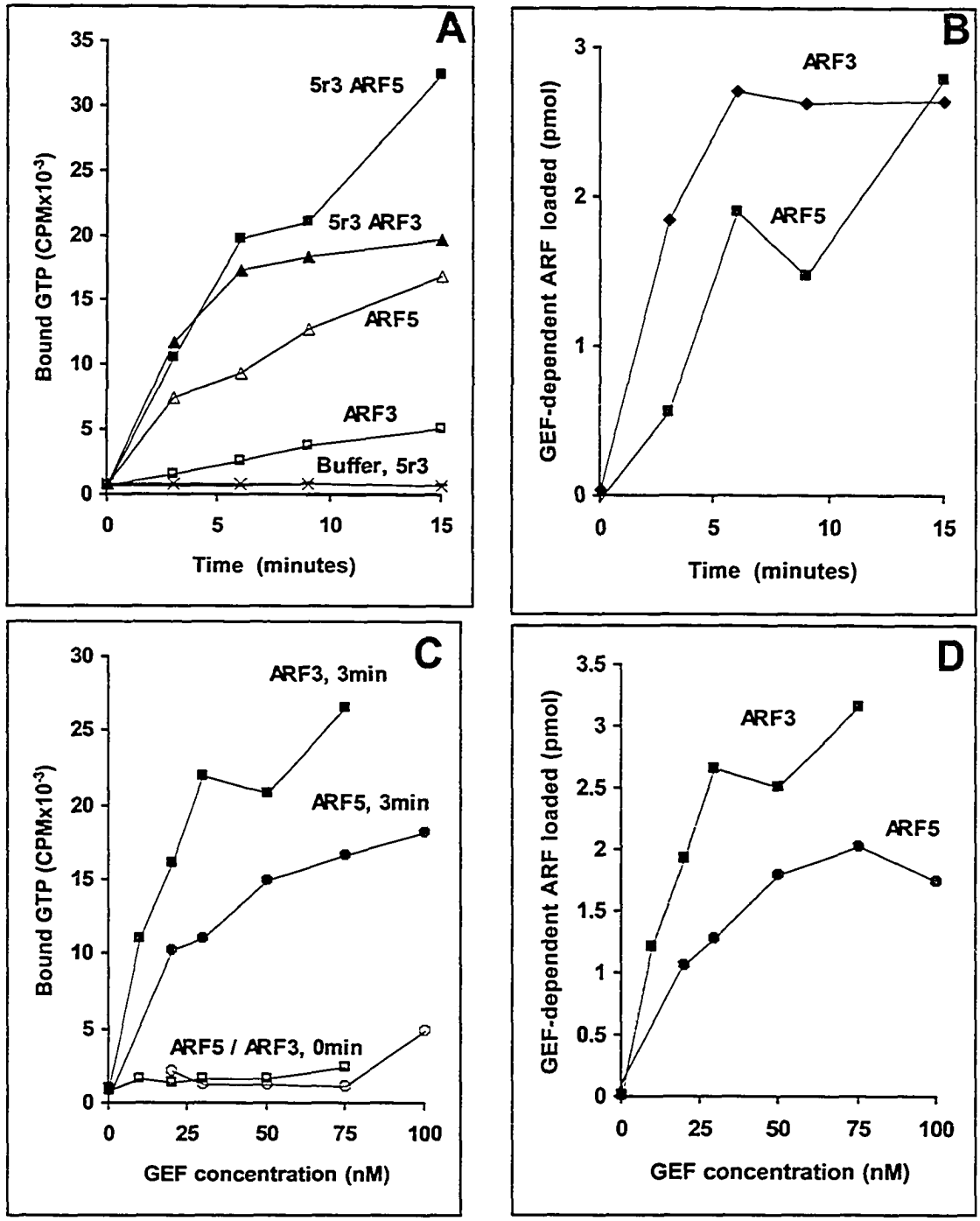

Figure 3.5 ***BRAG1 catalyses GTP exchange on class I and class II ARF***
Panels A and B. Kinetics of GTP binding on Arf3 (1μM) and Arf5 (1μM) in the absence or presence of 50 nM 5R3. The raw data from panel A was corrected and plotted in panel B. BRAG1a (5r3) is active both on class I and class II ARFs. Panels C and D. Arf3 (1μM) and Arf5 (1μM) were incubated with increasing concentrations of BRAG1a (5r3) and the extent of GTP binding was measured at either time zero or following a 3 min incubation at 30 C. The raw data from panel C was corrected and plotted in panel D. GTP loading on ARF3 and ARF5 is roughly correlated to the concentration of 5r3 added to the reaction.

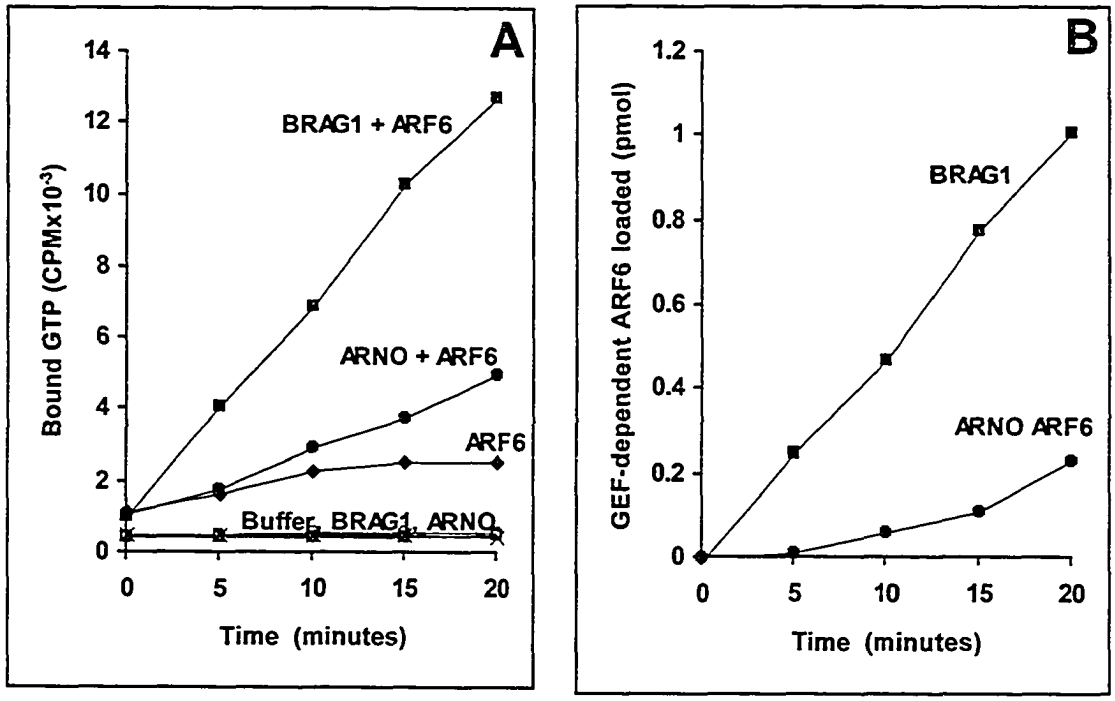

Figure 3.6 ***BRAG1 catalyzes GDP exchange on ARF6***

Kinetics of GTP binding on Arf 6 (1μM) in the absence or presence of either 20 nM 5R3 or 20 nM of full length ARNO1. Panel A and B show the raw data and corrected data, respectively. Assays were performed and quantitated as described in Chapter 2 section. BRAG1 is more active than ARNO on ARF6.

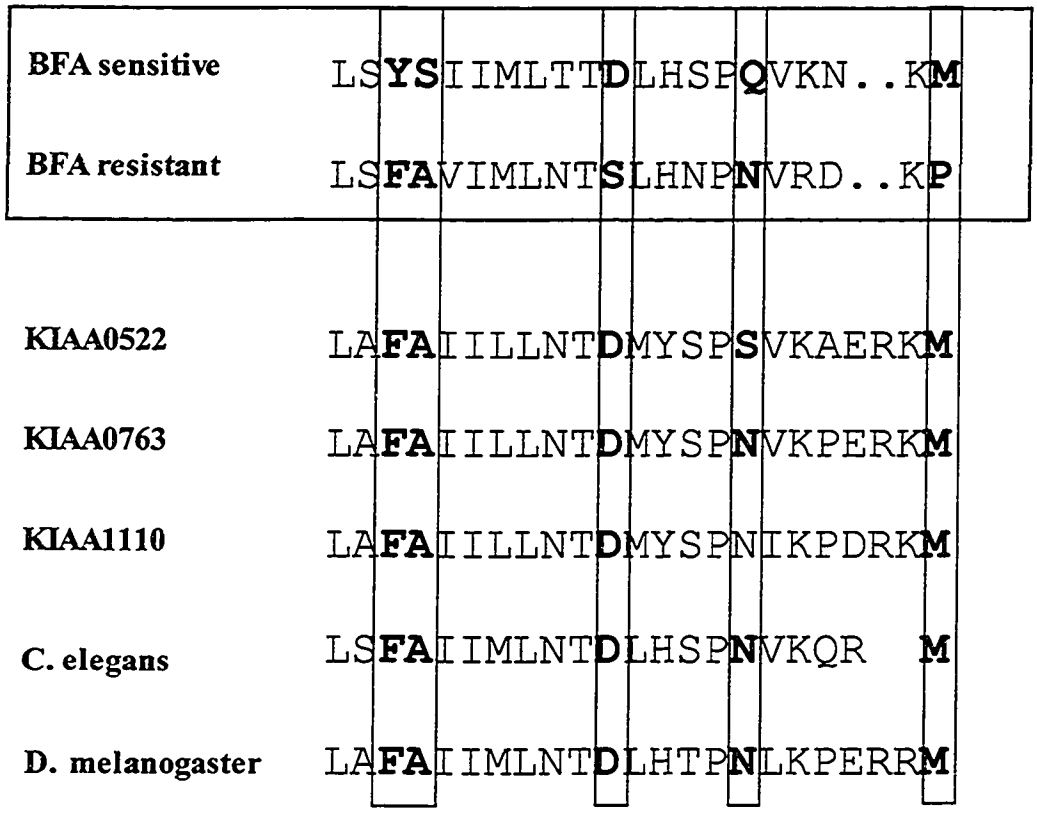

Figure 3.7 ***BFA resistance or susceptibility is encoded in motif 2 of the Sec7 domain***

Mutagenesis studies by several groups have identified key residues in motif 2 of the Sec7 domain which are important for the determination of BFA resistance. Examples of BFA-sensitive and BFA-resistant sequences were derived from hBIG1 and hARNO1, respectively. The 3 human BRAGs and their worm and fly homologs display identical pattern of residues at those key positions. The BFA sensitivity cannot be inferred from these sequences since all BRAGs contain an equal mixture of BFA resistance and BFA sensitivity determinants. However, the identical pattern does suggest that all BRAGs should show similar response to BFA.

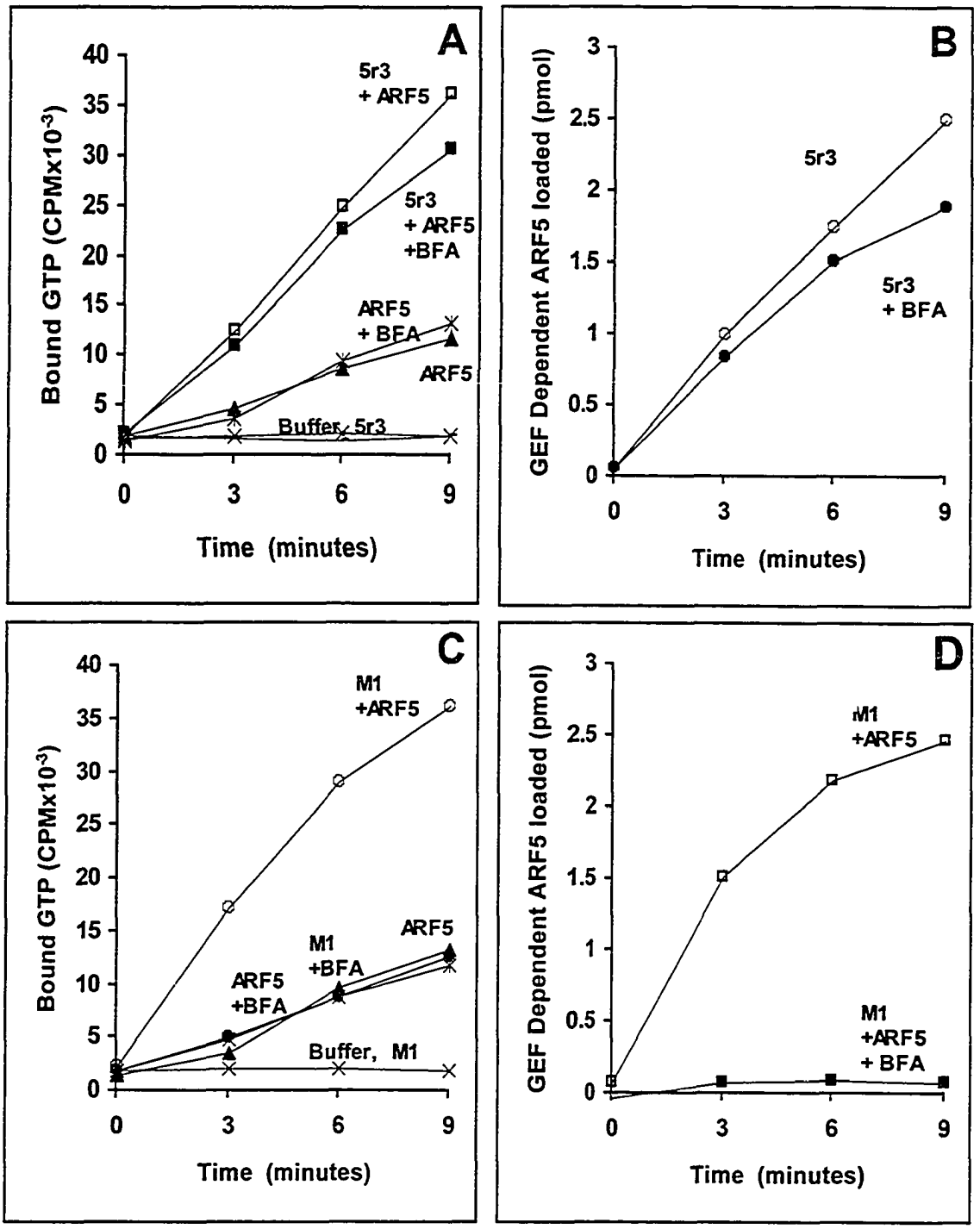

Figure 3.8 ***BRAG1 GTP exchange activity is resistant to BFA***

Exchange assays were performed with Arf5 (1μM) and either 50 nM BRAG1 (5r3) (Panel A and B) or 50 nM BIG1 (M1) (Panel C and D). Kinetics of GTP binding were measured in the absence and the presence of 300 μM BFA. The raw data from panels A and C were corrected and plotted in panels B and D, respectively. Under conditions where the sec7 domain of BIG 1 (M1) is completely inhibited by BFA, BRAG1 activity is not significantly affected.

Chapter 4:

Analysis of splicing and expression patterns of BRAGs

4.1 INTRODUCTION

Chapter 3 demonstrated that the three cDNAs KIAA0522, KIAA0763 and KIAA1110 form a novel family of sec7 domain proteins. Because this family of Arf-GEFs is exclusive to metazoans it is likely that they possess some function, which is vital to multi-cellularity. Quantitative RT-PCR at the Kazusa Institute published on their web site reveals tissue specific distribution of BRAG1, confirming differential distribution and therefore differential function of BRAG1 in different cell types (Fig 4.1).

The biochemical analysis of KIAA0522 and KIAA0763 Sec7d truncations established that BRAG1 and BRAG2 could function as Arf-GEFs. However, this provided limited insight as to the cellular function of BRAGs. To elucidate the cellular function of this novel Arf-GEF family, we must first address two sets of basic questions. First, we must determine what exactly are BRAGs, since published cDNAs appear to be partial and may not encode the full-length protein. Secondly, we must determine their intracellular distribution and also their relative expression in various tissues. Only then will we be able to identify candidate roles for these proteins. This will allow us to design tests to investigate their function with either neutralizing antibodies or various other molecular tools that interfere with their function in cells/tissues of interest.

4.2 OB4, A BRAG1 SPECIFIC SERUM IDENTIFIES MULTIPLE FORMS

To ensure success of localization we pursued both antibody production and construction of expression vectors encoding tagged forms of BRAG cDNAs. To generate polyclonal sera we took advantage of the fact that Heather Vandertol-Vanier had produced large quantities of the 5r3 protein that cold be used to obtain gel purified product for immunization. This electrophoretically pure protein was used to immunize and boost 2 rabbits (OB-4 and 6-17) at 6 weeks interval. Sera obtained after the third boost and the final bleed were affinity purified on nitrocellulose against 5r3 and tested for specificity.

The affinity-purified antisera were first characterized by immuno-fluorescence of cultured Normal Rat Kidney (NRK) cells (Fig 4.2). The 6-17 antiserum did not stain any specific organelles and was not pursued further. The OB4 serum gave a striking juxta-nuclear pattern (Fig 4.2, left middle panel) that appears identical to that observed with the

Figure 4.1 ***RT-PCR by the Kazusa Institute suggests that BRAG1 is abundant in multiple tissues***

The Kazusa Institute performed quantitative RT-PCR on RNA from multiple tissues. Lanes 1 - 5 were amplified from serial tenfold dilutions of plasmid DNA template (from 0.1 fg to 1 pg, respectively). Lanes 6-19 represent the RT-PCR amplification from different tissues.
The data was taken from the Kazusa Institute website: http://www.kazusa.or.jp/huge/gfimage/rt-pcr/html/KIAA0522.html

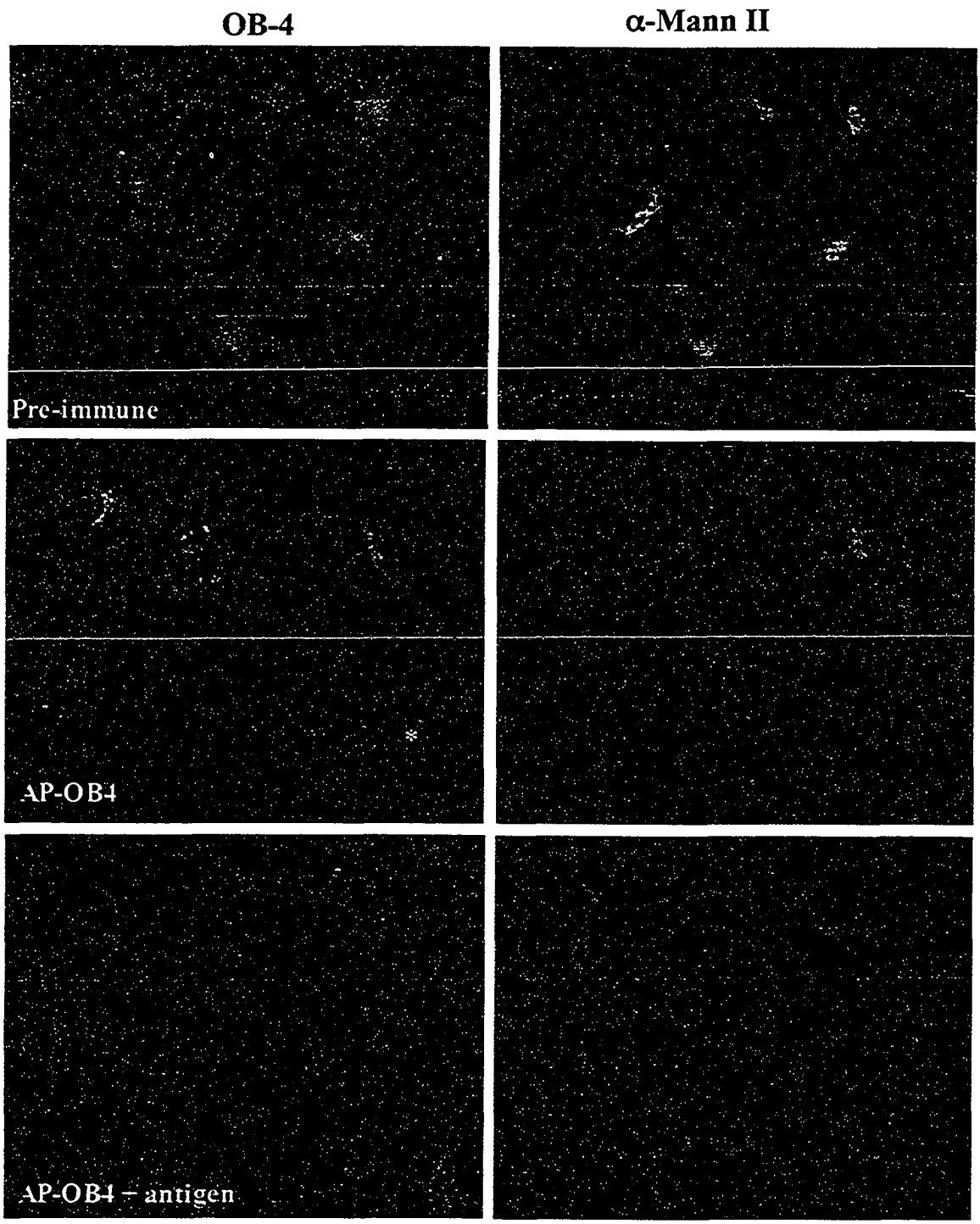

Fig 4.2, ***The anti-BRAG1 antibody (AP-OB4) detects BRAG1 in NRK***

Pre-immune α-BRAG1 signal shows little staining coincident with mannII (medial Golgi, antibody 53fc3) in comparison to AP-OB4. AP-OB4 stains juxta-nuclear structure in many cells. OB4 also stain the PM in some cells such as the one marked with asterix. Furthermore, pre-incubation of APOB4 with immunogen prior to staining eliminates both Golgi and PM staining.

Golgi marker mannosidase II (mannII) (Fig 4.2, right middle panel). In some cells (see bottom right cell marked with white asterix), OB4 yielded instead staining of the plasma membrane. The juxta-nuclear pattern revealed with OB4 was not observed with the pre-immune serum (left top panel). Furthermore, preincubation of the affinity purified OB4 with excess antigen eliminated both juxta-nuclear as well as plasma membrane staining, and yielded instead nuclear staining. Strong nuclear signal by an antibody-antigen complex has been observed by others and was not investigated further. These initial experiments suggested that BRAG1 is involved in the exocytic pathway.

The affinity-purified antisera were then used to probe blots of detergent extracts prepared from BHK cells (Fig 4.3). The crude pre-immune serum does not detect any major protein species, while the crude post-immune serum at the same dilution detects a number of bands. The largest of the new bands is very diffuse at about 160kDa. Several bands are also present around 97-116kDa.

Affinity purification caused a clear change in the pattern of proteins recognized by the OB4 serum (Fig 4.3A). Immunoblots of BHK lysates with the second preparation of affinity-purified OB4 (AP2) no longer displayed the 200 kDa species and showed much reduced levels of the 97-116 kDa proteins. This suggested that the higher molecular weight protein of a size similar to that predicted by KIAA0522 were actually not related to BRAG1. The lower molecular weight species may represent products of proteolysis, or of alternate BRAG1 transcripts. Note that we have not yet unambiguously established by competition experiments with purified antigen whether the band at 140 kDa represents endogenous BRAG1 expressed in BHK cells. [A preliminary competition experiment left only a band at 70kDa; however this experiment was never repeated].

To further characterize the sera and directly compare the size of endogenous BRAG1 to that encoded by the KIAA0522 cDNA, we repeated immunoblot analysis using lysates prepared from NRK cells transfected with empty expression vector (pCEP4), or with vectors containing either the original KIAA0522 cDNA or a form modified to encode a G tag at the N-terminus (see Chapter 2, section 2.11). The results shown in Fig 4.3 revealed that affinity-purified OB4 detects a 100 and 150 kDa species in lysates of NRK cells (panel B). A band at 160 kDa is also readily detected in cells that overexpress either tagged or untagged KIAA0522. As expected, probing with a serum raised against

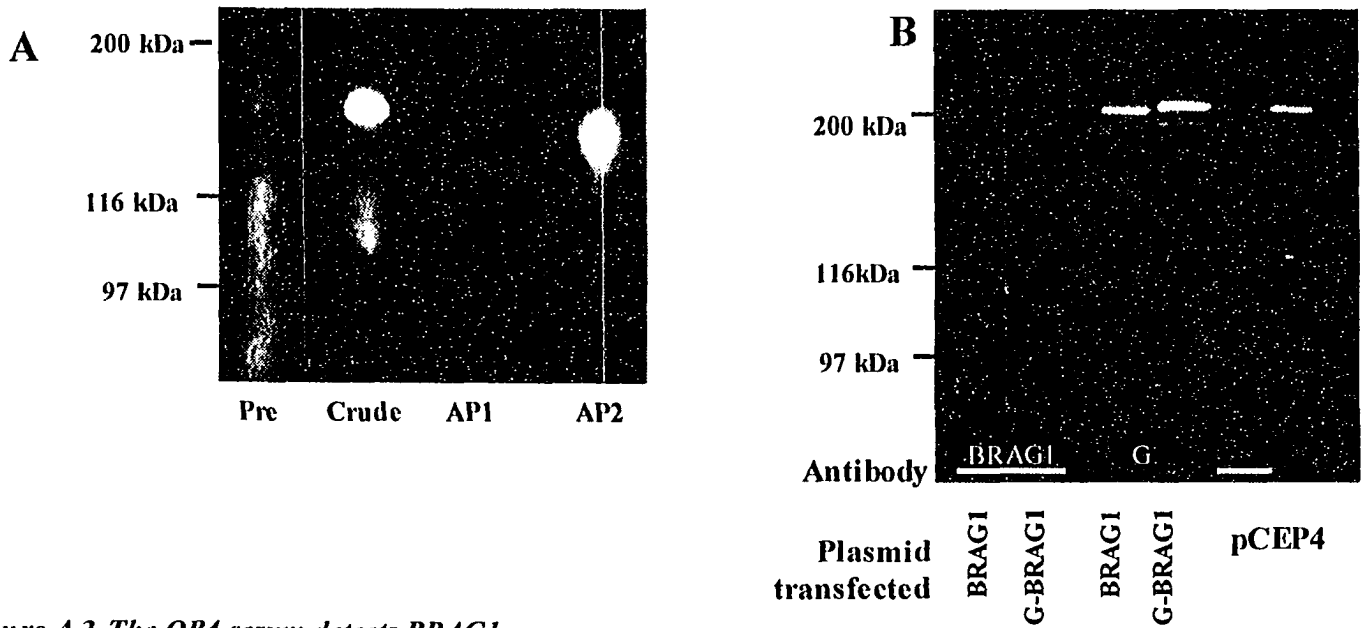

Figure 4.3 ***The OB4 serum detects BRAG1***

Panel A. The OB4 serum was affinity purified using nitrocellulose bound 5r3 protein on two separate occasions. The pre-immune, crude and purified sera were used to blot BHK lysates.
Panel B. The affinity purified OB4 and anti-VSV-G were used to probe immublots of lysates from NRK cells transfected either with empty vector (pCEP4), or vectors encoding untagged BRAG1 or G-tagged BRAG1 (G-BRAG1). Lysates were prepared as described in Chapter 2 thwenty-four hours post-transfection and resolved on SDS-PAGE. The largest endogenous BRAG1 species is 140kDa.

the G-tag revealed the same 160 kDa species, but only in cells transfected with the G-tagged form of the cDNA. I concluded that NRK cells express a BRAG1 form of 110 kDa and 135 kDa, clearly smaller than the 160 kDa species encoded by the KIAA0522 cDNA obtained from the Kazusa Institute.

4.3 Evidence for alternate splice forms of BRAG cDNAs

The immunoblot results described above suggested that NRK cells express preferentially a splice form of BRAG1 slightly different from that encoded by KIAA0522. Several additional lines of evidence suggested that some or all of the BRAG cDNAs may be incomplete and/or alternatively spliced. For example, the 5'UTR of longest of the cDNAs (KIAA0522) encodes an open reading frame (ORF) of 201 nt, which is in frame with the initiating methionine (Fig 4.4). Examination of genomic sequence upstream of the putative 5' UTR identified 192 additional nucleotides encoding an ORF that remains continuous and in-frame with the proposed initiating methionine of KIAA0522. This suggested the possibility that the KIAA0522 cDNA encodes a truncation lacking the N-terminus of full-length BRAG1.

Secondly, the use of the newly released Evidenceviewer on the NCBI web site revealed a number of expressed sequence tags (ESTs) that cluster within the second intron of KIAA0522 and identify three novel exons (Fig. 4.4). mRNAs submitted to Genebank at that time connected these 3 exons to one another, but never to exons present in KIAA0522. The third predicted exon possesses many stop codons in all 3 reading frames and is covered by a very large number of ESTs (42 at last count), several of which possess a polyA tail. This suggests that this novel exon might not be retained in BRAG1 mRNAs, but represents the end of a nested gene. The well-known bias of ESTs made from polyA mRNA towards the 3'-end would readily explain the preponderance of ESTs covering this exon. However, we cannot rule out the possibility that some BRAG1 transcripts retain the exon with the stop codons. Such transcripts would encode a truncated form of 183 residues that could have regulatory role if it competed with and modulated the function of a full-length protein encoded by a transcript retaining those exons.

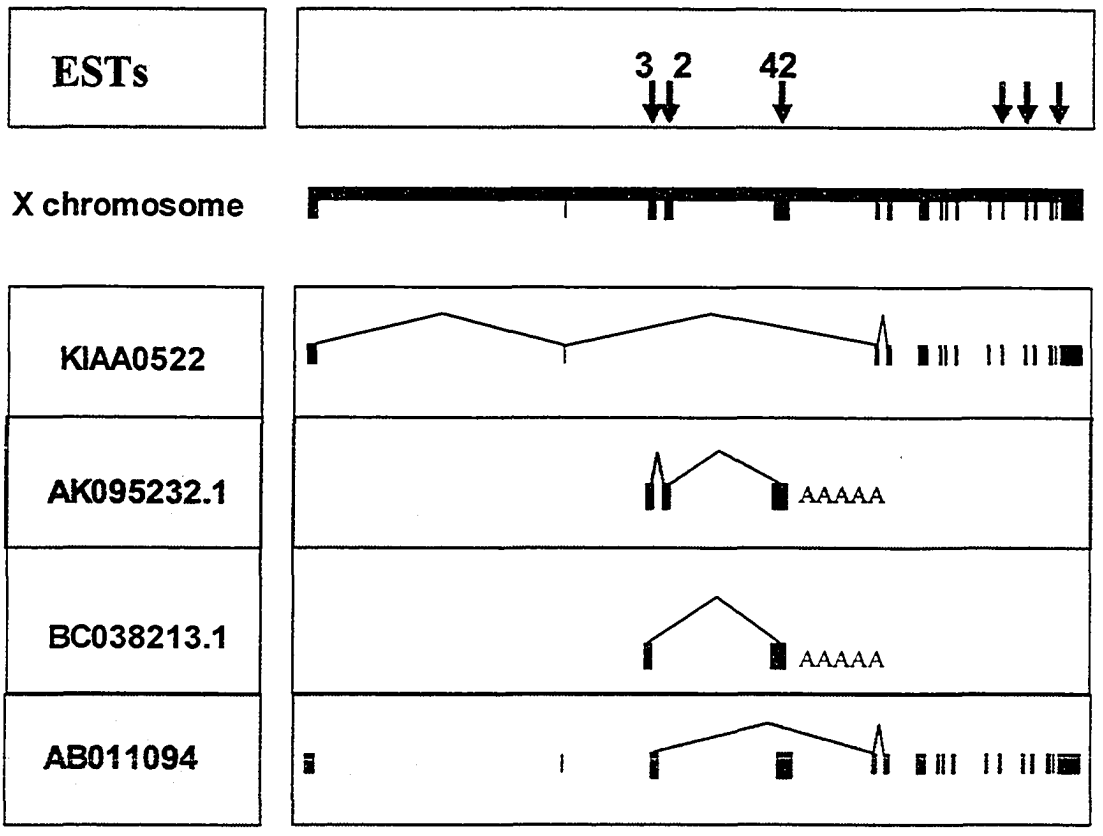

Figure 4.4 ***Analysis of BRAG1 cDNAs and ESTs suggests that other transcripts exist in vivo***

The boxed areas in the bottom portion of the figure illustrate the exon structure of several cDNAs encoded by the BRAG1 gene. The boxed area at the top shows all exons for which ESTs have been isolated. The number of such identified ESTs is given above the three novel exons absent from KIAA0522. Note that 2 of the cDNAs containing those novel exons have a poly-A tail.

4.4 5'RACE OF BRAG1 AND BRAG2

To determine if the BRAG1 cDNA had been truncated or alternatively spliced at the 5' end, I performed 5'RACE using an Invitrogen GeneRacer™ kit (Fig 4.5). This kit takes advantage of the 5' cap on full length mRNAs to protect those RNAs from de-phosphorylation by exogenously added calf intestine phosphatase (CIP). The 5' cap is then removed with Tobacco Acid Phosphatase (TAP), and those RNAs with a 5' phosphate are ligated to the Generacer™ oligo-nucleotide. The ligated Generacer™ oligo-nucleotide then acts as a nonspecific priming site for the 5' RACE reaction. Thereby, only descendants of capped mRNAs should be amplified by 5' RACE. The manufacturer provides an additional nested primer complementary to the 5' RACE oligo for subsequent nested PCR, if many products are observed after the initial 5'RACE reaction.

The 5'RACE primers for KIAA0522 were designed to address two specific questions: (1) Is KIAA0522 a 5' truncation of the full length mRNA?, and (2) Are the novel exons predicted by ESTs complementary to intron 2 actually part of BRAG1 or of some other gene?

To determine if the 5' end of BRAG1 had been truncated, four different primers were designed with identity to the first exon of KIAA0522 (Fig 4.6). The primer sequences were chosen to maximize AT content because of the high GC content at the N-terminus of KIAA0522. Most of the region is also composed of low complexity sequence (poly G and poly C tracts), so primers were chosen for high complexity sequence to ensure specificity. Two additional primers were designed in the opposite (forward) orientation (F1 & F2), which might be used to amplify BRAG1 from plasmid or 5'RACE products as positive controls.

The second set of primers was designed to determine if the 3 predicted exons nested within the 2nd intron of KIAA0522 are included in some of the BRAG1 transcripts. To detect the alternate splicing I wanted to perform 5' RACE from a region of BRAG1 encoding a domain critical to function and likely present in all splice forms. As a first step to identify regions essential to BRAG function, I compared the sequence of BRAG1 to it's closest relative, BRAG2. I found that the central third of BRAG1 (exons 4-12) encoding the sec7d and PH domains displayed greatest conservation with BRAG2.

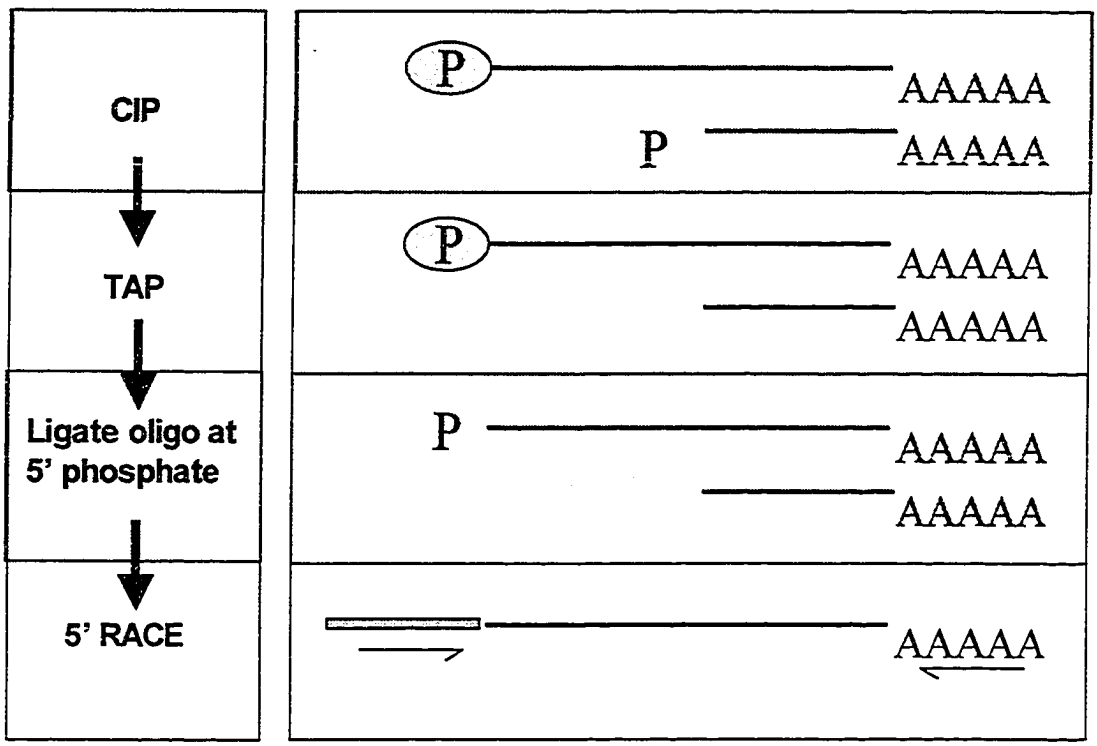

Figure 4.5 ***The GeneRacer kit amplifies only full length mRNAs***

Schematic description of the four steps leading to the amplification of full length mRNAs with the GeneRacer kit. In the first step, poly A mRNAs are treated with CIP to dephosphorylate all mRNAs lacking a 5' mRNA cap (blue oval). Subsequent treatment with TAP removes the cap to reveal a 5' phosphate. An oligo of defined sequence is then ligated to the 5'end. This oligo provides a shared 5' region for priming the final RACE reaction.

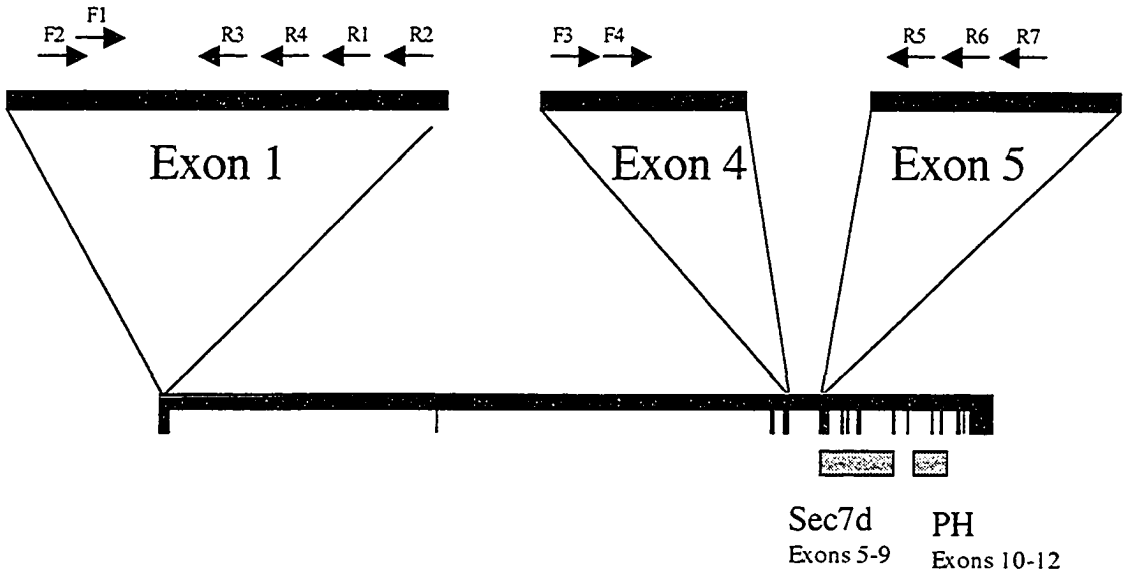

Figure 4.6 ***Placement of 5' RACE primers on BRAG1***

This diagram shows the distribution of BRAG1 exons along the X chromosome. Exons 1, 4 and 5 have been enlarged to show the relative distribution of the primers used in 5' RACE.

The three selected primers were ultimately derived from the 5th exon of BRAG1 because it encodes the beginning of the sec7d (Fig 4.6) and this domain is likely the more essential of the two. As before, I also designed two primers on the opposite strand (F3 & F4) to act as positive controls for amplification from plasmid for 5'RACE reactions. Both of these control primers were derived from exon 4. Please note that 5'RACE reactions with exon 5 primers may not only yield products with the putative novel exons but also those containing exons 1 and 2 present at the 5' end of KIAA0522.

The templates for the 5'RACE reactions were produced from poly A mRNA extracted from cultured HEK-293 cells, or from total HeLa RNA which was supplied with the commercial kit. Initially the reverse transcription of mRNA was performed using random priming (RP) hexamers. Because the first set of 5'RACE reactions failed to yield any specific bands (see below) I produced an additional Generacer library using mRNA obtained from HEK-393 cells and a mixture of 3 gene specific primers (GSP). These are the R1, R2 and R3 primers that were used in the production of GST tagged BRAG1-sec7d (see Fig 3.1). By selectively reverse transcribing BRAG1 mRNA I could use lower stringency conditions for the PCR without producing nonspecific products.

4.4.1 5' RACE of KIAA0522 from exon 1 fails to amplify BRAG1

5'RACE using the reverse primers R1 and R2 specific to exon 1 failed to produce any specific bands from either the HEK-293 mRNA and HeLa total RNA libraries (data not shown). Optimization of the reactions using several concentrations of DMSO, template, Mg++ and several annealing temperatures failed to yield products. Specifically, 5'RACE bands corresponding to the mRNAs with 5' end of KIAA0522 equal to or larger than 750nt (R1) and 830nt (R2) were never observed. In contrast, control reactions performed in parallel with manufacturer-supplied primers complementary for the actin mRNA yielded strong bands of the expected size.

To enhance the chance of recovering 5'RACE products containing exon 1, I produced an additional Generacer library from HEK-293 mRNA using a mixture of 3 gene specific primers. In addition, I designed two additional reverse primers, R3 and R4 (see Fig 4.6), to increase the likelihood of obtaining specific products in the 5'RACE

reaction. Unfortunately, as observed previously, none of the 5'RACE reactions with the new library and primers yielded identifiable products.

Negative results are notoriously difficult to interpret. I concluded that there was no problem inherent to the reverse transcribed template because control reactions performed with the actin primers readily amplified products of the expected size. This left us with two alternate explanations. The primers I designed either failed to anneal with sufficient strength and/or specificity or the level of full length mRNA containing exon1 expressed by HeLa or HEK293 cells was too low to yield readily identifiable 5'RACE products.

4.4.2 5' RACE from the 5th exon of BRAG1 identifies BRAG1b and BRAG1c splice variants.

Amplification using primers complementary to the 5th exon of BRAG1 was successful using both the random primed (RP) and gene specific (GSP) libraries (see Chapter 2 for details) prepared from HEK 293 mRNA (Fig 4.7). The HeLa library was never tested with these primers.

Amplification of the 5' end of BRAG1 from the random primed library was successful with only one of three primers tested (B1RACER5). This reaction yielded two bands of about 900bp and 1000bp (Fig. 4.7). These products were cloned using the Zero Blunt® TOPO® PCR Cloning Kit as before (see Material and Methods). The resulting colonies were screened for the presence of inserted DNA fragments. The majority of the 42 plasmids screened contained inserts ranging between 300bp and 500bp. Eight plasmids bearing larger insertions were recovered. Inserts were sequenced from both classes of clones and 2 species of cDNA were identified bearing homology to BRAG1 (Fig 4.8).

The longer of these inserts, termed BRAG1c, differs from the 5'end of KIAA0522 through removal of the first 2 exons of KIAA0522 and inclusion of 2 of the three novel exons described in figure 4.8 above. This species was isolated twice, from 2 independent 5'RACE and cloning reactions. The predicted molecular weight of BRAG1 containing these alternate exons, termed BRAG1c, is 141kDa, a size similar to that observed by

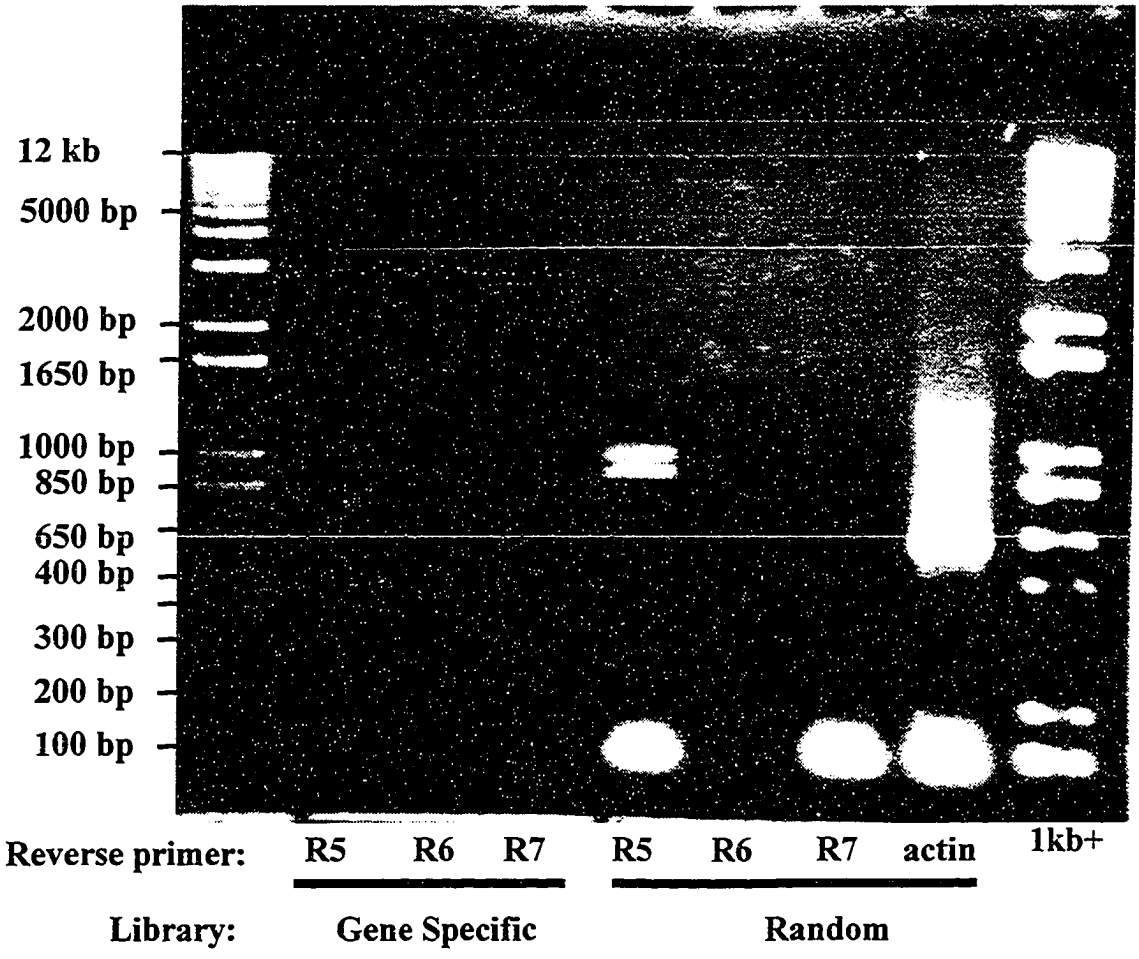

Figure 4.7 *5' RACE of BRAG1 amplifies several species of DNA*

The R1 primed reaction produced three bands at 900bp, 1kb and 100nt, from the random primed library. The Gene Specific library produced a single weak band at 700bp.

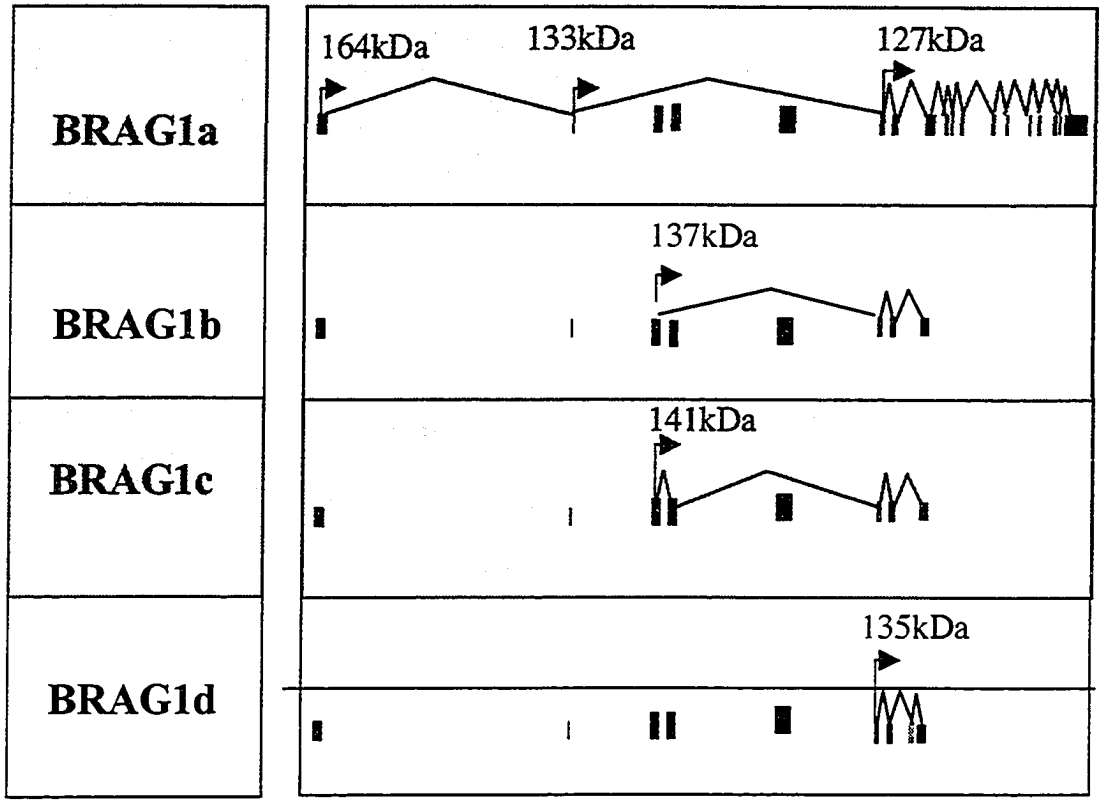

Figure 4.8 ***BRAG1 is differentially spliced at the 5' end***

Schematic of alternate splicing at the 5' end of BRAG1. BRAG1b/c lack the first two exons of BRAG1a, which are replaced with one or two exons predicted from ESTs. BRAG1d removes the alternate beginnings of BRAG1a, b and c and inserts a novel 3rd exon.

immunoblots (Fig. 4.3) encodes a protein which is larger than endogenous BRAG1 in NRK).

The second insert discovered, termed BRAG1b, also lacks the first two exons of the KIAA0522 cDNA and includes only the first novel exon present in BRAG1c (Fig 4.8). The predicted molecular weight of the species encoded by this alternate splice form is 137kDa, a size also very close to that observed by immunoblots of NRK lysates (see Fig 4.3). It may also be important to note that the shared initiating codon of the longest ORF predicted from the sequence of those two variants [ACCCAUGG] matches well the Kozak consensus sequence (ACCAUGG).

Amplification of the 5' end of BRAG1 from the GSP library was successful with only one primer (B1RACER5), the same one that yielded product with the RP library. In this case, the reaction produced a single weak band of approximately 680 nt (Fig 4.7). Molecular cloning of this product led to identification of a third species of 5' exon from every clone screened (n=6) (Fig. 4.8). This encodes a novel 5' end for KIAA0522 that is appreciably smaller than the other variants. In this transcript, the first four exons of the published cDNA were skipped and a novel exon was inserted prior to the 5^{th} exon. The predicted molecular weight of the protein encoded by this transcript is 127kDa, which is appreciably smaller than the 140kDa band that corresponds to the endogenous KIAA0522 found in NRK.

It is interesting to note that the 5' end of the published KIAA0522 sequence was never isolated in these screens. This might be explained by lack of expression or very low abundance of this transcript in those cell types. Alternatively, the sequence between the true capped 5'end and the first published exon may be to great to allow efficient recovery with this approach.

4.4.3 PCR CONFIRMS THE PRESENCE OF BRAG1B AND BRAG1C TRANSCRIPTS IN HEK293 CELLS

To demonstrate that transcripts for BRAG1b and BRAG1c could be isolated from the HEK293 mRNA, a new forward primer was designed with homology to the first exon of BRAG1b/c (F1RT)(Fig 4.6). PCR was then performed on the random-primed HEK293

cDNA library with this primer and B1RACER5, the primer that had been successful in the 5' RACE of BRAG1 (Fig 4.9).

The PCR reactions produced a single band from the random primed library at 900bp. This is similar in size to the original BRAG1b amplification (Fig 4.7). This suggests the BRAG1b splice variant is abundant enough to be detected while the BRAG1C variant is not. Under less stringent PCR conditions we observed additional bands at 1300bp, 1900bp and 2500bp. Because no additional cryptic exons have been identified downstream of the second exon of BRAG1c, these larger fragments are likely non-specific products. We made no further attempts to clone and characterize these products.

4.4.4 5' RACE of BRAG2:

The identification of several alternatively spliced forms of BRAG1 suggested diversity of BRAG1 function through regulated alternate splicing of the 5' terminus. BRAG2 is very similar to BRAG1 both in domain structure and sequence, and could also be subject to regulation by alternate splicing. The 5'end of KIAA0763, the longest available BRAG2 cDNA is shorter than that of KIAA0522 and lacks a variable 5' region. However, this could have resulted from truncation during mRNA isolation and BRAG2 may well possess a variable 5' end like BRAG1. Three primers were designed to perform 5' RACE of BRAG2 and address this possibility. Each was located within the second exon of BRAG2, no more than 700bp into the mRNA (Fig 4.10). As before, primers were designed to maximize AT content in a GC rich region and to maximize primer complexity.

One of the three BRAG2 primers used for 5'RACE amplified DNA from the random primed library (Fig 4.11). The R1 primer amplifies three species of DNA from the random primed library. There are distinct bands at 800bp, 450bp and a weak smear is evident at 100bp.

The amplified DNA was cloned into pTOPO and clones were screened for insertions similar in size to the 5'RACE products. Amongst the digested clones there was a preponderance of lower molecular weight insertions most of which proved to be vector-derived fragments. One clone had a 731bp insertion with homology to the 5' end

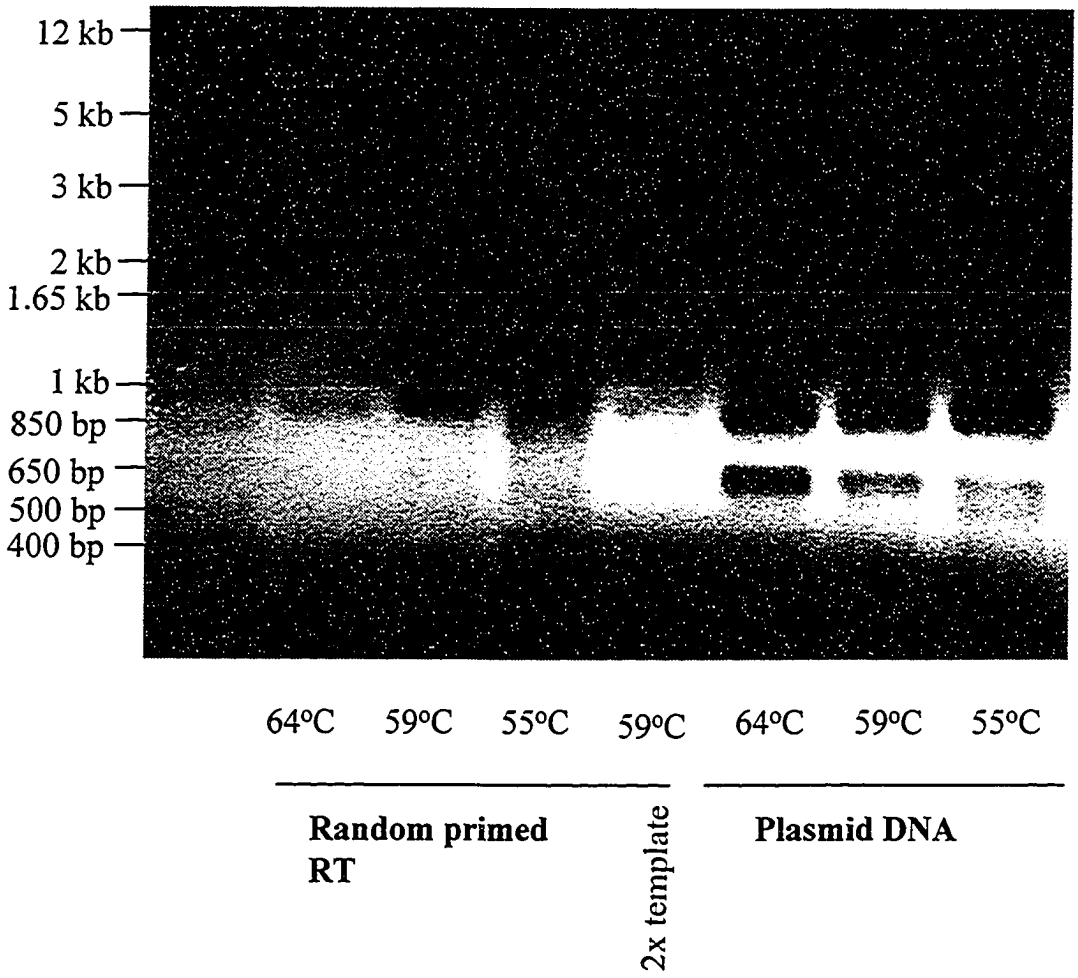

Figure 4.9 ***The 5' end of BRAG1 can be amplified from random primed library***

Novel sequence derived from the 5' RACE reaction of BRAG1 was used to perform PCR on either the RP library or plasmid DNA encoding GBRAG1c. Under the most stringent conditions (64°C) a single band was amplified from RP library. Under similar conditions, 2 bands are amplified from the plasmid DNA with primers B1RACER5 and F1RT. The expected size was 900 nt. We do not know the origin of the band migrating at 650 nt.

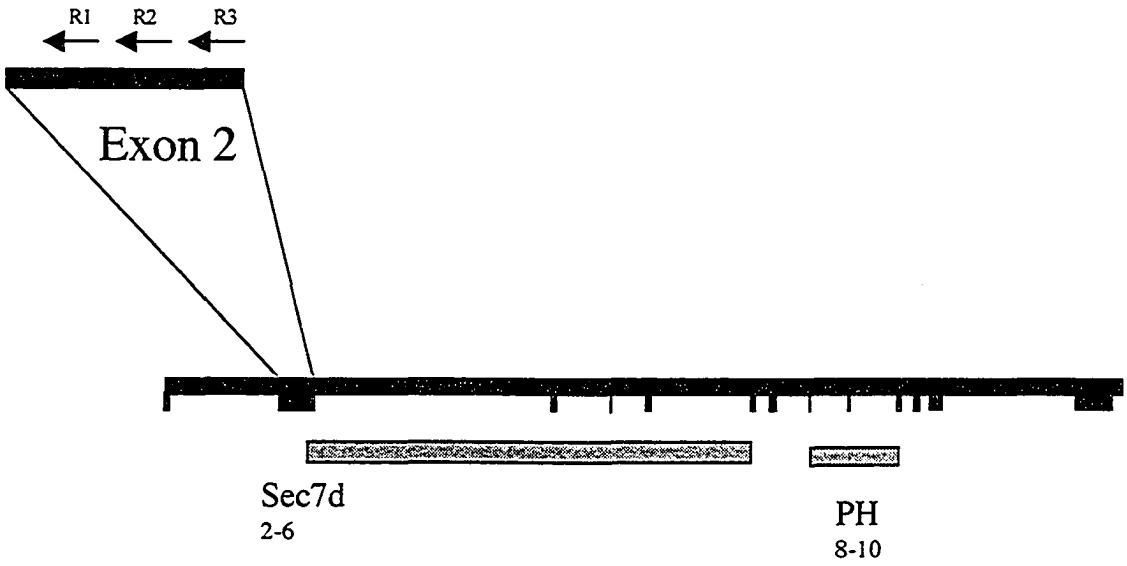

Figure 4.10 ***Placement of 5' RACE primers on BRAG2***

This diagram shows the distribution of BRAG2 exons along chromosome 3. Exon 2 has been enlarged to show the relative distribution of the primers used in 5' RACE.

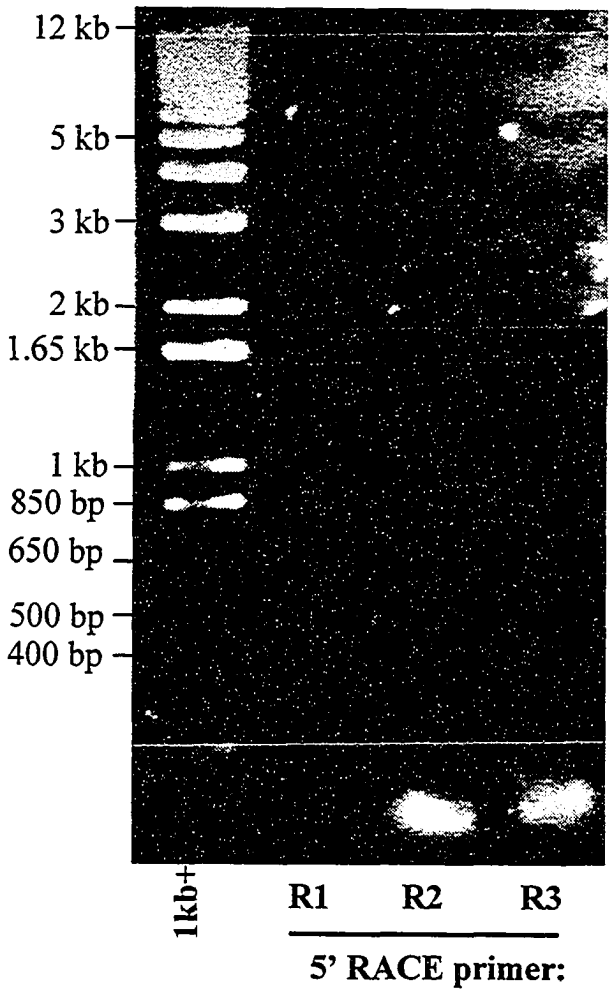

Figure 4.11 ***5' RACE of BRAG2 was successful using the R1 primer***

5' RACE of BRAG2 was successful using the R1 primer. This amplification yielded bands at 450 base pairs (bp) and 800 bp.

of BRAG2 (Fig 4.12). The clone is homologous to BRAG2 at its 3' end. There is an additional 296nt of sequence which maps to chromosome 3, 100kb upstream of the first published exon (this is twice the length of the rest of the gene!!).

4.4.5 5' RACE of BRAG3

BRAG3 is the shortest of the 3 human cDNAs. It is truncated at the N-terminus, such that it is 684nt shorter than BRAG2 and 1828nt shorter than BRAG1a. Three primers were designed with homology to the 1st exon of BRAG3, using the same criteria as was used for the 5' RACE of BRAG1 and BRAG2.

5' RACE using the 3 BRAG3 specific primers failed to yield any products. I believe that this was simply a matter of bad luck. Only 1/3 of the primers designed for BRAG1 or BRAG2 were able to produce 5' RACE products. Alternatively, the 5' fragment of BRAG3 might have been too long for efficient amplification and cloning. The recent cDNA submission AK091953 demonstrates that KIAA1110 is a truncation of BRAG3, with 2 additional exons at the 5' end (Fig 4.13)

4.5 Northern analysis of BRAG1

To determine if there is tissue specific expression of the BRAG1 splice variants, a northern blot was performed using a Clonetech Multiple Tissue Northern (MTN) blot (cat # 7780-1, lot#3020545). We chose to use a commercially available blot to circumvent difficulties with procurement of human tissues and reproducibility of the transfer.

Three probes were designed to determine if there was tissue specific expression of BRAG1 (Fig 4.14). The first probe was designed to detect all BRAG1 isoforms, the second probe was designed to specifically detect the published BRAG1 cDNA, and the third probe was designed to detect both BRAG1b and BRAG1c.

4.5.1 BRAG1-PH specific probe

To detect all splice forms of the BRAG1 mRNA, the northern probe must be designed to a region that is not subject to alternate splicing. Our approach was based on the assumption that highly conserved regions should encode domains that perform an essential function and be less likely to exhibit variance. To identify those regions, I

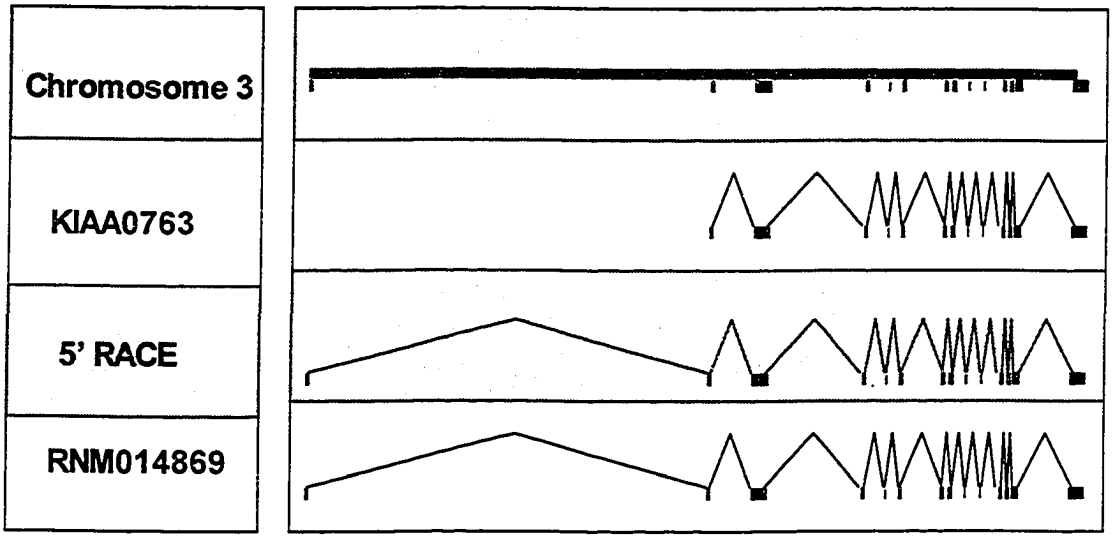

Figure 4.12 ***KIAA0763 is a 5' truncation of the full length cDNA***

5' RACE of BRAG2 yields an additional exon at the 5' end of the cDNA. This result is confirmed by the recent submission RNM014869, which is identical to the 5' end to BRAG2

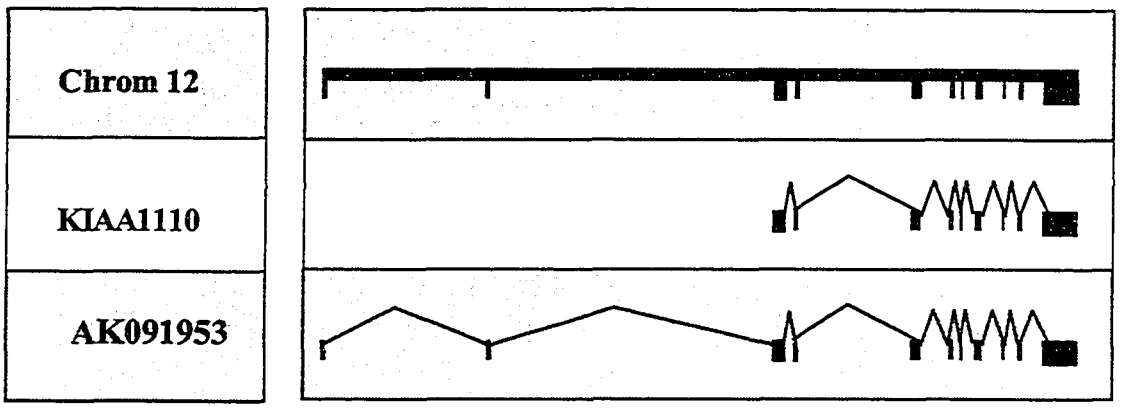

Figure 4.13 ***KIAA110 is a 5' deletion of the full length mRNA***

5' RACE reactions were unsuccessful for KIAA1110. A recent Genebank submission confirms that the KIAA1110 cDNA is incomplete, with two additional additional exons at the 5' end.

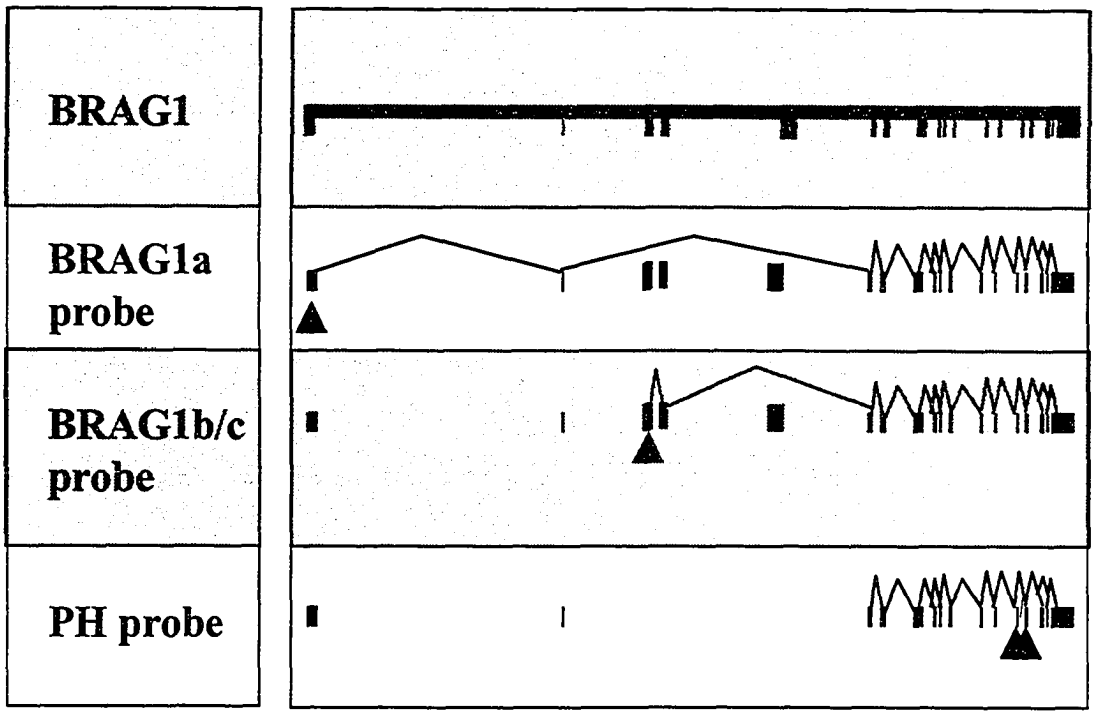

Figure 4.14 ***BRAG1 northern probes differentiate between the BRAG1 isoforms***

The BRAG1b/c and BRAG1a probes are complementary to isoform specific sequences. The PH domain probe should detect all BRAG1 isoforms.

performed a pairwise comparison of the genomic sequences of BRAG1 and BRAG2 and identified several regions of high conservation between BRAG1 and BRAG2.

The region encoding the sec7d may appears at first glance to offer the best candidate. However, a probe complementary to a region with such a high level of conservation with BRAG2 (80% identity) may not be specific enough for our purpose. The probe was therefore designed to detect another highly conserved region encoding the only other domain with known function, the PH domain. I used about half of the PH domain as a probe. We expect the PH domain to play a critical regulatory function and be present in all BRAG splice forms. Pairwise BLAST searching determined that BRAG2 does not have a homologous region.

The BRAG1 PH domain specific probe revealed expression restricted to a limited set of tissues (Fig 4.15A). The probe hybridized efficiently with mRNA species in the heart, skeletal muscle and placenta samples. Low signal was also detected in the brain and colon samples. The lack of significant expression in most tissues did not result from uneven loading. Probing of the same blot with the actin probe at the end of a series of blotting and stripping steps confirmed that all wells received similar levels of mRNA (Fig 4.15B).

There were at least 4 species of mRNA detected by the BRAG1-PH domain probe. In the brain, heart and skeletal muscle the predominant mRNA detected was about 6kb. The heart and skeletal muscle samples displayed an additional band at 1kb, suggesting that either one of the bands is non-specific, or that multiple, very distinct splice variants exist within a single tissue.

mRNAs of sizes different from 6 kb were detected in other tissues as well. The colon sample contained an mRNA of approximately 6.6kb detected slightly above the band present in the brain, heart and skeletal muscle samples. In the placental sample, the PH domain probe detected a single very strong band at 2kb.

The smaller mRNAs that were detected in the heart, skeletal muscle and placenta were unexpected. Because they are much smaller than predicted, they could represent artefactual abundant species that were erroneously detected. This is unlikely because these results are similar to what is detected by the KIAA0522 probe (below).

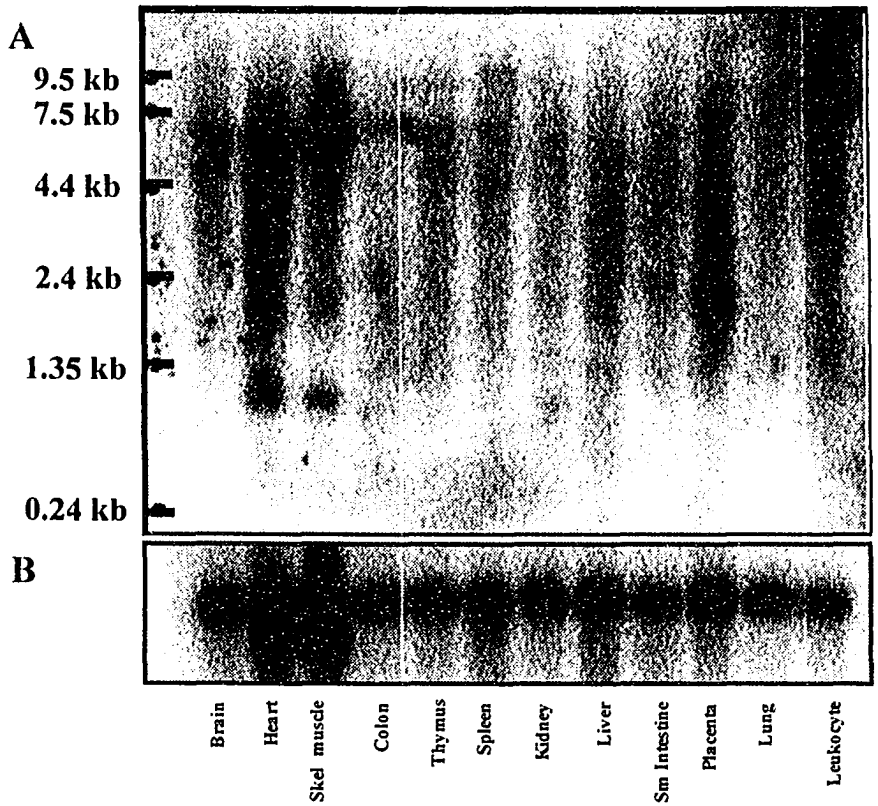

Figure 4.15 ***Northern blotting using the PH-domain probe reveals tissue-specific expression***
Panel A. A multiple tissue northern blot was probed with a radiolabeled fragment derived from the PH domain coding regions of BRAG1. The BRAG1-PH domain probe shows strong expression of BRAG1 in the brain, heart, skeletal muscle, colon and placenta.
Panel B. The blot was stripped and reprobed several times. The fourth probing was performed with a radiolabeled fragment derived from actin gene.

4.5.2 KIAA0522 probe:

To specifically detect the published splice variant KIAA0522, a probe was designed in the first variable exon of BRAG1 (see Fig 4.14). Because the 5' end of this splice variant is unique, the probe should only detect a single variant of BRAG1. This probe revealed a tissue distribution that is identical to that obtained with PH-domain specific probe. Specifically, mRNAs are detected at 6kb in brain, heart and skeletal muscle, at 1kb in heart and skeletal muscle, and 2kb in placenta (Fig 4.16).

The observation of identical patterns with the PH-domain and the KIAA0522 probes is striking and significant. Several lines of evidence establish that it does not result from poor stripping of the commercial blot. Probing the MTN blot with the BRAG1a probe was performed 3rd, and followed one with the BRAG1b/c probe that gave a completely different pattern (see below). Furthermore, we had confirmed by prolonged fluorography prior to blotting that all radio-labeled material had been removed. Because the pattern detected with the KIAA0522 probe is identical to that detected by the PH-domain probe, we conclude that the KIAA0522 variant represents the primary splice form in those tissues. Furthermore, the mRNAs detected by both probes are likely specific as two entirely separate probes detect them both.

4.5.3 BRAG1b/c specific probe

Because the only difference between the BRAG1c and BRAG1b splice variants is the presence of an additional exon in BRAG1c, the design of a BRAG1b-specific probe is possible but challenging. This would involve creating a probe whose sequence overlaps the intron boundary between exon 1 and exon 2 of BRAG1b. Furthermore, the length of the two arms would have to be experimentally adjusted such that it would efficiently bind transcripts with exons 1 and 2 when they are joined (as in BRAG1b), but not those containing these exons when separated by an additional exon (as in BRAG1c). In our initial studies we chose to bypass this problem and first design a probe specific to the exon shared by BRAG1b and BRAG1c.

The northern probe specific to both BRAG1b and BRAG1C detected mRNAs that have different molecular weight and relative abundance from those observed with the KIAA0522 and PH domain experiments (Fig 4.17). For example, the expression of

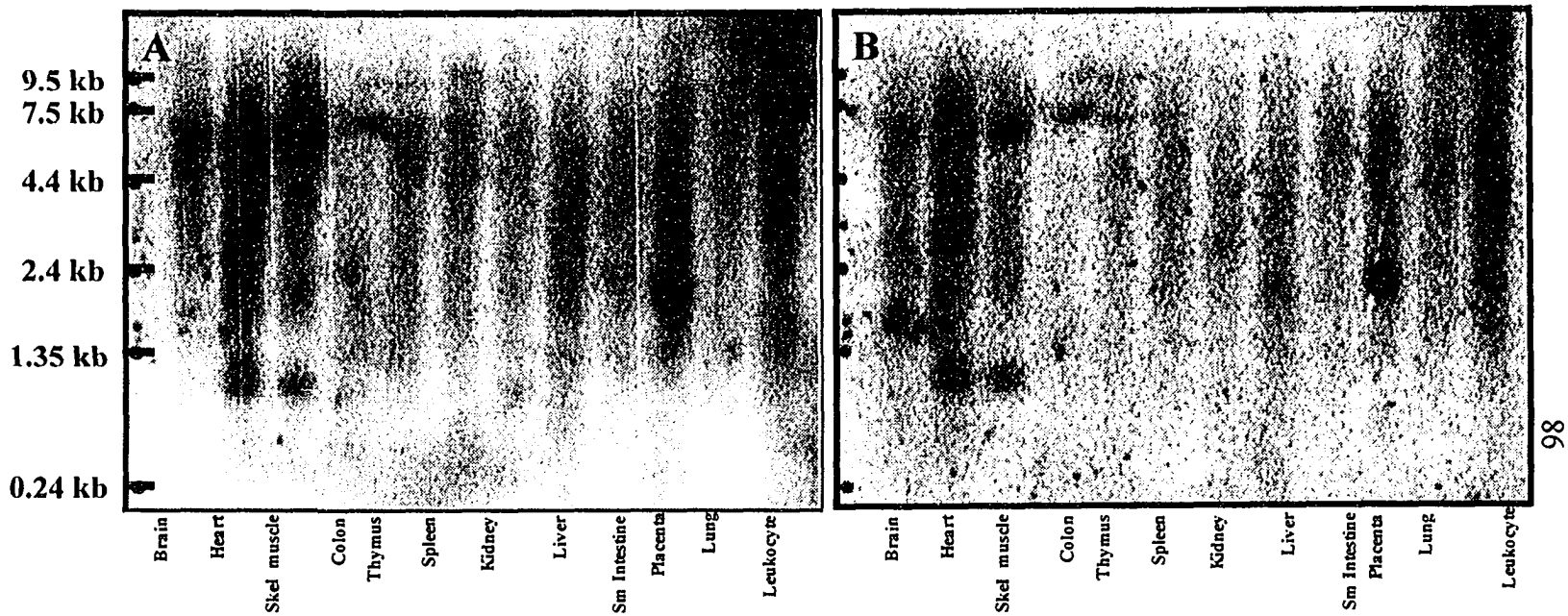

Figure 4.16 ***Northern blotting using the PH-domain probe and the BRAG1a probe shows striking similarities***

Panel A. This panel shows a Northern blot obtained with the PH domain-derived probe and is the same as that shown in Panel A of Fig. 4.15

Panel B. This blot stripped and reprobed several times. The third probing was performed with a radiolabeled fragment derived from a region specific to BRAG1a. Comparison with panel A demonstrates that this probe gives a similar expression profile as that of the cDNA.

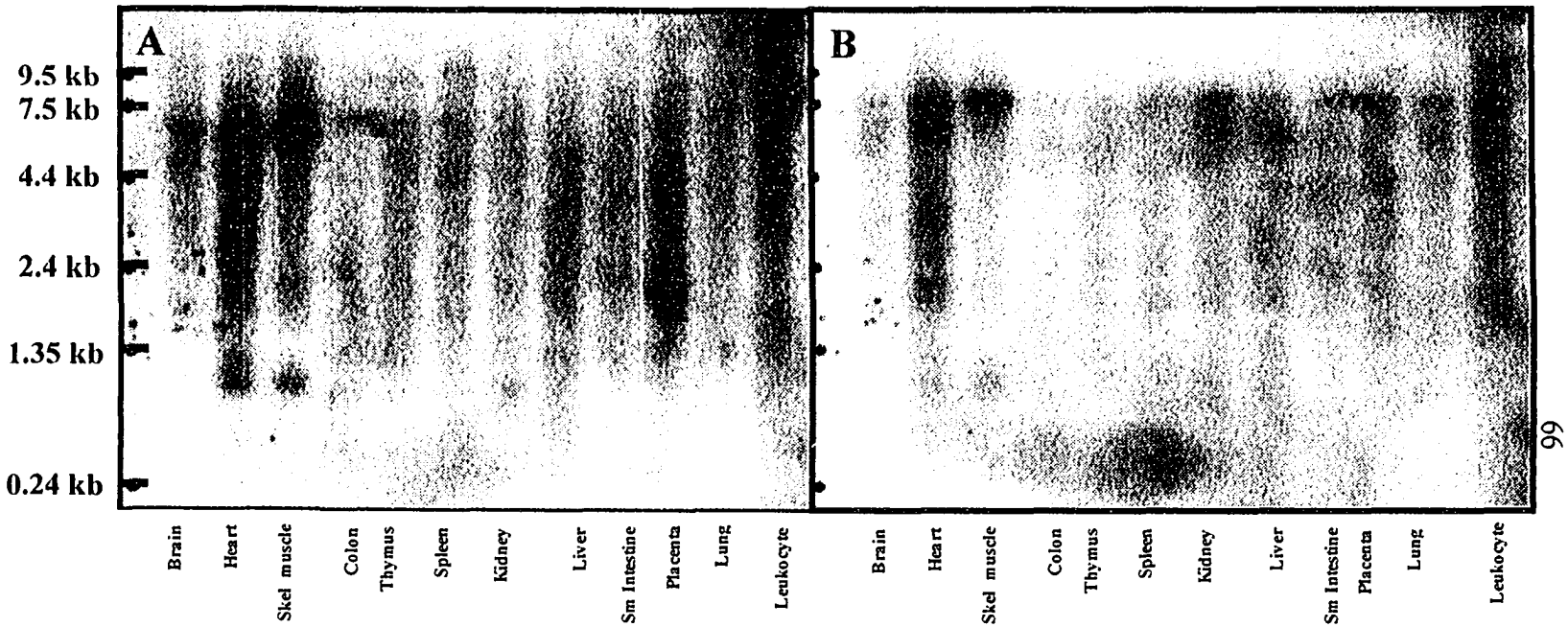

Figure 4.17 ***Northern blotting using the PH-domain probe and the BRAG1b/c probe shows striking dissimilarities***

Panel A. This panel shows a Northern blot obtained with the PH domain-derived probe and is the same as that shown in Panel A of Fig. 4.15

Panel B. This blot stripped and reprobed several times. The second probing was performed with a radiolabeled fragment derived from a region specific to BRAG1b,c. The BRAG-PH domain probe and the BRAG1b/c are both abundant in heart and skeletal muscle. Aside from this, the RNA species seen with the b/c probe seems more ubiquitous and the signal is a higher molecular weight than the PH-domain probe.

BRAG1b,c bearing cDNAs was more ubiquitous than observed with the two other probes. Indeed, signal was detected in samples from brain, heart, skeletal muscle, colon, liver, small intestine, placenta, lung and peripheral blood leukocyte. The size of the transcript was more homogeneous than observed with the cDNA and PH probes, with a single species detected at 6.6kb. Overlay of the three blots demonstrated that the BRAG1b/c transcripts were of identical size to the species detected in the colon sample by both the PH and cDNA probe and clearly larger than the major 6 kb species expressed in muscle tissues.

Because the BRAG1b/c probe detected a single species in a wide range of tissues, I postulate that either BRAG1b or BRAG1c play an important role in some housekeeping function of the cell. The other isoforms are likely to play a role in tissue specific development.

4.6 Localization of endogenous BRAG1

Initial localization studies focused on the endogenous protein expressed by normal rat kidney (NRK) cells, as RT-PCR data posted by the Kazusa Institute indicated abundant expression in that tissue (Fig 4.1). As shown at the beginning of this chapter in Figure 4.2, three types of staining were prevalent, a cytosolic pool, a plasma membrane pool and a Golgi pool (Fig. 4.2). Subsequent studies were focused primarily on the Golgi pool of BRAG1.

To investigate the intracellular localization of BRAG1 in more detail, I chose to first compare various fixation procedures to optimize resolution (see Chapter 2, for details). Affinity purified OB4 α-BRAG1 serum was used to localize BRAG1. These preliminary experiments established that methanol-acetone fixation yielded sharper images with less background than observed with paraformaldehyde. Furthermore, cross-linking of acetone-methanol fixed samples with 100μM *bis* (sulfosuccinamidyl) suberate (BS^3) prior to staining yielded further improvements in resolution.

I first examined the relative distribution of BRAG1 with that of mannosidase II (mannII), a well-characterized Golgi marker (Fig 4.18). This analysis confirmed that OB-4 stained a juxta-nuclear structure in a significant fraction of NRK cells. As shown in the merge panel on the right, there was extensive overlap between OB04 and mannII,

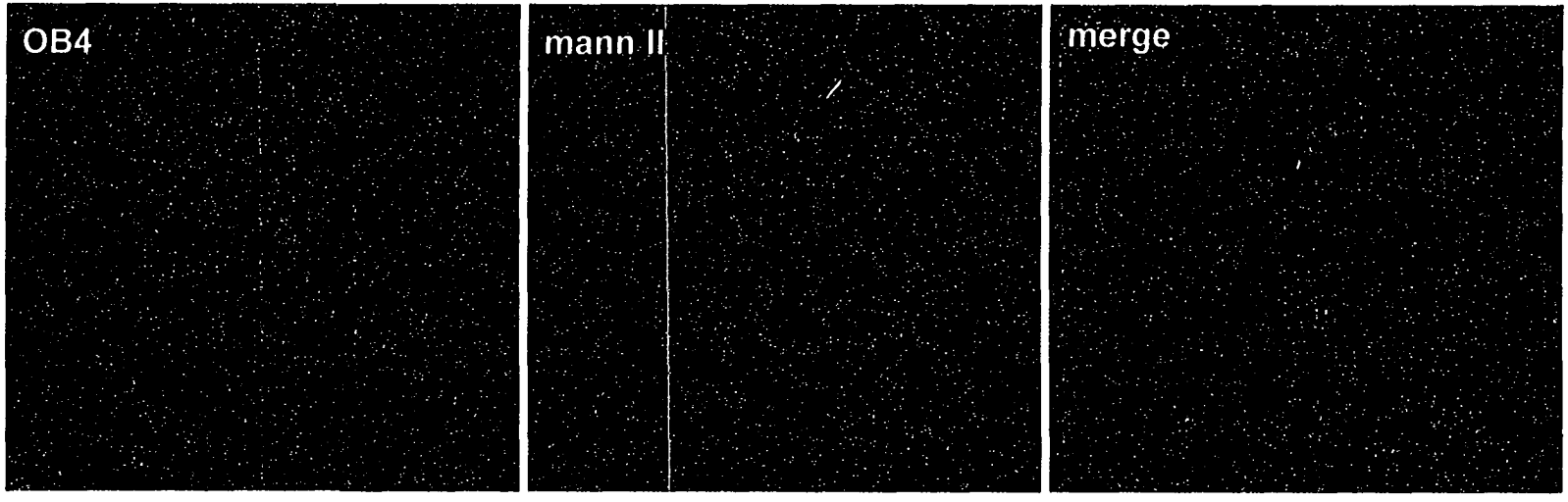

Figure 4.18 ***BRAG1 localizes to the*** **cis** ***Golgi***

BRAG1 localization was compared, by confocal microscopy, to the cis Golgi marker p115 and the medial Golgi marker (mannII). In the merged images, BRAG1 has some overlap with the medial Golgi marker, but nearly complete overlap with the p115 marker.

confirming that the juxtanuclear staining observed with OB-4 corresponded to Golgi localization.

Zhao et al showed that proteins can be resolved across the Golgi stack by confocal laser microscopy. As such I used a monoclonal antibody that recognizes α-p115 as a cis-Golgi marker, and transfected HA-furin as a *trans* Golgi marker (Fig 4.19). To better illustrate the differences in extent of signal overlap, I show in this figure a higher magnification of merged images. We see again that the BRAG1 signal overlaps significantly with mannII (Fig 4.19, middle panel). However, the OB4 signal is nearly completely coincident with p115 (Fig 4.19, left panel). These results suggested that BRAG1 localizes preferentially to cis-compartments of the Golgi complex in NRK cells. To test this more directly, I examined the relative distribution of endogenous BRAG1 and exogenously expressed HA-furin (Fig 4.19, right panel). In sharp contrast to complete or partial overlap observed with p115 and mann II, respectively (Figure 4.19 left panels), the BRAG1 signal was clearly distinct from the HA-furin (Fig 4.19, right panel).

There has been no effort to characterize the cytosolic or plasma membrane staining of BRAG1. I had originally thought that most of this was background staining since pre-incubation of the α-BRAG1 antibody with excess antigen prior to staining eliminated staining at both the plasma membrane and the Golgi and yielded instead strong nuclear staining (Fig 4.2).

4.7 Localization of overexpressed BRAG1 isoforms

To elucidate in more detail the relative role of the multiple splice forms described in the previous sections, I constructed mammalian expression vectors in which the unique BRAG1b,c 5' sequences identified by RACE were spliced with the remainder of the cDNA derived from KIAA0522 (see section 2.13 in Methods for details). Because of the questionable specificity (see Fig 4.2) and poor reliability of the OB4 antibody, I chose to create additional versions of BRAG1a, BRAG1b and BRAG1c modified with an epitope tag at the N-terminus. We expected tagged versions of these proteins to allow detection of transient transfectants with low level of expression. This is of interest because heavy over-expression might disrupt regular functioning of the cell. We would also be able to

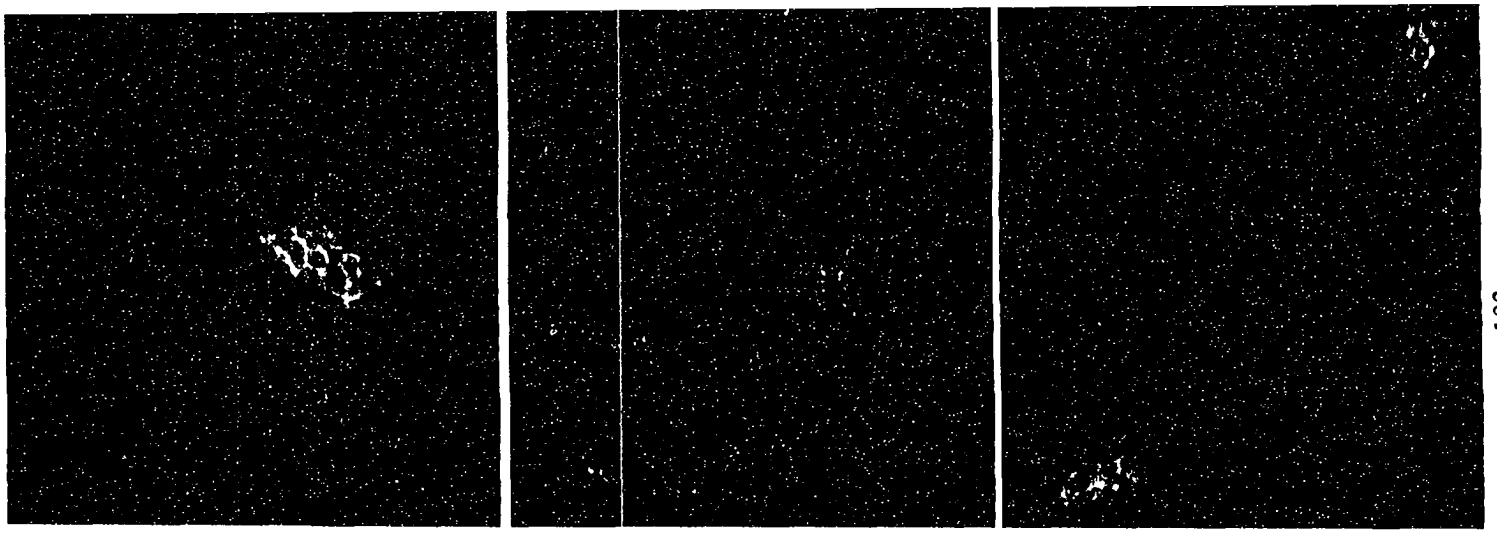

Figure 4.19 ***BRAG1 localizes primarily to cis-elements of the Golgi complex***

NRK cells were fixed and stained as described in Chapter 2. Images shown were obtained by confocal laser microscopy. The image in the left panel was obtained after staining cells with AP-OB4 and a monoclonal antibody raised against p115. The image in the center panel was obtained after staining cells with AP-OB4 and a monoclonal antibody raised against mannII. The image in the right panel was obtained after first transfecting cells with a plasmid encoding HA-tagged furin and staining cells with AP-OB4 and a monoclonal antibody raised against HA.

compare the tagged constructs to the affinity purified OB4 to determine if the antibody is reliable.

In the first attempt to immunolocalize these isoforms of BRAG1, I transfected pCEP4-derived plasmids encoding untagged BRAG1a and BRAG1c isoforms into NRK cells (Fig 4.20). The untagged BRAG1a reproducibly localized to discrete structures. However, as illustrated in Fig 4.20A-C, the nature of these structures varied widely between transfectants. In most cases, BRAG1a stained large and bright patches or the PM (Fig 20, top panels). In some cases, BRAG1 also localized to juxtanuclear structures that were also positive for the Golgi marker HA-furin (Fig 4.20, middle panels). In contrast, untagged BRAG1c displayed a primarily cytosolic, possibly reticular, pattern with no obvious concentration on juxtanuclear structures (Fig 4.20, bottom left panel) identified by the medial Golgi marker mannII (Fig 4.20, bottom right panel). In all cases, I observed very few transfectants stained with OB-4 and those showed very high expression levels. This might be a concern because it may disrupt cell physiology. The potentially disruptive effect of overexpression and the low frequency at which transfectants were identified precluded detailed characterization and made it very difficult to determine what to call representative data.

The VSV-G tagged versions of the BRAG1a gave a pattern dissimilar to the untagged forms (Fig 4.21). As mentioned above, NRK cells transfected with untagged forms of BRAG1a usually showed several large bright patches (Fig 4.21, top panels). In contrast, NRK cells transfected with the G-tagged form of BRAG1a showed abundant diffuse staining and lacked the clear labeling of variable but discrete structures (Fig 4.21, bottom panels). This suggests that N-terminal tagging interfered with localization of this isoform. In contrast, the G-tagged forms of BRAG1b and BRAG1c showed a diffuse somewhat reticular pattern similar to that observed with the untagged forms of these proteins (Fig 4.22).

To circumvent the problem with low transfection efficiency obtained with NRK cells, the constructs were transfected and expressed in BHK cells. Unfortunately the staining pattern of BRAG1 in BHK was dissimilar to that which was seen in NRK. This cell line was not pursued further.

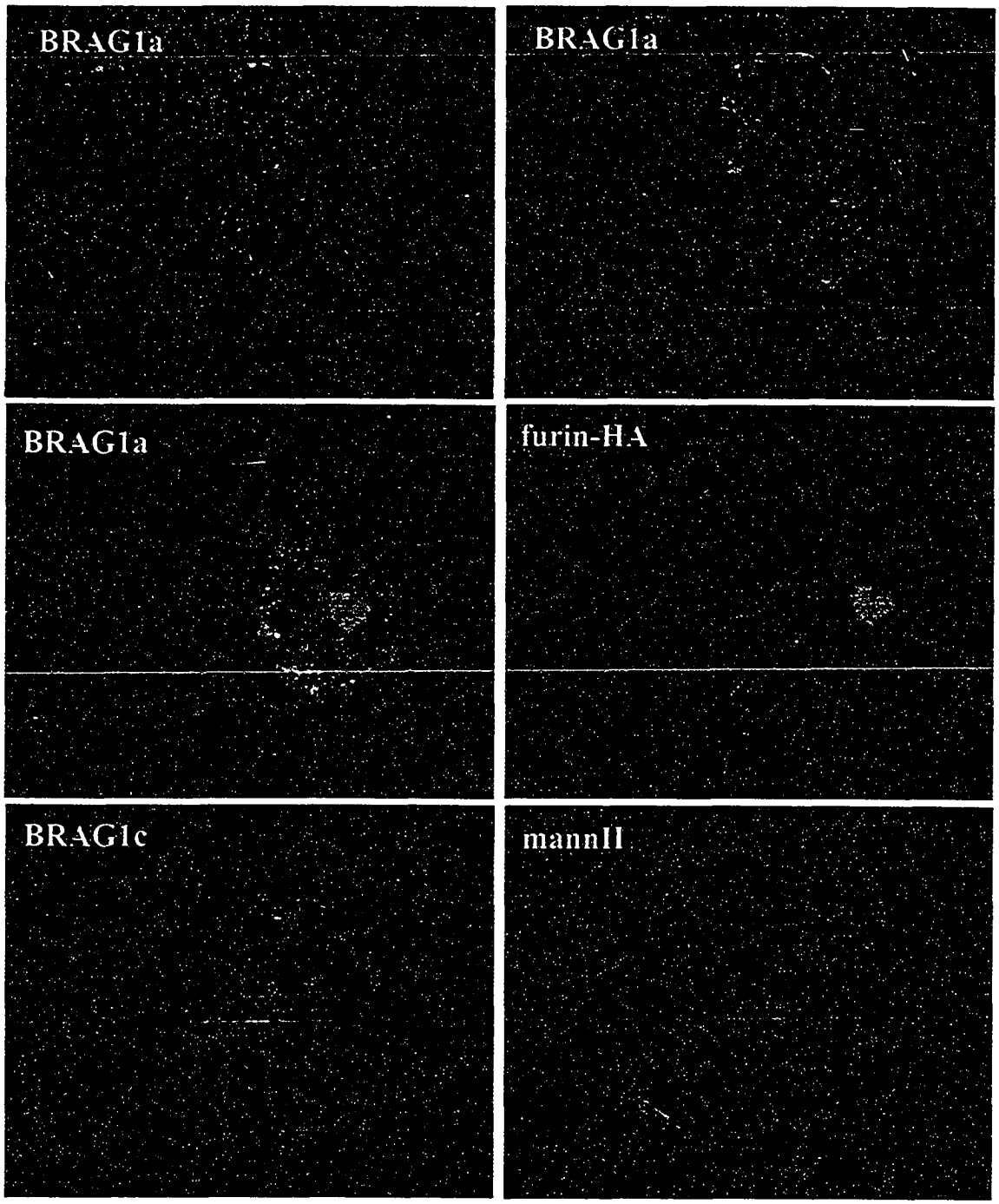

Figure 4.20 Overexpressed *BRAG1a accumulates at various locations in the cell*

Overexpressed BRAG1a (red) localizes to the plasma membrane, cytosol and large cytosolic punctae. Middle panels shows same cells staining either for BRAG1a of HA-furin. In contrast, BRAG1c displays more disperse reticular staining that does not coincide with the the medial Golgi marker, mannII shown in green.

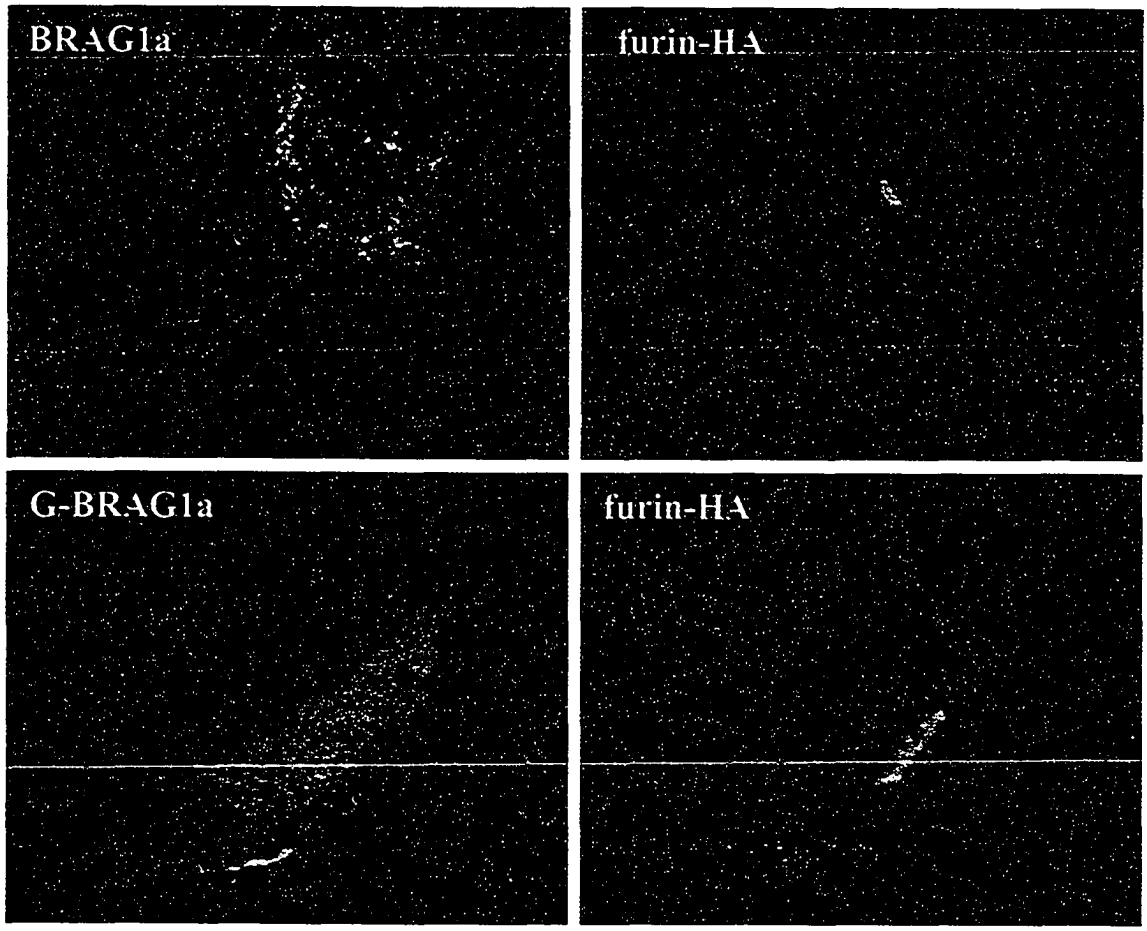

Figure 4.21 ***Tagging BRAG1a with the VSV-G epitope interferes with localization***

NRK cells were transfected with G-tagged and untagged BRAG1a. UntaggedBRAG1a localizes to punctae, while G-tagged BRAG1a/b/c are primarily cytosolic with some PM staining.

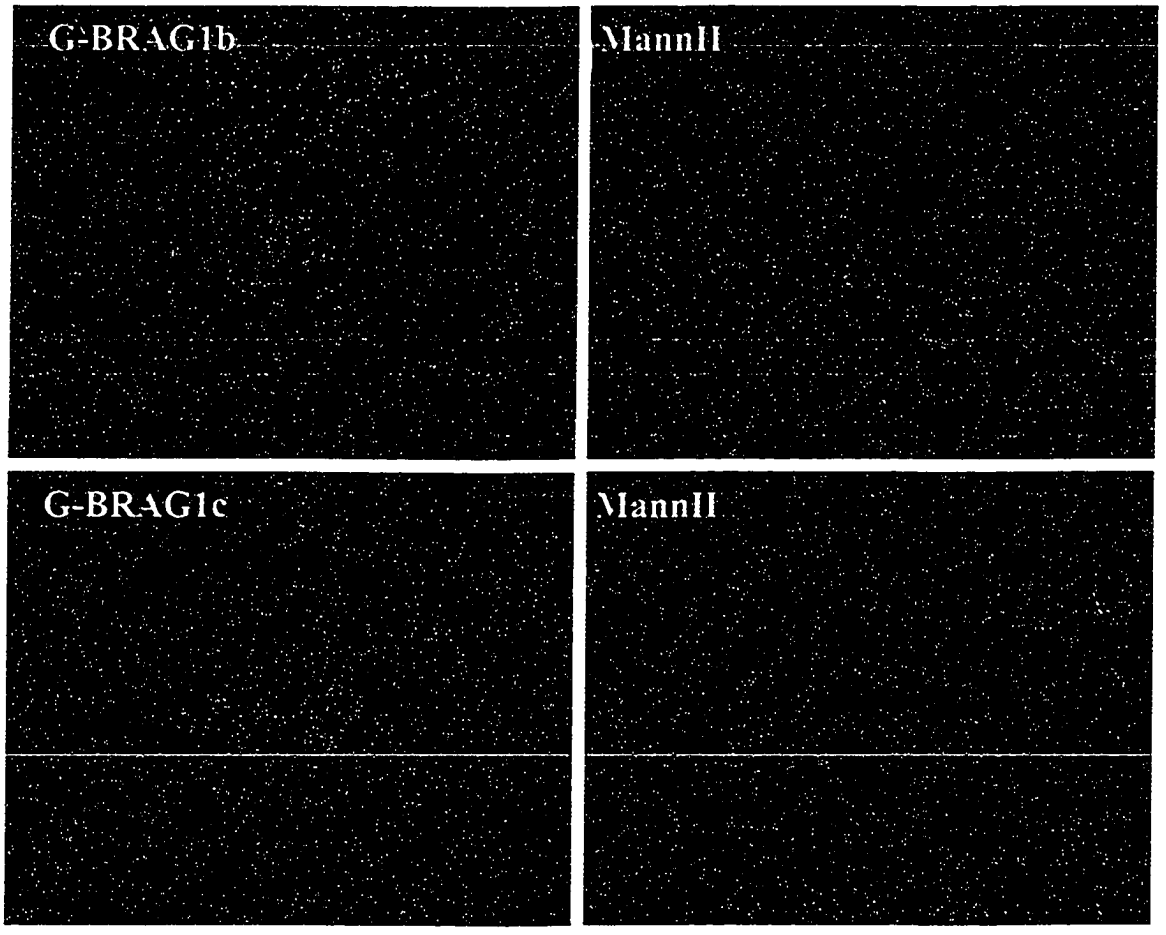

Figure 4.22 ***Tagging BRAG1b and BRAG1c with the VSV-G epitope does not interferes with localization***

NRK cells were transfected with G-tagged BRAG1b and BRAG1c. Untagged BRAG1b and c localizes to a fine reticular pattern clearly distinct from the juxtanuclear Golgi complex identified with the Golgi marker mannII.

4.8 CONSTRUCTION AND PRELIMINARY CHARACTERIZATION OF P5/TO VECTORS FOR BRAGA,B,C LOCALIZATION.

Because the pCEP4-based plasmids were not functioning as had been anticipated, we decided to re-tag the construct with several changes. Specifically, we wanted:

1. Smaller vector size. The first tagging attempt used pCEP4, which is a very large vector. To improve the transfection efficiency it was suggested that I should use a smaller vector.
2. C-terminal tag. The first attempt to tag the construct used an N-terminal tag. A C-terminal tag may yield better results, if the N-terminus plays an important functional role.
3. FLAG tag. There were some initial problems concerning the α-VSV-g antibody. There are many commercially available FLAG antibodies, including at least one with a sensitivity to Mg++.

I created tagged and untagged versions of BRAG1b,c and untagged versions of BRAG1b,c. p5/TO vectors expressing BRAG1a were planned but not obtained. Each plasmid DNA was then transfected into Hela cells and the distribution of overexpressed protein examined following induction with doxycycline. Protein distribution was examined using new polyclonal crude sera 3b2 and 3b5 raised more recently against the same antigen used originally for production of OB-4. Both antisera were able to detect BRAG1b, yielding strong reticular staining throughout the cytoplasm in some transfected cells, and a strong nuclear envelope staining in others (Fig 4.23). Figure 4.23 also compares the patterns observed with the old OB-4 and the better new serum 3B5 in NRK cells transfected with a vector encoding BRAG1b. The diffuse reticular pattern observed with OB-4 in NRK cells was similar to that observed in Hela cells. Surprisingly, 3B5 yielded a reticular pattern with pronounced nuclear rim in un-transfected cells NRK cells (Fig 4.23, bottom panels). Such a pattern was not observed with OB-4 (see Fig 4.2). We have no explanation for the variable distribution of endogenous BRAG1 in NRK cells.

The results of transfections of HeLa cells with the new BRAG1b,c vectors are similar to those obtained with the BRAG1-pCEP4 vectors. Transfectants expressing either untagged or FLAG-tagged BRAG1b,c appeared flatter and displayed characteristic cytosolic staining, or staining of the nuclear envelope with a fine reticulum throughout

the cytoplasm (Fig 4.24). The two sera gave similar results. Significantly, none of the transfectants displayed juxtanuclear staining similar to the Golgi pattern initially observed in NRK cells (see Fig 4.2).

In summary, 3B5 and OB4 detect distinct patterns for endogenous BRAG1 in NRK cells. Whereas OB-4 reveals primarily juxta-nuclear and PM staining, 3B5 shows a fine reticulum and clear nuclear rim. Overexpressed BRAG1a, like the endogenous rat protein, localizes to a variety of distinct structures such as peripheral punctae, juxtanuclear structure or PM; tagging BRAG1a with a G-epitope at the N-terminus abrogates this localization. In contrast, overexpressed BRAG1b and BRAG1c localize to a diffuse reticular pattern consistent with the ER. This pattern is similar to that detected for the endogenous protein with the 3B5 sera. Tagging with a FLAG epitope at the C-terminus does not impact the reticular staining of BRAG1b and BRAG1c.

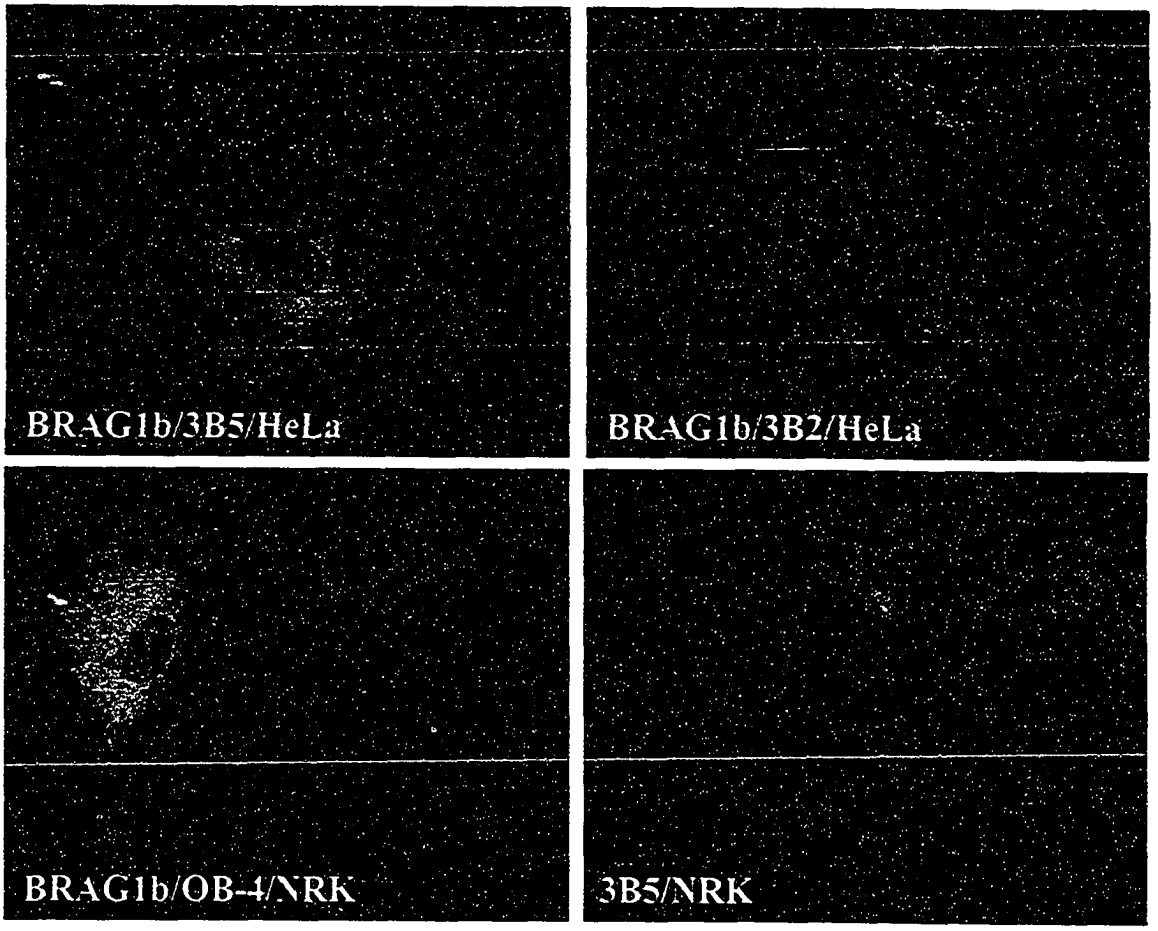

Figure 4.23 ***Characterization of new antiBRAG1 sera 3B2 and 3B5***

The OB4 antibody detects cytosolic, exogenous BRAG1b. The 3b2 antibody stains the nuclear membrane, with tubules emanating towards the cell periphery. 3b5 gives a similar phenotype to 3b2. These transfected cells are similar in signal to the endogenous BRAG1 in NRK.

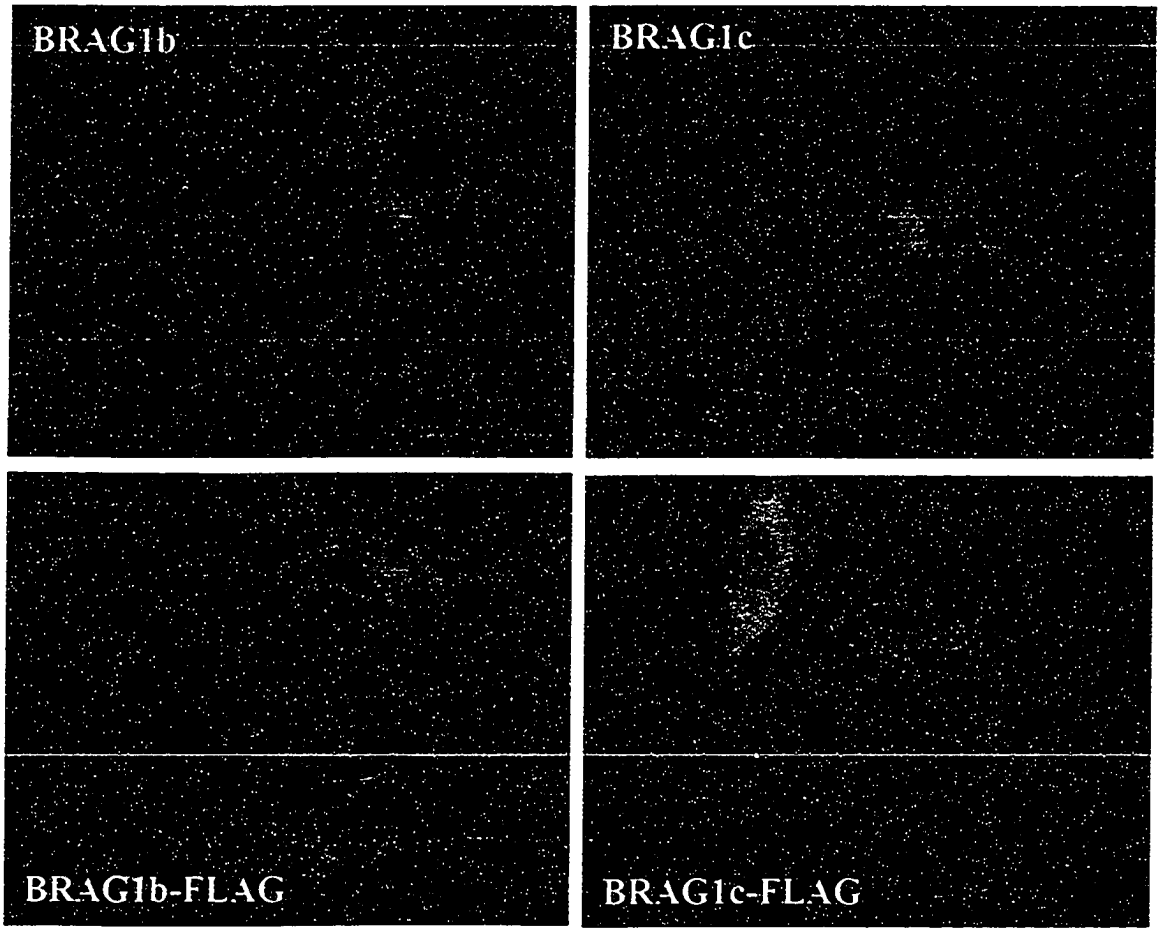

Figure 4.24 ***BRAG1b and BRAG1c tagged with the FLAG epitope at the C-terminus localize to a reticular pattern***

Cells were transfected with BRAG1b or BRAG1c, with or without a C-terminal FLAG epitope. For this experiment I used FITC to label BRAG structures, because the red channel was probed with with an anti-ER polyclonal. The untagged BRAG1b and c both localize to the nuclear membrane, with some cytosolic staining. This is not apparent in the FLAG-tagged constructs which are more cytosolic.

Chapter 5

Discussion

5.1 Identification of BRAGs

We have determined that the cDNAs KIAA0522, KIAA0763 and KIAA1110 form a novel family of ARF-GEFs. This is evident by pairwise BLAST searches, phylogenetic analysis, and comparison of the domain organization. These proteins are clearly larger than EFA6s and the ARNOs, but unlike the other large Arf-GEFs GBF1 and BIGs, they contain a PH domain. It is interesting to note that only GBF1 and BIGs are shared among all eukaryotes (Cox et al., 2004) and that all three classes of Arf-GEFs unique to metazoans contain PH domains. A clear function for these unique PH domains has not been established yet.

When we initially compared the three human BRAG cDNAs, we found that KIAA0522 was considerably longer than the other two cDNAs. This suggested that one or more of the cDNAs was a truncation, because we expected them all to be very similar in size. Of course this expectation proved to be true. The 5' RACE reactions performed with BRAG2 primers determined that BRAG2 was a partial cDNA. As discussed below, this result, and the presence of extra 5' sequence for BRAG3 were later confirmed by new Genebank submissions for all three clones.

5.2 Characterization of GST-tagged Sec7d truncation of BRAG1

The sec7 domain – GST truncations were initially tested for GEF activity on ARF5. I subsequently found that 5r3 was active on class I, II and III ARFs. In contrast, Vaughan and colleagues concluded that a recombinant form of BRAG2 activated Arf6 preferentially (Someya et al., 2001). Olson and colleagues reported similar specificity for class III Arfs with the single D. melanogaster BRAG called LONER (Chen et al., 2003).

The specificity of BRAG1 could be different *in vivo*, because other factors might add specificity to the GEF reaction, such as N- or C-termini or binding partners. Such change in specificity has been reported for ARNO1 that activates Arf1 preferentially over Arf6 *in vitro* but appears more selective for Arf6 *in vivo* (Macia et al., 2001); (Frank et al., 1998). It is also possible that BRAG1 is a highly promiscuous GEF. Of course, if the PH domains were spliced out of BRAG1b,c, there may be a soluble form of BRAG1 with altered substrate specificity.

It is interesting to note that the most active GEF truncation possesses the complete PH domain while the other two truncations tested do not (see Fig 3.1). This might be important because the PH domain could interact with phosphoinositides present on synthetic liposomes, thereby allowing recruitment to the membrane for productive interaction with Arf-GDP.

It is also interesting to note that GST forms a homo-dimer. This could mean that the 5r3 GST fusion proteins would dimerize through the GST. This is potentially important for BRAG1 activity, because other GEFs such as the BIGs or the ARNOs also dimerize (Yamaji et al., 2000); (Chardin, 1996). Therefore, even without the N- or C-termini, BRAG1 sec7 domain truncations may still act as dimers.

5.3 Identification of BRAG1 splice variants

5'RACE of BRAG1 was performed with two questions in mind. Is KIAA0522 truncated at the 5' end, and are there alternate beginnings for BRAG1. I used several primers with this method, but never retrieved product from the 5'RACE reactions based on exon 1 of BRAG1a. This might be because the KIAA0522 clone may only be expressed in tissues other than those that we used. Alternatively, the length of sequence between the true 5'end and exon 1 may be too long for amplification. I cannot exclude the possibility that the amplification reaction itself did not work.

To address the second question, I performed 5'RACE of BRAG1 using primers derived from exon 3 of KIAA0522. The random primed library yielded two major products that defined novel termini. These alternate 5'ends were cloned and named BRAG1b and BRAG1c respectively. The library created using BRAG1 specific primers produced yet another variant at a very high frequency (100% of clones tested). This BRAG1d was not further characterized. It seems to represent an even shorter version of BRAG1.

5'RACE of BRAG2 yielded three products, at 100bp, 450bp and 800bp. In my efforts, I completed the 5'end of KIAA0763 (450bp). It seems likely that the other bands also represent novel 5' variants of BRAG2. This would infer that BRAG2 is regulated in a manner similar to BRAG1.

I used PCR to confirm the existence of mRNAs containing the novel BRAG1b exon and exon 5 of BRAG1a (section 4.4.3). Further support for my BRAG1 5'RACE results and the existence of BRAG1b was recently provided by a new Genebank submission. An mRNA (AK095232; gi:21754444) with a 5'end identical to that of BRAG1c was isolated from tongue tissue. This cDNA is nearly identical over most of its length with the chimeric cDNA I assembled for BRAG1c and includes the exons that encode the PH domain. This observation demonstrates that the BRAG1b,c chimeras I assembled with the RACE products and the remaining 3' half of KIAA0522 are physiologically relevant. No evidence has yet been obtained for alternate splicing at the 5'end of BRAG3. However, a cDNA with homology to BRAG3 has been submitted that adds two novel exons to the 5' end of BRAG3 (gi: 21750435). More are likely to come.

A recent publication by Olson and colleagues demonstrated that the single drosophila BRAG, named LONER is vital to muscle development (Chen et al., 2003). This cDNA is most similar to BRAG1a. The authors also determined that LONER is subject to alternate splicing at the 5' end. Interestingly, none of the three splice forms published have homology to the BRAG1a/b/c/d isoforms.

Finally, it may be worth noting that AK095232 differs from the original KIAA0522 (AB011094.1; gi: 3043567) not at the 5'end but also at the 3'end. Direct comparison of these two sequences reveals that AK095232 lacks a stretch of 49 residues that corresponds to exon14. AK095232 is also shorter at the 3'end and lacks the last 1245 nt of KIAA0522. Interestingly, loss of exon 14 causes a frame-shift, which leads to premature translation termination after the first 12 nt of exon 15. This mRNA variant likely represents a splicing mistake. However, I cannot exclude the possibility that the protein with the truncated and alternate C-terminus may have alternate function.

5.4 Localization of BRAG1 splice variants

In NRK, the pCEP4-BRAG1a expression construct gave a distinct and reproducible localization. These large cytosolic blotches may represent aggregated protein, vacuoles, or even sites of attachment to the substrate. The BRAG1b and BRAG1c expression constructs seem to be reticular, surrounding the nucleus. All or none of these constructs may be localizing properly. The proper localization machinery

may not be expressed in the cell types used, which was shown to be important for LONER localization. Perhaps we detect extra localizations because the antibody may not be specific for the BRAG1 sec7 domain.

Furthermore, it is possible that BRAG1b/c that may be soluble (ie. no PH domain). This would explain the diffuse BRAG1 staining observed by immunofluorescence.

Vaughan and colleagues have demonstrated that GEP100/BRAG2 is most active on ARF6, and is found primarily at the PM and endosomes. This is expected because all sec7 domain proteins bearing PH domains are active at PM and endosomes. The surprising result was our localization of BRAG1 to the *cis*-Golgi, not only because of the PH domain, but because two family members, BRAG1 and BRAG2 do not possess similar localizations. All other ARF-GEF families are specifically active in a certain region of the cell, eg BIGs at the TGN, ARNOs at the PM and endosome.

5.5 Tissue specific expression of BRAG1 splice variants

Using the novel sequence derived from 5'RACE of BRAG1, I performed Northern blots with three probes corresponding to either sequences unique to BRAG1a and BRAG1b/c or sequences (PH domain) that we expected shared among all three isoforms all BRAGs.

Surprisingly, the PH domain probe gave an expression profile nearly identical to that of BRAG1a. I had expected that all of the splice variants would be represented in the PH domain blot. This turned out not to be true, since the higher molecular weight species detected with BRAG1b/c probe was clearly absent from the pattern observed with the other two probes. Furthermore, the large species recognized by the PH domain probe, like that observed with the BRAG1a probe, was particularly enriched in heart and skeletal muscle with some expression in brain and colon. Both of these patterns clearly differ from the more ubiquitous and slightly larger signal detected with the BRAG1b,c probe.

The wider, nearly ubiquitous distribution of BRAG1b/c suggests that it may be a housekeeping gene. The results obtained with this probe may have been different from those obtained with the BRAG1a and PH probes because the BRAG1b/c isoforms are expressed at very low levels. In this scenario, the signal observed with the PH probe

would be dominated by the more abundant BRAG1a species. On the other hand, the PH domain itself could be alternately spliced, as is observed with ARNO, for which alternate splicing yields PH domains with altered phosphoinositide binding characteristics (Ogasawara et al., 2000); (Cullen and Chardin, 2000). This may be important to the localization and function of BRAGs since the PH domain could allow responsiveness to changes in levels of phosphoinositides. Intracellular compartments vary not only in the level but also in the types of phosphoinositides they produce (De Matteis and Godi, 2004). Whereas the trans-Golgi cisternae produce primarily Pi4P, membranes of the endosomes contain PI3P and the PM PI(4,5)P2. Isoforms lacking the pH domain may therefore localize to different compartments.

AK095232 is a cDNA that has recently been submitted to Genebank. It includes all the sequence of BRAG1b, including the 5' BRAG1b N-terminus. Because this clone encodes a PH domain, I must conclude that at least some of the BRAG1b cDNAs do possess a PH domain. However, this does no preclude the possibility that some BRAG1b splice variants lack PH domains.

5.6 Final comments

The alternate splicing of BRAGs may provide a new paradigm in regulation of the central vacuolar system. In this model, the BRAGs consist of the central sec7 domain flanked by variable termini. These alternate termini might confer different localization, different coats, effectors, membership to large molecular complexes, GAPs, ARF specificity and homo/hetero-oligomerization.

CHAPTER 6

References

REFERENCES

Aikawa, Y., and T.F. Martin. 2003. ARF6 regulates a plasma membrane pool of phosphatidylinositol(4,5)bisphosphate required for regulated exocytosis. *J Cell Biol.* 162:647-59.

Al-Awar, O., H. Radhakrishna, N.N. Powell, and J.G. Donaldson. 2000. Separation of membrane trafficking and actin remodeling functions of ARF6 with an effector domain mutant. *Mol Cell Biol.* 20:5998-6007.

Antonny, B., S. Beraud-Dufour, P. Chardin, and M. Chabre. 1997. N-terminal hydrophobic residues of the G-protein ADP-ribosylation factor-1 insert into membrane phospholipids upon GDP to GTP exchange. *Biochemistry.* 36:4675-84.

Antonny, B., D. Madden, S. Hamamoto, L. Orci, and R. Schekman. 2001. Dynamics of the COPII coat with GTP and stable analogues. *Nat Cell Biol.* 3:531-7.

Antonny, B., and R. Schekman. 2001. ER export: public transportation by the COPII coach. *Curr Opin Cell Biol.* 13:438-43.

Aoe, T., I. Huber, C. Vasudevan, S.C. Watkins, G. Romero, D. Cassel, and V.W. Hsu. 1999. The KDEL receptor regulates a GTPase-activating protein for ADP-ribosylation factor 1 by interacting with its non-catalytic domain. *Journal of Biological Chemistry.* 274:20545-9.

Aridor, M., K.N. Fish, S. Bannykh, J. Weissman, T.H. Roberts, J. Lippincott-Schwartz, and W.E. Balch. 2001. The Sar1 GTPase coordinates biosynthetic cargo selection with endoplasmic reticulum export site assembly. *Journal of Cell Biology.* 152:213-29.

Aridor, M., J. Weissman, S. Bannykh, C. Nuoffer, and W.E. Balch. 1998. Cargo selection by the COPII budding machinery during export from the ER. *J Cell Biol.* 141:61-70.

Bader, M.F., F. Doussau, S. Chasserot-Golaz, N. Vitale, and S. Gasman. 2004. Coupling actin and membrane dynamics during calcium-regulated exocytosis: a role for Rho and ARF GTPases. *Biochim Biophys Acta.* 1742:37-49.

Bannykh, S.I., and W.E. Balch. 1997. Membrane dynamics at the endoplasmic reticulum-Golgi interface. *J Cell Biol.* 138:1-4.

Bannykh, S.I., T. Rowe, and W.E. Balch. 1996. The organization of endoplasmic reticulum export complexes. *J Cell Biol.* 135:19-35.

Barlowe, C. 2003a. Molecular recognition of cargo by the COPII complex: a most accommodating coat. *Cell.* 114:395-7.

Barlowe, C. 2003b. Signals for COPII-dependent export from the ER: what's the ticket out? *Trends Cell Biol.* 13:295-300.

Barr, F.A., and B. Short. 2003. Golgins in the structure and dynamics of the Golgi apparatus. *Curr Opin Cell Biol.* 15:405-13.

Beraud-Dufour, S., S. Robineau, P. Chardin, S. Paris, M. Chabre, J. Cherfils, and B. Antonny. 1998. A glutamic finger in the guanine nucleotide exchange factor ARNO displaces Mg2+ and the beta-phosphate to destabilize GDP on ARF1. *Embo J.* 17:3651-9.

Berger, S.J., K.A. Resing, T.C. Taylor, and P. Melancon. 1995. Mass-spectrometric analysis of ADP-ribosylation factors from bovine brain: identification and evidence for homogeneous acylation with the C14:0 fatty acid (myristate). *Biochem J.* 311:125-32.

Bevis, B.J., and B.S. Glick. 2002. Rapidly maturing variants of the Discosoma red fluorescent protein (DsRed). *Nat Biotechnol.* 20:83-7.

Bi, X., R.A. Corpina, and J. Goldberg. 2002. Structure of the Sec23/24-Sar1 pre-budding complex of the COPII vesicle coat. *Nature*. 419:271-7.

Bigay, J., P. Gounon, S. Robineau, and B. Antonny. 2003. Lipid packing sensed by ArfGAP1 couples COPI coat disassembly to membrane bilayer curvature. *Nature*. 426:563-6.

Block, M.R., B.S. Glick, C.A. Wilcox, F.T. Wieland, and J.E. Rothman. 1988. Purification of an N-ethylmaleimide-sensitive protein catalyzing vesicular transport. *Proc Natl Acad Sci U S A*. 85:7852-6.

Bock, J.B., H.T. Matern, A.A. Peden, and R.H. Scheller. 2001. A genomic perspective on membrane compartment organization. *Nature*. 409:839-41.

Boman, A.L., and R.A. Kahn. 1995. Arf proteins: the membrane traffic police? *Trends Biochem Sci*. 20:147-50.

Boman, A.L., C. Zhang, X. Zhu, and R.A. Kahn. 2000. A family of ADP-ribosylation factor effectors that can alter membrane transport through the trans-Golgi. *Mol Biol Cell*. 11:1241-55.

Bonifacino, J.S. 2004. The GGA proteins: adaptors on the move. *Nat Rev Mol Cell Biol*. 5:23-32.

Bonifacino, J.S., and B.S. Glick. 2004. The mechanisms of vesicle budding and fusion. *Cell*. 116:153-66.

Bonifacino, J.S., and C.L. Jackson. 2003. Endosome-specific localization and function of the ARF activator GNOM. *Cell*. 112:141-2.

Bonifacino, J.S., and J. Lippincott-Schwartz. 2003. Coat proteins: shaping membrane transport. *Nat Rev Mol Cell Biol*. 4:409-14.

Bremser, M., W. Nickel, M. Schweikert, M. Ravazzola, M. Amherdt, C.A. Hughes, T.H. Sollner, J.E. Rothman, and F.T. Wieland. 1999. Coupling of coat assembly and vesicle budding to packaging of putative cargo receptors. *Cell*. 96:495-506.

Brown, F.D., A.L. Rozelle, H.L. Yin, T. Balla, and J.G. Donaldson. 2001. Phosphatidylinositol 4,5-bisphosphate and Arf6-regulated membrane traffic. *J Cell Biol*. 154:1007-17.

Burd, C.G., T.I. Strochlic, and S.R. Gangi Setty. 2004. Arf-like GTPases: not so Arf-like after all. *Trends Cell Biol*. 14:687-94.

Burridge, K., and K. Wennerberg. 2004. Rho and Rac take center stage. *Cell*. 116:167-79.

Busch, M., U. Mayer, and G. Jürgens. 1996. Molecular analysis of the Arabidopsis pattern-formation gene GNOM: gene structure and intragenic complementation. *Molec. Gen. Genet*. 250: 681-691.

Carlton, J., M. Bujny, B.J. Peter, V.M. Oorschot, A. Rutherford, H. Mellor, J. Klumperman, H.T. McMahon, and P.J. Cullen. 2004. Sorting nexin-1 mediates tubular endosome-to-TGN transport through coincidence sensing of high- curvature membranes and 3-phosphoinositides. *Curr Biol*. 14:1791-800.

Chardin, P., Paris, S., Antonny, B., Robineau, S., Beraud-Dufour, S., Jackson, C.L. and Chabre, M. 1996. A human exchange factor for ARF contains sec7 and pleckstrin-homology domains. *Nature*. 384:481-484.

Chen, E.H., and E.N. Olson. 2004. Towards a molecular pathway for myoblast fusion in Drosophila. *Trends Cell Biol*. 14:452-60.

Chen, E.H., B.A. Pryce, J.A. Tzeng, G.A. Gonzalez, and E.N. Olson. 2003. Control of myoblast fusion by a guanine nucleotide exchange factor, loner, and its effector ARF6. *Cell.* 114:751-62.

Claing, A.e.a. 2001. Beta arrestin-mediated ARF6 activation and beta2-adrenergic receptor

endocytosis. *J. Biol. Chem.* epub.

Clary, D.O., I.C. Griff, and J.E. Rothman. 1990. SNAPs, a family of NSF attachment proteins involved in intracellular membrane fusion in animals and yeast. *Cell.* 61:709-21.

Claude, A., B.P. Zhao, C.E. Kuziemsky, S. Dahan, S.J. Berger, J.P. Yan, A.D. Armold, E.M. Sullivan, and P. Melancon. 1999. GBF1: A novel Golgi-associated BFA-resistant guanine nucleotide exchange factor that displays specificity for ADP-ribosylation factor 5. *J Cell Biol.* 146:71-84.

Corthesy-Theulaz, I., A. Pauloin, and S.R. Pfeffer. 1992. Cytoplasmic dynein participates in the centrosomal localization of the Golgi complex. *J Cell Biol.* 118:1333-45.

Cosson, P., and F. Letourner. 1994. Coatomer interaction with dilysine endoplasmic reticulum retention motifs. *Science.* 263:1629-1631.

Cox, R., R.J. Mason-Gamer, C.L. Jackson, and N. Segev. 2004. Phylogenetic analysis of Sec7-domain-containing Arf nucleotide exchangers. *Mol Biol Cell.* 15:1487-505.

Cukierman, E., I. Huber, M. Rotman, and D. Cassel. 1995. The ARF1 GTPase-activating protein: zinc finger motif and Golgi complex localization. *Science.* 270:1999-2002.

Cullen, P.J., and P. Chardin. 2000. Membrane targeting: what a difference a G makes. *Curr Biol.* 10:R876-8.

D'Souza-Schorey, C., G. Li, M.I. Colombo, and P.D. Stahl. 1995. A regulatory role for ARF6 in receptor-mediated endocytosis. *Science.* 267:1175-8.

De Matteis, M.A., and A. Godi. 2004. Protein-lipid interactions in membrane trafficking at the Golgi complex. *Biochim Biophys Acta.* 1666:264-74.

Derrien, V., C. Couillault, M. Franco, S. Martineau, P. Montcourrier, R. Houlgatte, and P. Chavrier. 2002. A conserved C-terminal domain of EFA6-family ARF6-guanine nucleotide exchange factors induces lengthening of microvilli-like membrane protrusions. *J Cell Sci.* 115:2867-79.

Donaldson, J.G. 2003. Multiple roles for Arf6: sorting, structuring, and signaling at the plasma membrane. *J Biol Chem.* 278:41573-6.

Dupre, S., D. Urban-Grimal, and R. Haguenauer-Tsapis. 2004. Ubiquitin and endocytic internalization in yeast and animal cells. *Biochim Biophys Acta.* 1695:89-111.

Eitzen, G. 2003. Actin remodeling to facilitate membrane fusion. *Biochim Biophys Acta.* 1641:175-81.

Eitzen, G., N. Thorngren, and W. Wickner. 2001. Rho1p and Cdc42p act after Ypt7p to regulate vacuole docking. *Embo J.* 20:5650-6.

Engqvist-Goldstein, A.E., and D.G. Drubin. 2003. Actin assembly and endocytosis: from yeast to mammals. *Annu Rev Cell Dev Biol.* 19:287-332.

Franco, M., J. Boretto, S. Robineau, S. Monier, B. Goud, P. Chardin, and P. Chavrier. 1998. ARNO3, a Sec7-domain guanine nucleotide exchange factor for ADP ribosylation factor 1, is involved in the control of Golgi structure and function. *Proc Natl Acad Sci U S A.* 95:9926-31.

Franco, M., P. Chardin, M. Chabre, and S. Paris. 1996. Myristoylation-facilitated binding of the G protein ARF1GDP to membrane phospholipids is required for its activation by a soluble nucleotide exchange factor. *J Biol Chem.* 271:1573-8.

Franco, M., P.J. Peters, J. Boretto, E. van Donselaar, A. Neri, C. D'Souza-Schorey, and P. Chavrier. 1999. EFA6, a sec7 domain-containing exchange factor for ARF6, coordinates membrane recycling and actin cytoskeleton organization. *Embo J.* 18:1480-91.

Frank, S., S. Upender, S.H. Hansen, and J.E. Casanova. 1998. ARNO is a guanine nucleotide exchange factor for ADP-ribosylation factor 6. *J Biol Chem.* 273:23-7.

Gillingham, A.K., and S. Munro. 2003. Long coiled-coil proteins and membrane traffic. *Biochim Biophys Acta.* 1641:71-85.

Goldberg, J. 1998. Structural basis for activation of ARF GTPase: mechanisms of guanine nucleotide exchange and GTP-myristoyl switching. *Cell.* 95:237-48.

Goldberg, J. 1999. Structural and functional analysis of the ARF1-ARFGAP complex reveals a role for coatomer in GTP hydrolysis. *Cell.* 96:893-902.

Graham, T.R. 2004. Membrane targeting: getting Arl to the Golgi. *Curr Biol.* 14:R483-5.

Grebe, M., J. Gadea, T. Steinmann, M. Kientz, J.U. Rahfeld, K. Salchert, C. Koncz, and G. Jurgens. 2000. A conserved domain of the arabidopsis GNOM protein mediates subunit interaction and cyclophilin 5 binding. *Plant Cell.* 12:343-56.

Hammer, J.A., 3rd, and X.S. Wu. 2002. Rabs grab motors: defining the connections between Rab GTPases and motor proteins. *Curr Opin Cell Biol.* 14:69-75.

Holthuis, J.C., and K.N. Burger. 2003. Sensing membrane curvature. *Dev Cell.* 5:821-2.

Houndolo, T., P.L. Boulay, and A. Claing. 2005. G protein-coupled receptor endocytosis in ADP-ribosylation factor 6-depleted cells. *J Biol Chem.* 280:5598-604.

Huang, M., J.T. Weissman, S. Beraud-Dufour, P. Luan, C. Wang, W. Chen, M. Aridor, I.A. Wilson, and W.E. Balch. 2001. Crystal structure of Sar1-GDP at 1.7 A resolution and the role of the NH2 terminus in ER export. *J Cell Biol.* 155:937-48.

Hunzicker-Dunn, M., V.V. Gurevich, J.E. Casanova, and S. Mukherjee. 2002. ARF6: a newly appreciated player in G protein-coupled receptor desensitization. *FEBS Lett.* 521:3-8.

Jackson, C.L., and J.E. Casanova. 2000. Turning on ARF: the Sec7 family of guanine-nucleotide-exchange factors. *Trends Cell Biol.* 10:60-7.

Jahn, R., T. Lang, and T.C. Sudhof. 2003. Membrane fusion. *Cell.* 112:519-33.

Johannes, L., and C. Lamaze. 2002. Clathrin-dependent or not: is it still the question? *Traffic.* 3:443-51.

Kahn, R.A., J. Clark, C. Rulka, T. Stearns, C.J. Zhang, P.A. Randazzo, T. Terui, and M. Cavenagh. 1995. Mutational analysis of Saccharomyces cerevisiae ARF1. *J Biol Chem.* 270:143-50.

Kam, J.L., K. Miura, T.R. Jackson, J. Gruschus, P. Roller, S. Stauffer, J. Clark, R. Aneja, and P.A. Randazzo. 2000. Phosphoinositide-dependent activation of the ADP-ribosylation factor GTPase-activating protein ASAP1. Evidence for the pleckstrin homology domain functioning as an allosteric site. *J Biol Chem.* 275:9653-63.

Kawamoto, K., Y. Yoshida, H. Tamaki, S. Torii, C. Shinotsuka, S. Yamashina, and K. Nakayama. 2002. GBF1, a Guanine Nucleotide Exchange Factor for ADP-Ribosylation Factors, is Localized to the cis-Golgi and Involved in Membrane Association of the COPI Coat. *Traffic.* 3:483-95.

Klarlund, J.K., L.E. Rameh, L.C. Cantley, J.M. Buxton, J.J. Holik, C. Sakelis, V. Patki, S. Corvera, and M.P. Czech. 1998. Regulation of GRP1-catalyzed ADP ribosylation factor guanine nucleotide exchange by phosphatidylinositol 3,4,5-trisphosphate. *J Biol Chem.* 273:1859-62.

Klarlund, J.K., W. Tsiaras, J.J. Holik, A. Chawla, and M.P. Czech. 2000. Distinct polyphosphoinositide binding selectivities for pleckstrin homology domains of GRP1-like proteins based on diglycine versus triglycine motifs. *J Biol Chem.* 275:32816-21.

Ladinsky, M.S., D.N. Mastronarde, J.R. McIntosh, K.E. Howell, and L.A. Staehelin. 1999. Golgi structure in three dimensions: functional insights from the normal rat kidney cell. *J Cell Biol.* 144:1135-49.

Ladinsky, M.S., C.C. Wu, S. McIntosh, J.R. McIntosh, and K.E. Howell. 2002. Structure of the Golgi and Distribution of Reporter Molecules at 20 degrees C Reveals the Complexity of the Exit Compartments. *Mol Biol Cell.* 13:2810-25.

Laemmli, U.K., and F.A. Eiserling. 1968. Studies on the morphopoiesis of the head of phage T-even. V. The formation of polyheads. *Mol Gen Genet.* 101:333-45.

Lanoix, J., J. Ouwendijk, A. Stark, E. Szafer, D. Cassel, K. Dejgaard, M. Weiss, and T. Nilsson. 2001. Sorting of Golgi resident proteins into different subpopulations of COPI vesicles: a role for ArfGAP1. *J Cell Biol.* 155:1199-212.

Lee, M.C., E.A. Miller, J. Goldberg, L. Orci, and R. Schekman. 2004. Bi-directional protein transport between the ER and Golgi. *Annu Rev Cell Dev Biol.* 20:87-123.

Lee, M.C., and R. Schekman. 2004. Cell biology. BAR domains go on a bender. *Science.* 303:479-80.

Lee, S.Y., and B. Pohajdak. 2000. N-terminal targeting of guanine nucleotide exchange factors (GEF) for ADP ribosylation factors (ARF) to the Golgi. *J Cell Sci.* 113:1883-9.

Lefkowitz, R.J., and E.J. Whalen. 2004. beta-arrestins: traffic cops of cell signaling. *Curr Opin Cell Biol.* 16:162-8.

Letourneur, F., E.C. Gaynor, S. Hennecke, C. Demolliere, R. Duden, S.D. Emr, H. Riezman, and P. Cosson. 1994. Coatomer is essential for retrival of dilysine-tagged proteins to the endoplasmic reticulum. *Cell.* 79:1199-1207.

Liang, J.O., T.C. Sung, A.J. Morris, M.A. Frohman, and S. Kornfeld. 1997. Different domains of mammalian ADP-ribosylation factor 1 mediate interaction with selected target proteins. *J Biol Chem.* 272:33001-8.

Lippincott-Schwartz, J., L. Yuan, C. Tipper, M. Amherdt, L. Orci, and R.D. Klausner. 1991. Brefeldin A's effects on endosomes, lysosomes, and the TGN suggest a general mechanism for regulating organelle structure and membrane traffic. *Cell.* 67:601-16.

Macia, E., M. Chabre, and M. Franco. 2001. Specificities for the small g proteins arf1 and arf6 of the guanine nucleotide exchange factors arno and efa6. *J Biol Chem.* 276:24925-30.

Mansour, S.J., J.A. Herbrick, S.W. Scherer, and P. Melancon. 1998. Human GBF1 is a ubiquitously expressed gene of the sec7 domain family mapping to 10q24 [In Process Citation]. *Genomics.* 54:323-7.

Mansour, S.J., J. Skaug, X.H. Zhao, J. Giordano, S.W. Scherer, and P. Melancon. 1999. p200 ARF-GEP1: a Golgi-localized guanine nucleotide exchange protein whose Sec7 domain is targeted by the drug brefeldin A. *Proc Natl Acad Sci U S A.* 96:7968-73.

Marsh, B.J., D.N. Mastronarde, J.R. McIntosh, and K.E. Howell. 2001. Structural evidence for multiple transport mechanisms through the Golgi in the pancreatic beta-cell line, HIT-T15. *Biochem Soc Trans.* 29:461-7.

Martinez, O., C. Antony, G. Pehau-Arnaudet, E.G. Berger, J. Salamero, and B. Goud. 1997. GTP-bound forms of rab6 induce the redistribution of Golgi proteins into the endoplasmic reticulum. *Proc Natl Acad Sci U S A.* 94:1828-33.

Martinez-Menarguez, J.A., H.J. Geuze, J.W. Slot, and J. Klumperman. 1999. Vesicular tubular clusters between the ER and Golgi mediate concentration of soluble secretory proteins by exclusion from COPI-coated vesicles. *Cell.* 98:81-90.

Matsuoka, K., L. Orci, M. Amherdt, S.Y. Bednarek, S. Hamamoto, R. Schekman, and T. Yeung. 1998. COPII-coated vesicle formation reconstituted with purified coat proteins and chemically defined liposomes. *Cell.* 93:263-75.

McNew, J.A., F. Parlati, R. Fukuda, R.J. Johnston, K. Paz, F. Paumet, T.H. Sollner, and J.E. Rothman. 2000. Compartmental specificity of cellular membrane fusion encoded in SNARE proteins. *Nature.* 407:153-9.

Melancon, P., B.S. Glick, V. Malhotra, P.J. Weidman, T. Serafini, M.L. Gleason, L. Orci, and J.E. Rothman. 1987. Involvement of GTP-binding "G" proteins in transport through the Golgi stack. *Cell.* 51:1053-62.

Melancon, P., X. Zhao, and T.K. Lasell. 2004. Large Arf-GEFs of the Golgi complex: In search of mechanisms for the cellular effects of BFA. *In* ARF Family GTPases. R.A. Kahn, editor. Kluwer Academic Publishers, Dordrecht. 101-119.

Miller, E., B. Antonny, S. Hamamoto, and R. Schekman. 2002. Cargo selection into COPII vesicles is driven by the Sec24p subunit. *Embo J.* 21:6105-13.

Miller, E.A., T.H. Beilharz, P.N. Malkus, M.C. Lee, S. Hamamoto, L. Orci, and R. Schekman. 2003. Multiple cargo binding sites on the COPII subunit Sec24p ensure capture of diverse membrane proteins into transport vesicles. *Cell.* 114:497-509.

Miura, K., K.M. Jacques, S. Stauffer, A. Kubosaki, K. Zhu, D.S. Hirsch, J. Resau, Y. Zheng, and P.A. Randazzo. 2002. ARAP1: a point of convergence for Arf and Rho signaling. *Mol Cell.* 9:109-19.

Mogelsvang, S., B.J. Marsh, M.S. Ladinsky, and K.E. Howell. 2004. Predicting function from structure: 3D structure studies of the mammalian Golgi complex. *Traffic.* 5:338-45.

Morinaga, N., J. Moss, and M. Vaughan. 1997. Cloning and expression of a cDNA encoding a bovine brain brefeldin A- sensitive guanine nucleotide-exchange protein for ADP-ribosylation factor. *Proc Natl Acad Sci U S A.* 94:12926-31.

Morinaga, N., S.C. Tsai, J. Moss, and M. Vaughan. 1996. Isolation of a brefeldin A-inhibited guanine nucleotide-exchange protein for ADP ribosylation factor (ARF) 1 and ARF3 that contains a Sec7-like domain. *Proc Natl Acad Sci U S A.* 93:12856-60.

Mossessova, E., L.C. Bickford, and J. Goldberg. 2003. SNARE selectivity of the COPII coat. *Cell.* 114:483-95.

Mouratou, B., V. Biou, A. Joubert, J. Cohen, D.J. Shields, N. Geldner, G. Jurgens, P. Melancon, and J. Cherfils. 2005. The domain architecture of large guanine nucleotide exchange factors for the small GTP-binding protein Arf. *BMC Genomics.* 6:20.

Muller, O., D.I. Johnson, and A. Mayer. 2001. Cdc42p functions at the docking stage of yeast vacuole membrane fusion. *Embo J.* 20:5657-65.

Muniz, M., P. Morsomme, and H. Riezman. 2001. Protein sorting upon exit from the endoplasmic reticulum. *Cell*. 104:313-20.

Nabi, I.R., and P.U. Le. 2003. Caveolae/raft-dependent endocytosis. *J Cell Biol*. 161:673-7.

Nie, Z., M. Boehm, E.S. Boja, W.C. Vass, J.S. Bonifacino, H.M. Fales, and P.A. Randazzo. 2003a. Specific regulation of the adaptor protein complex AP-3 by the Arf GAP AGAP1. *Dev Cell*. 5:513-21.

Nie, Z., D.S. Hirsch, and P.A. Randazzo. 2003b. Arf and its many interactors. *Curr Opin Cell Biol*. 15:396-404.

Ogasawara, M., S.C. Kim, R. Adamik, A. Togawa, V.J. Ferrans, K. Takeda, M. Kirby, J. Moss, and M. Vaughan. 2000. Similarities in function and gene structure of cytohesin-4 and cytohesin-1, guanine nucleotide-exchange proteins for ADP-ribosylation factors. *J Biol Chem*. 275:3221-30.

Oka, T., and M. Krieger. 2005. Multi-component protein complexes and Golgi membrane trafficking. *J Biochem (Tokyo)*. 137:109-14.

Oprins, A., R. Duden, T.E. Kreis, H.J. Geuze, and J.W. Slot. 1993. Beta-COP localizes mainly to the cis-Golgi side in exocrine pancreas. *J Cell Biol*. 121:49-59.

Oprins, A., C. Rabouille, G. Posthuma, J. Klumperman, H.J. Geuze, and J.W. Slot. 2001. The ER to Golgi interface is the major concentration site of secretory proteins in the exocrine pancreatic cell. *Traffic*. 2:831-8.

Orci, L., B.S. Glick, and J.E. Rothman. 1986. A new type of coated vesicular carrier that appears not to contain clathrin: its possible role in protein transport within the Golgi stack. *Cell*. 46:171-84.

Orci, L., A. Perrelet, and J.E. Rothman. 1998. Vesicles on strings: morphological evidence for processive transport within the Golgi stack. *Proc Natl Acad Sci U S A*. 95:2279-83.

Palade, G. 1975. Intracellular aspects of the process of protein synthesis. *Science*. 189:347-58.

Parton, R.G., and A.A. Richards. 2003. Lipid rafts and caveolae as portals for endocytosis: new insights and common mechanisms. *Traffic*. 4:724-38.

Pasqualato, S., J. Menetrey, M. Franco, and J. Cherfils. 2001. The structural GDP/GTP cycle of human Arf6. *EMBO Reports*. 2:234-8.

Pasqualato, S., L. Renault, and J. Cherfils. 2002. Arf, Arl, Arp and Sar proteins: a family of GTP-binding proteins with a structural device for 'front-back' communication. *EMBO Rep*. 3:1035-41.

Pearse, B.M., and M.S. Robinson. 1990. Clathrin, adaptors, and sorting. *Annu Rev Cell Biol*. 6:151-71.

Pelham, H.R. 1988. Evidence that luminal ER proteins are sorted from secreted proteins in a post-ER compartment. *Embo J*. 7:913-8.

Pelham, H.R. 2001. Traffic through the Golgi apparatus. *J Cell Biol*. 155:1099-101.

Pelham, H.R. 2004. Membrane traffic: GGAs sort ubiquitin. *Curr Biol*. 14:R357-9.

Perry, S.J., and R.J. Lefkowitz. 2002. Arresting developments in heptahelical receptor signaling and regulation. *Trends Cell Biol*. 12:130-8.

Peyroche, A., B. Antonny, S. Robineau, J. Acker, J. Cherfils, and C.L. Jackson. 1999. Brefeldin A acts to stabilize an abortive ARF-GDP-Sec7 domain protein complex: involvement of specific residues of the Sec7 domain. *Mol Cell*. 3:275-85.

Pfeffer, S. 2003. Membrane domains in the secretory and endocytic pathways. *Cell.* 112:507-17.

Presley, J.F., N.B. Cole, T.A. Schroer, K. Hirschberg, K.J. Zaal, and J. Lippincott-Schwartz. 1997. ER-to-Golgi transport visualized in living cells [see comments]. *Nature.* 389:81-5.

Puertollano, R., R.C. Aguilar, I. Gorshkova, R.J. Crouch, and J.S. Bonifacino. 2001. Sorting of mannose 6-phosphate receptors mediated by the GGAs. *Science.* 292:1712-6.

Radhakrishna, H., and J.G. Donaldson. 1997. ADP-ribosylation factor 6 regulates a novel plasma membrane recycling pathway. *J Cell Biol.* 139:49-61.

Radhakrishna, H., R.D. Klausner, and J.G. Donaldson. 1996. Aluminum fluoride stimulates surface protrusions in cells overexpressing the ARF6 GTPase. *J Cell Biol.* 134:935-47.

Randazzo, P.A., and D.S. Hirsch. 2004. Arf GAPs: multifunctional proteins that regulate membrane traffic and actin remodelling. *Cell Signal.* 16:401-13.

Reggiori, F., and H.R. Pelham. 2002. A transmembrane ubiquitin ligase required to sort membrane proteins into multivesicular bodies. *Nat Cell Biol.* 4:117-23.

Reinhard, C., M. Schweikert, F.T. Wieland, and W. Nickel. 2003. Functional reconstitution of COPI coat assembly and disassembly using chemically defined components. *Proc Natl Acad Sci U S A.* 100:8253-7.

Renault, L., B. Guibert, and J. Cherfils. 2003. Structural snapshots of the mechanism and inhibition of a guanine nucleotide exchange factor. *Nature.* 426:525-30.

Robinson, M.S. 2004. Adaptable adaptors for coated vesicles. *Trends Cell Biol.* 14:167-74.

Rossanese, O.W., J. Soderholm, B.J. Bevis, I.B. Sears, J. O'Connor, E.K. Williamson, and B.S. Glick. 1999. Golgi structure correlates with transitional endoplasmic reticulum organization in Pichia pastoris and Saccharomyces cerevisiae. *J Cell Biol.* 145:69-81.

Santy, L.C., S.R. Frank, and J.E. Casanova. 2001. Expression and analysis of ARNO and ARNO mutants and their effects on ADP-ribosylation factor (ARF)-mediated actin cytoskeletal rearrangements. *Methods in Enzymology.* 329:256-64.

Sata, M., J.G. Donaldson, J. Moss, and M. Vaughan. 1998. Brefeldin A-inhibited guanine nucleotide-exchange activity of Sec7 domain from yeast Sec7 with yeast and mammalian ADP ribosylation factors. *Proc Natl Acad Sci U S A.* 95:4204-8.

Sata, M., J. Moss, and M. Vaughan. 1999. Structural basis for the inhibitory effect of brefeldin A on guanine nucleotide-exchange proteins for ADP-ribosylation factors. *Proc Natl Acad Sci U S A.* 96:2752-7.

Scales, S.J., R. Pepperkok, and T.E. Kreis. 1997. Visualization of ER-to-Golgi transport in living cells reveals a sequential mode of action for COPII and COPI. *Cell.* 90:1137-48.

Schledzewski, K., H. Brinkmann, and R.R. Mendel. 1999. Phylogenetic analysis of components of the eukaryotic vesicle transport system reveals a common origin of adaptor protein complexes 1, 2, and 3 and the F subcomplex of the coatomer COPI. *J Mol Evol.* 48:770-8.

Seabra, M.C., and C. Wasmeier. 2004. Controlling the location and activation of Rab GTPases. *Curr Opin Cell Biol.* 16:451-7.

Shiba, Y., Y. Katoh, T. Shiba, K. Yoshino, H. Takatsu, H. Kobayashi, H.W. Shin, S. Wakatsuki, and K. Nakayama. 2004. GAT (GGA and Tom1) domain responsible for ubiquitin binding and ubiquitination. *J Biol Chem.* 279:7105-11.

Shin, H.W., N. Morinaga, M. Noda, and K. Nakayama. 2004. BIG2, a guanine nucleotide exchange factor for ADP-ribosylation factors: its localization to recycling endosomes and implication in the endosome integrity. *Mol Biol Cell.* 15:5283-94.

Shinotsuka, C., Y. Yoshida, K. Kawamoto, H. Takatsu, and K. Nakayama. 2002. Overexpression of an ADP-ribosylation factor-guanine nucleotide exchange factor, BIG2, uncouples brefeldin A-induced adaptor protein-1 coat dissociation and membrane tubulation. *J Biol Chem.* 277:9468-73.

Soderholm, J., D. Bhattacharyya, D. Strongin, V. Markovitz, P.L. Connerly, C.A. Reinke, and B.S. Glick. 2004. The transitional ER localization mechanism of Pichia pastoris Sec12. *Dev Cell.* 6:649-59.

Sollner, T., S.W. Whiteheart, M. Brunner, E.-B. H., S. Germanos, P. Tempst, and J.E. Rothman. 1993. SNAP receptors implicated in vesicle targeting and fusion. *Nature.* 362:318-324.

Someya, A., M. Sata, K. Takeda, G. Pacheco-Rodriguez, V.J. Ferrans, J. Moss, and M. Vaughan. 2001. ARF-GEP100, a guanine nucleotide-exchange protein for ADP-ribosylation factor 6. *Proc Natl Acad Sci U S A.* 98:2413-8.

Song, J., Z. Khachikian, H. Radhakrishna, and J.G. Donaldson. 1998. Localization of endogenous ARF6 to sites of cortical actin rearrangement and involvement of ARF6 in cell spreading. *J Cell Sci.* 111:2257-67.

Storrie, B., and T. Nilsson. 2002. The Golgi apparatus: balancing new with old. *Traffic.* 3:521-9.

Szafer, E., M. Rotman, and D. Cassel. 2001. Regulation of GTP hydrolysis on ADP-ribosylation factor-1 at the Golgi membrane. *J Biol Chem.* 276:47834-9.

Tarricone, C., B. Xiao, N. Justin, P.A. Walker, K. Rittinger, S.J. Gamblin, and S.J. Smerdon. 2001. The structural basis of Arfaptin-mediated cross-talk between Rac and Arf signalling pathways. *Nature.* 411:215-9.

Taylor, T.C., R.A. Kahn, and P. Melancon. 1992. Two distinct members of the ADP-ribosylation factor family of GTP- binding proteins regulate cell-free intra-Golgi transport. *Cell.* 70:69-79.

Turner, C.E., K.A. West, and M.C. Brown. 2001. Paxillin-ARF GAP signaling and the cytoskeleton. *Curr Opin Cell Biol.* 13:593-9.

Van Valkenburgh, H., J.F. Shern, J.D. Sharer, X. Zhu, and R.A. Kahn. 2001. ADP-ribosylation factors (ARFs) and ARF-like 1 (ARL1) have both specific and shared effectors: characterizing ARL1-binding proteins. *Journal of Biological Chemistry.* 276:22826-37.

Wang, Y., J. Seemann, M. Pypaert, J. Shorter, and G. Warren. 2003. A direct role for GRASP65 as a mitotically regulated Golgi stacking factor. *Embo J.* 22:3279-90.

Ward, T.H., R.S. Polishchuk, S. Caplan, K. Hirschberg, and J. Lippincott-Schwartz. 2001. Maintenance of Golgi structure and function depends on the integrity of ER export. *J Cell Biol.* 155:557-70.

Warren, G., and I. Mellman. 1999. Bulk flow redux? *Cell.* 98:125-7.

Watanabe, R., and H. Riezman. 2004. Differential ER exit in yeast and mammalian cells. *Curr Opin Cell Biol.* 16:350-5.

Waters, M.G., T. Serafini, and J.E. Rothman. 1991. 'Coatomer': a cytosolic protein complex containing subunits of non- clathrin-coated Golgi transport vesicles. *Nature*. 349:248-51.

Watson, P.J., G. Frigerio, B.M. Collins, R. Duden, and D.J. Owen. 2004. Gamma-COP appendage domain - structure and function. *Traffic*. 5:79-88.

Weber, T., B.V. Zemelman, J.A. McNew, B. Westermann, M. Gmachl, F. Parlati, T.H. Sollner, and J.E. Rothman. 1998. SNAREpins: minimal machinery for membrane fusion. *Cell*. 92:759-72.

Weissman, J.T., M. Aridor, and W.E. Balch. 2001. Purification and properties of rat liver Sec23-Sec24 complex. *Methods in Enzymology*. 329:431-8.

Wherlock, M., and H. Mellor. 2002. The Rho GTPase family: a Racs to Wrchs story. *J Cell Sci*. 115:239-40.

Whyte, J.R., and S. Munro. 2002. Vesicle tethering complexes in membrane traffic. *J Cell Sci*. 115:2627-37.

Yamaji, R., R. Adamik, K. Takeda, A. Togawa, G. Pacheco-Rodriguez, V.J. Ferrans, J. Moss, and M. Vaughan. 2000. Identification and localization of two brefeldin A-inhibited guanine nucleotide-exchange proteins for ADP-ribosylation factors in a macromolecular complex. *Proc Natl Acad Sci U S A*. 97:2567-72.

Yoshida, T., C.C. Chen, M.S. Zhang, and H.C. Wu. 1991. Disruption of the Golgi apparatus by brefeldin A inhibits the cytotoxicity of ricin, modeccin, and Pseudomonas toxin. *Exp Cell Res*. 192:389-95.

Zhao, X., T.K. Lasell, and P. Melancon. 2002. Localization of large ADP-ribosylation factor-guanine nucleotide exchange factors to different Golgi compartments: evidence for distinct functions in protein traffic. *Mol Biol Cell*. 13:119-33.